THESIS APPROVAL

GRADUATE SCHOOL, KASETSART UNIVERSITY

Master of Engineering (Civil Engineering)

DEGREE

Civil Engineering — **FIELD**

Civil Engineering — **DEPARTMENT**

TITLE: Anchorage Behavior of Headed Reinforcement Bar in CCT Nodes

NAME: Mr. Wichian Kaewkhampa

THIS THESIS HAS BEEN ACCEPTED BY

.... **THESIS ADVISOR**

(Assistant Professor Wanchai Yodsudjai, D.Eng.)

.... **THESIS CO-ADVISOR**

(Associate Professor Trakool Aramraks, Ph.D.)

.... **DEPARTMENT HEAD**

(Associate Professor Korchoke Chantawarangul, Ph.D.)

APPROVED BY THE GRADUATE SCHOOL ON ....

.... **DEAN**

(Associate Professor Gunjana Theeragool, D.Agr.)

THESIS

ANCHORAGE BEHAVIOR OF HEADED REINFORCEMENT BAR IN CCT NODES

WICHIAN KAEWKHAMPA

A Thesis Submitted in Partial Fulfillment of
the Requirements for the Degree of
Master of Engineering (Civil Engineering)
Graduate School, Kasetsart University
2011

Wichian Kaewkhampa 2011: Anchorage Behavior of Headed Reinforcement Bar in CCT Nodes. Master of Engineering (Civil Engineering), Major Field: Civil Engineering, Department of Civil Engineering. Thesis Advisor: Assistant Professor Wanchai Yodsudjai, D.Eng. 155 pages.

The paper expresses the observation of anchorage performance of headed bar reinforced concrete beam specimens, including the behavior of the compression-compression-tension CCT Nodes. The CCT Nodes are modeled in reinforced concrete beams with various types of reinforcing bars e.g. two different models of headed bar connections named BARTEC and GRIPTEC which provide the contradiction in surface roughness assembled with small and large circular shape headed bar also including 90° standard hooked bars.

Specimens were cast with two different compressive strength concretes 23.5 MPa and 31.4 MPa as well as two sizes of reinforcing bars 20 mm and 32 mm. The test result present the anchorage mechanism of headed reinforcing bar in (CCT) nodes and the influence of head type varieties including CCT Node behavior. The current provision related to Strut and Tie Modeling and technical limitation in ACI-318 is evaluated against the observed result. This will eventually lead to the conclusion of the versatility and restriction of use of headed bars to replace the conventional use of hooked bars in congested discontinuity area.

The result indicated that the final anchorage capacity consists of peak bearing capacity of head and reduced bond. For the same head type, the ultimate head capacity was increased with the increasing relative head area. With the same bar size Bartec headed bar had greater ultimate anchorage capacity than Griptec headed bar. The ultimate head capacity of Griptec headed bar was not influenced by the obstruction of rebar deformation which was greater than 2_{db}. The ultimate anchorage capacity of headed reinforcement bar was equal or greater than the 90° standard hooked reinforcement bar.

___________________________ ___________________________ ___ / ___ / ___

Student's signature Thesis Advisor's signature

ACKNOWLEDGEMENT

I would like to grateful thank to Assistant Professor Wanchai Yodsudjai my thesis advisor for advice, encouragement and valuable suggestion for completely writing of thesis. I would sincerely like to thank Associate Professor Trakool Aramraks, my committee member for his valuable comments and suggestion.

The support of the Dextra Manufacturing Co., Ltd. is gratefully acknowledged. The test program was conducted at the Concrete Laboratory of Kasetsart University. The help of the laboratory staff was essential to the conduct of the study, and is greatly appreciated.

I am especially appreciated my parents for their continuing encouragements. Finally, I am deeply appreciated to my wife who always devotes time and support and also my daughter and my son who always gives me heartfelt love during my graduate study.

Wichian Kaewkhampa
March 2011

TABLE OF CONTENTS

Page

LIST OF TABLES

LIST OF TABLES (Continued)

Appendix Table **Page**

LIST OF TABLES (Continued)

LIST OF FIGURES

Figure **Page**

LIST OF FIGURES (Continued)

Figure **Page**

LIST OF FIGURES (Continued)

Figure **Page**

LIST OF FIGURES (Continued)

LIST OF FIGURES (Continued)

Figure **Page**

Appendix Figure

LIST OF FIGURES (Continued)

Appendix Figure **Page**

LIST OF FIGURES (Continued)

Appendix Figure **Page**

LIST OF ABBREVIATIONS

fy	=	Specified yield strength of the reinforcement (psi)
f 'c	=	Specified 28-day compressive strength of the concrete
α	=	Bar location factor,
β	=	Bar coating factor,
γ	=	Bar size factor,
λ	=	Lightweight concrete factor
c	=	Spacing / cover dimension
ktr	=	Transverse reinforcement index
db	=	Diameter of the bar being developed
Anh	=	Net head area
Ab	=	Nominal bar area
D	=	Outside diameter of head
d	=	Outside diameter of Griptec sleeve
T	=	Thickness of head
L1	=	Obstruction length
STM	=	Strut and Tie Model
CCT	=	Compression- Compression- Tension
CCC	=	Compression-Compression-Compression
CTT	=	Compression-Tension-Tension
$n_{5\%}$	=	Statistical adjustment parameter. A value of 0.7 is recommended
c_2	=	Minimum cover dimension, measured in direction orthogonal to c , mm
ψ	=	Radial disturbance factor, $0.6 + 0.4(c_2 / c) \leq 2.0$
L_a	=	Anchorage length,
L_d	=	Development length
χ	=	Reduction factor

LIST OF ABBREVIATIONS (Continued)

$f_{s,\,head}$ = Head bearing capacity

$f_{s,\,bond}$ = Bond Capacity

ANCHORAGE BEHAVIOR OF HEADED REINFORCEMENT BAR IN CCT NODES

INTRODUCTION

The thesis expressed the observation of anchorage performance of headed bars in comparison with the conventional hooked bars. This will eventually lead to the conclusion of the versatility and restriction of use of headed bars to replace the conventional use of hooked bars in congested discontinuity area.

The study examined the various types of headed bars such as small / large circular shape headed bar assembled with special type of connection named BARTEC and GRIPTEC which provide the contradiction in surface roughness.

The strut and tie modeling method with the compression-compression-tension (CCT) nodes specimen was selected to observe the behavior of various specimens. The modeling CCT node test specimens were developed by using a single headed bar in a CCT node.

The CCT node companion specimens with conventional 90˚ hooked bars were also tested to compare with the various types of headed bar specimens.

Finally the observed result of the anchorage performance of headed bars was compared to the theoretical results evaluated from the current formula presented in ACI technical paper.

OBJECTIVES

1. To observe the behavior and anchorage capacity of headed bars in CCT node under the different variables

    1.1 cracking behavior

    1.2 stress/strain development in the bars

    1.3 head slip

    1.4 failure mode

2. To observe the obstruction effect on the anchorage capacity for the different types of headed bars

3. To compare the behavior and capacity of headed bars to standard hooked bar

4. To compare the anchorage capacity of headed bars in CCT node with the theoretical model

Scope of Research

1. Use only the small and large round head shape with minimum relative head area 4.10 and 9.59 respectively

2. Use only the Thai reinforcing bar grade SD 40 with minimum yield strength 400 MPa

3. Use two types of concrete i.e. 23.5 MPa and 31.4 MPa compressive strength

4. Casting 20 numbers of CCT node reinforced concrete beam with various types of headed reinforcing bars.

5. Observe the following effects on anchorage capacity of headed bars in CCT node

    5.1. Bar size 20mm and 32 mm

    5.2. Relative head area with 4.10 and 9.59

    5.3. Obstruction effect of two models of headed bars i.e. BARTEC and GRIPTEC

6. Testing with fully equipped instruments to observe the following behavior of each specimen.

    6.1. Cracking development

    6.2. Stress/strain and bond development in the bar

    6.3. Head slip

    6.4. Failure mode

7. To observe the obstruction effect on anchorage capacity of headed bars in CCT node

8. Compare the observed anchorage capacity of headed bars in CCT node with theoretical model.

LITERATURE REVIEW

Bond and Development Length of Deformed Bars

Loads generally arrive at reinforced concrete members via the concrete, whether across the faces of the concrete, fasteners, anchors, etc., or the weight or mass (mass times acceleration) of the concrete itself. For reinforced concrete to `work' these loads (at least the tension ones) must be transferred to the steel. For cast-in-place concrete the transfer mechanism is the shear resistance of the concrete in contact along the reinforcement via the ribs of the rebar deformations. Hence, transfer is across the surface area of contact. To ensure there is enough contact area for the load transfer to take place we will specify minimum lengths of contact related to bar size.

In this regard, if we consider a certain amount of load to be carried by some arrangement of reinforcement, smaller bars will have more surface area *per bar*, and the lengths of contact required will be relatively smaller. The smaller bars are more efficiently developed. Or, a big bar will also have a greater development length, maybe cumbersomely so.

Before discussing the state-of-the-art of headed reinforcement, a brief overview of conventional anchorage of reinforcing bars will be presented emphasizing bond of straight reinforcement and standard hook details. The nature and mechanism of bond stress development of reinforcement will be studied. The behavior of hooked bar anchorages is also discussed. The research will eventually be compared to the design provisions focuses on the ACI 318-08 (American Concrete Institute, 2008).

The Mechanics of Bond

Bond is the interaction between reinforcing steel and the surrounding concrete that allows for transfer of tensile stress from the steel into the concrete. Bond is the mechanism that allows for anchorage of straight reinforcing bars and influences many other important features of structural concrete such as crack control and section stiffness. Figure 1 shows a straight bar embedded into a block of concrete. When the bond stress is sufficient to resist design tensile loads in the bar, then the bar is "developed" and the embedment length necessary for anchorage of the fully stressed reinforcing bar is referred to as its development length.

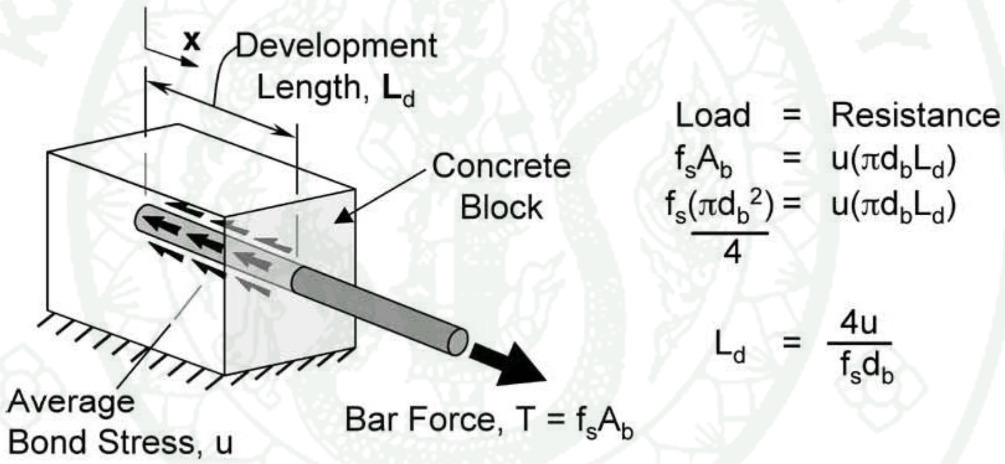

Figure 1 Simple concept of bond stress

Source: Thompson et al. (2002)

Development Length of Deformed Bars in Tension

From Chapter 12 in the ACI 318-08 (American Concrete Institute, 2008), the basic equation for development length, l_d, is, ...

$$l_d = \{ (3/40) (fy /\sqrt{f'c}) (\alpha \beta \gamma \lambda) / [(c + kt\ r) / db] \} db$$

where,

fy = specified yield strength of the reinforcement (psi)
f 'c = specified 28-day compressive strength of the concrete (psi) and where $\sqrt{f'c}$ carries the units of psi,
α = bar location factor, which is 1.0 except for horizontal bars with more than 12 in. of fresh concrete cast below them,
β = bar coating factor, which is 1.0 for uncoated bars, and 1.2 or so for epoxy coating the epoxy somewhat smoothing out the ribs.
γ = bar size factor, 0.8 for # 6 and smaller bars; 1.0 otherwise;
λ = lightweight concrete factor, 1.0 for normal weight concrete
c = spacing / cover dimension, being the smaller of the distance from the center of the bar to the nearest face of concrete, or half the center-to-center spacing of the reinforcement,
ktr is a transverse reinforcement index ... (see below, but) which may be taken as 0, and
db is the diameter of the bar being developed.
The Code places an upper limit on the quantity (c + kt r) / db of 2.5.

Note: the *minimum* development length is 12 in., regardless of the equation.

In many cases by satisfying other spacing and cover limitations in the Code (Ch. 7) a value of 1.5 can be obtained, and some authors generate *tables* of development length values using the 1.5.

Deformed reinforcing bars develop bond stresses by means of transverse ribs that bear directly on the concrete. As tensile forces develop in a reinforcing bar, transverse cracks propagate from the edges of the ribs. This was experimentally shown by Goto (1971) and is reproduced in Figure 2. The bond stress produced by the bearing of the ribs is not uniform. Mains (1951) showed experimentally that local bond stress can be more than twice the average bond stress. Figure 2 also shows the distribution of tensile and bond stresses for a bar embedded in a concrete prism and loaded in tension. Bond stress peaks near cracks and tapers off as the concrete carries more of the tensile load. The bond stress then reverses sign when another primary crack is formed. The process by which concrete around reinforcing bars shares tensile loads is called “tension stiffening.” It is important to note that a bar does not uniformly yield in cracked concrete when it is properly bonded. Yielding occurs only locally near cracks.

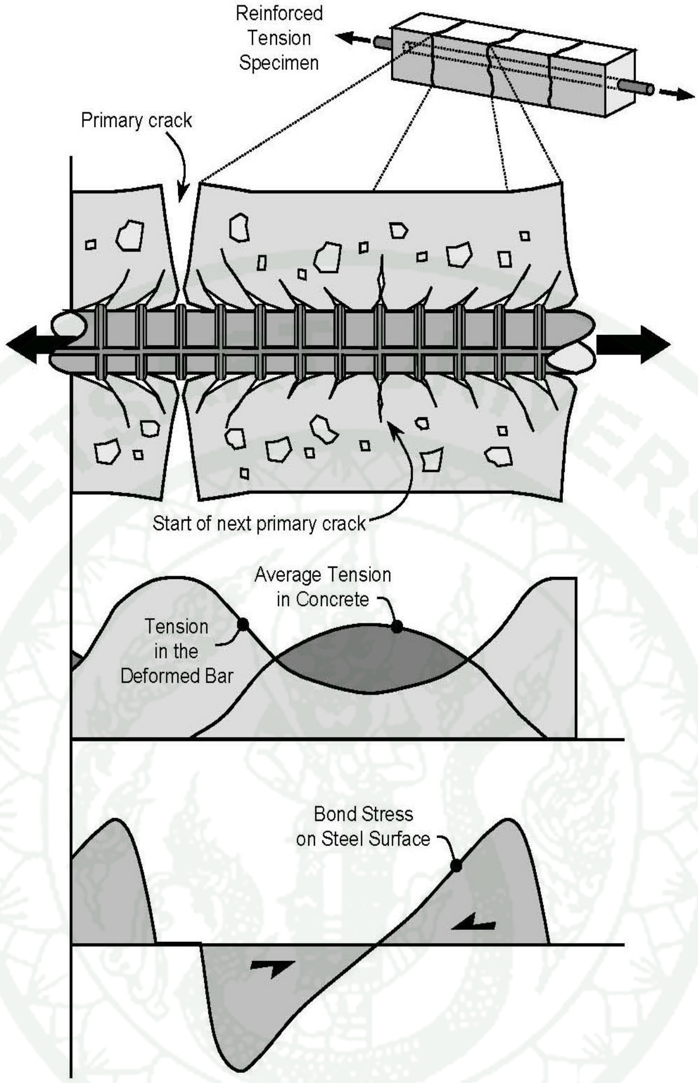

Figure 2 Transverse cracking at deformations

Source: Thompson et al. (2002)

Bearing stresses on the ribs act in a direction roughly normal to the face of the rib. Figure 3, part I shows bearing stresses acting at an angle, bond, relative to the bar axis. These bearing forces can be split into parallel and perpendicular components (Figure 3, part ii). The components parallel to the bar constitute the bond responsible for resisting the tensile force in the reinforcement. The components perpendicular to the bar act outward from the bar surface as splitting stresses on the concrete. These radial splitting stresses must be counteracted by ring tension stresses in the concrete surrounding the reinforcing bar, section A-A of Figure 3, part iii. Ultimately, the radial splitting stresses exceed the tensile capacity of the surrounding concrete and splitting cracks begin to propagate from the bar surface.

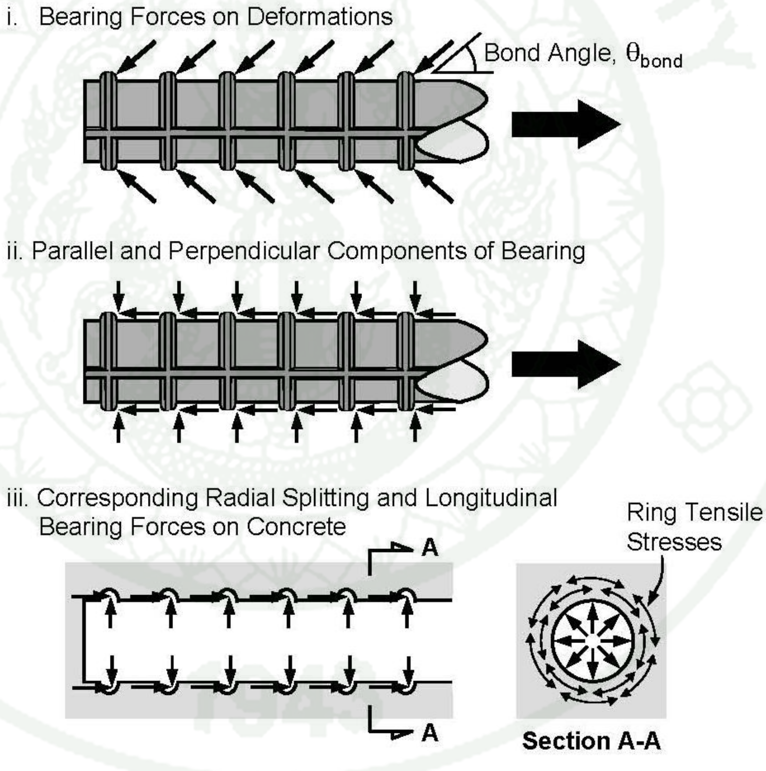

Figure 3 Bond and splitting components of rib bearing stress

Source: Thompson et al. (2002)

Bond can fail in multiple ways. The longitudinal bond stresses can exceed the shear strength of the concrete keys between ribs and the bar can pull free. This is referred to as a “pullout” failure. It is also sometimes termed a “shear-out” failure, but this report will use the more common term of pullout. More commonly though, splitting cracks will propagate from the bar to the surface of the concrete and the cover will spall off.

This eventually leads to the conclusion of bond development process of the headed bar which is composed of a combination of bond plus a contribution from head bearing. The variation of bond under loading is observed to understand the contribution from bond when peaked and then began to decrease before the contribution from head bearing reached its maximum capacity.

Background on Headed Bars

Headed bars are created by the attachment of a plate or nut to the end of a reinforcing bar to provide a large bearing area that can help anchor the tensile force in the bar. Figure 10 shows an example of a headed bar. The tensile force in the bar can be anchored by a combination of bearing on the ribs and on the head.

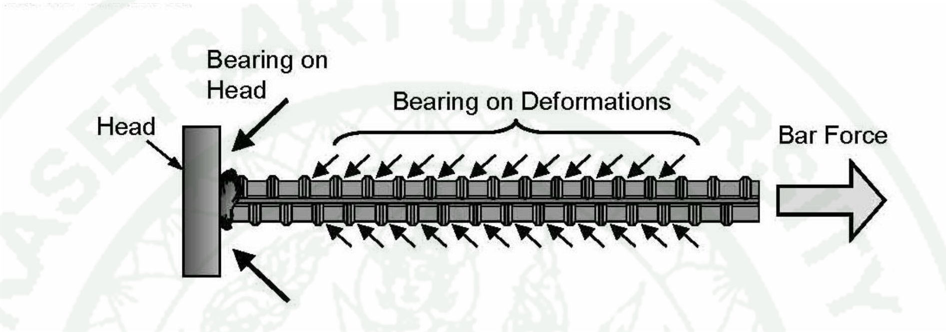

Figure 4 Anchorage of a headed bar

Source: Thompson et al. (2002)

$$\text{Relative Head Area} = \frac{A_{nh}}{A_b} = \frac{A_{gh} - A_b}{A_b}$$

A_{nh} = the net head area (in^2)

A_{gh} = the gross head area (in^2)

A_b = the nominal bar area defined by ASTM A615 [3] (in^2)

Types of Headed Bar

Basically the headed bar consists of a steel plate attached to the reinforcing bar end. The fixing method of head to bar could be as following.

1. By friction welding as shown in Figure 5
2. By bolt connection as shown in Figure 6
3. By nut connection method as shown in Figure 7
4. By swaging method as shown in Figure 8
5. By hot forging method as shown in Figure 9
6. By parallel threaded as shown in Figure 10

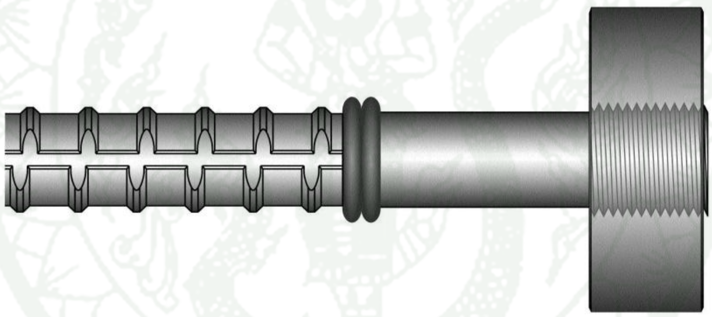

Figure 5 Friction welding method

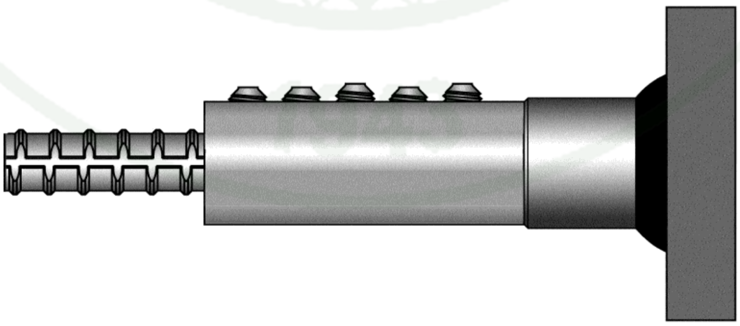

Figure 6 Bolt connection method

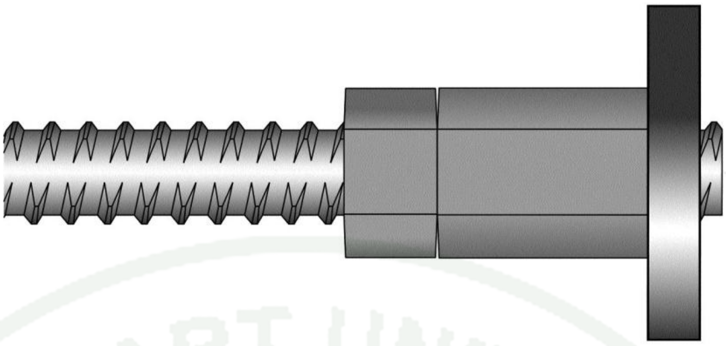

Figure 7 Nut connection method

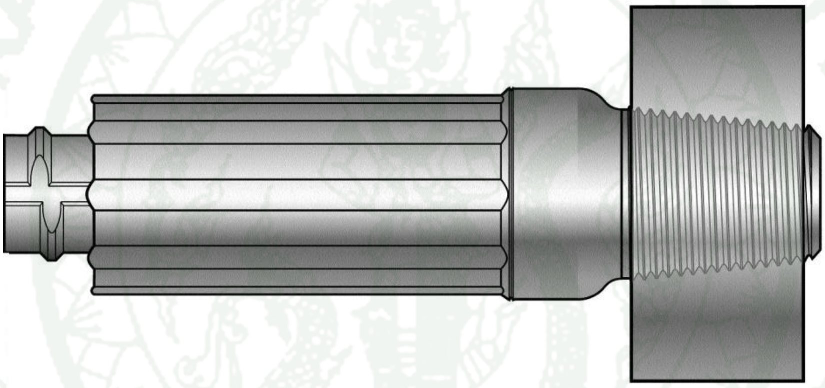

Figure 8 Swaging connection method

Figure 9 Hot forging method

Figure 10 Parallel threaded connection method

Application of Headed Bar

Headed bar is widely used in many applications particularly in large scale structure elements like bridge, oil and gas platform. Its provision in structure member could resolve the present detailing problems due to the long development lengths and large bend diameters that are required particularly when large-diameter reinforcing bars are used. Occasionally, the provision of hooked bar requires enough space for bend of bar, that may not fit within the dimensions of a member or the hooks create congestion and make an element difficult to construct. Figures 11- 18 show the provisions of headed bars to replace the hooked bars in various types of concrete structural members.

Figure 11 Headed bars in bridge structure

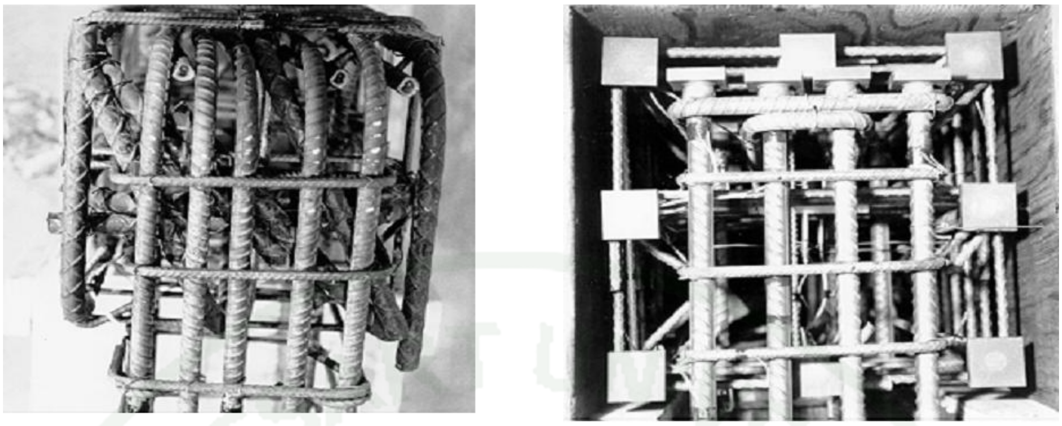

Figure 12 Headed bars in column structure

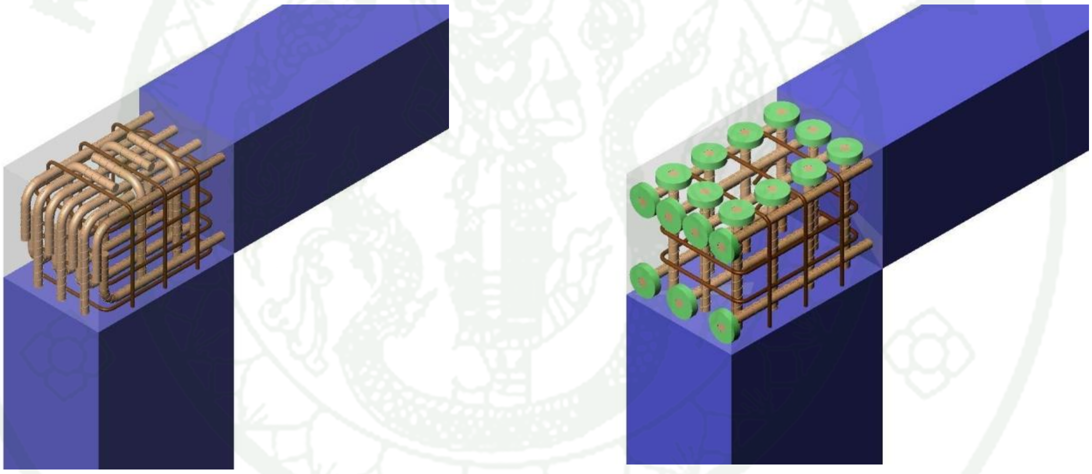

Figure 13 Headed bars in exterior beam-column connection

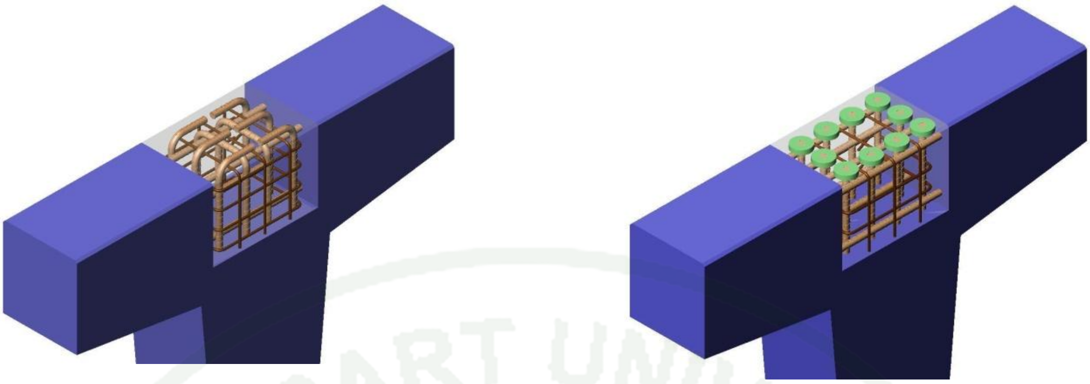

Figure 14 Headed bars in bridge pier structure

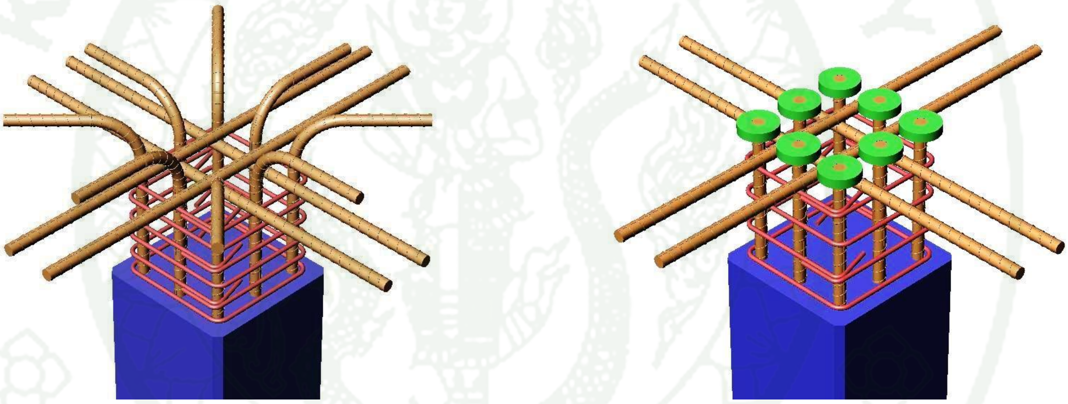

Figure 15 Headed bars in column structure

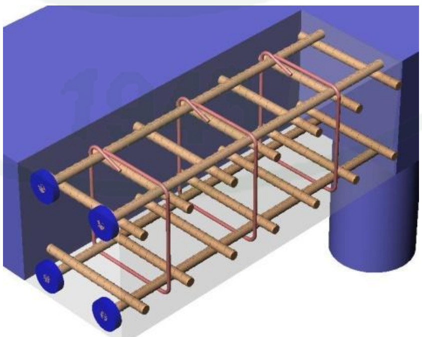

Figure 16 Headed bars in slab structure

Figure 17 Headed bars in corbel structure

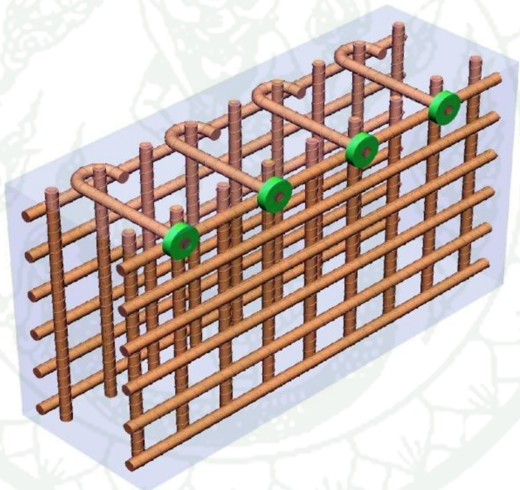

Figure 18 Headed bars in wall structure

Dextra's Headed Bar

BARTEC

Development of reinforcement is the main use of headed bars: They conveniently replace hooked bars as end anchorages in congested areas. They can also be used to reduce lapping length, or as confinement or shear reinforcement where placing of stirrups is difficult.

Typical applications include exterior beam-column connections, roof corners, pile feet, pile caps, cantilevered members, corbels, etc.

Just like hooked bars, headed bars provide end anchorage by a combination of bond and end bearing on the concrete. But headed bars bond better with the concrete because, for a given embedment length, the straight portion of a headed bar is longer than that of a hook, due to the bending radius of the hook. Under cyclic loading headed bars therefore display a smaller slip relative to the concrete than hooked bars do.

Bartec® Standard mechanical anchorages are circular in shape. Two sizes of heads are proposed. Other head sizes can be manufactured upon request to fit the application requirements. The dimensions of all bar sizes are listed in table 1 and 2.

The small heads, with a net bearing area of four times the cross-section area of the reinforcing bar, work with a combination of head bearing capacity and bond. The minimum anchorage length required to provide the bond must be computed according to the code provisions by the structural engineer, depending on the grade of reinforcement and the class of concrete. Again, due to the absence of a bending radius, the development length of a headed bar is typically shorter than that of a hook.

The large heads, with a net bearing area of nine times the cross-section area of the reinforcing bar, develop the yield strength of the bars without exceeding the concrete bearing strength. Figure 19 shows the relative head area characteristic.

The embedment length should however not be less than 8 times the bar diameter or 6”, whichever is greater.

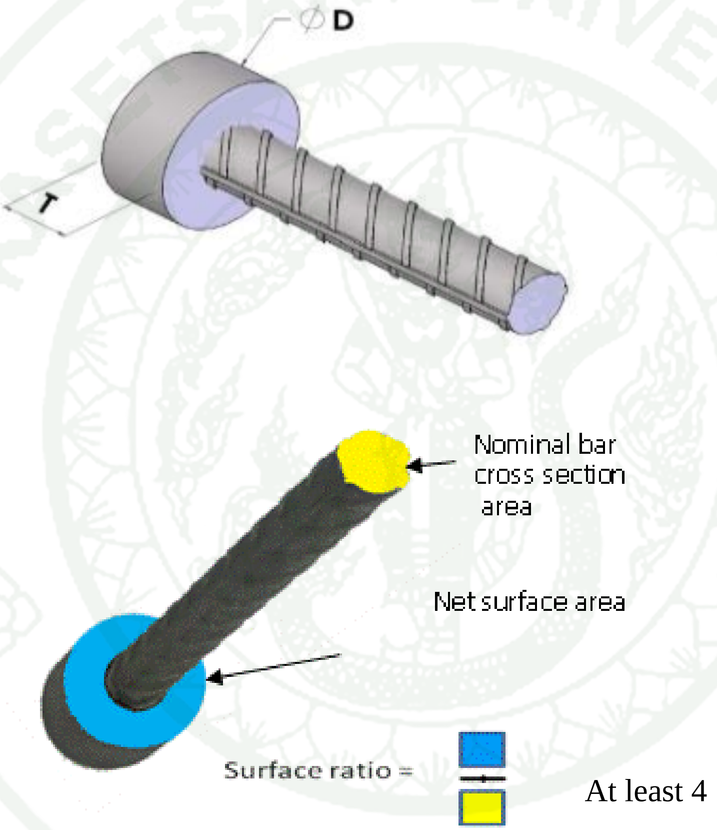

Figure 19 BARTEC headed bar relative head area

Table 1 BARTEC small headed bar dimension

Bar size	Model	Approximate external dimensions Small round heads			
		∅ D (mm)	Thickness (mm)	Net surface area (mm^2)	Surface ratio
12	BEASC12	30	14	553	4.89
14	BEASC14	34	16	707	4.59
16	BEASC16	38	20	820	4.08
18	BEASC18	45	22	1,210	4.76
20	BEASC20	48	24	1,357	4.32
22	BEASC22	52	27	1,551	4.08
25	BEASC25	60	30	2,121	4.32
28	BEASC28	70	33	2,993	4.86
32	BEASC32	75	36	3,400	4.23
34	BEASC34	80	39	3,832	4.22
36	BEASC36	85	42	4,289	4.21
40	BEASC40	95	45	5,498	4.38
43	BEASC43	100	48	6,849	4.72
50	BEASC50	115	56	7,924	4.04
56	BEASC56	130	64	10,056	4.08

Table 2 BARTEC large headed bar dimension

Bar size	Model	Approximate external dimensions Large round heads			
		∅ D (mm)	Thickness (mm)	Net surface area (mm^2)	Surface ratio
12	BEALC12	42	14	1,232	10.89
14	BEALC14	45	16	1,389	9.03
16	BEALC16	52	20	1,810	9.00
18	BEALC18	60	22	2,447	9.62
20	BEALC20	65	24	2,866	9.12
22	BEALC22	75	27	3,845	10.12
25	BEALC25	85	30	4,968	10.12
28	BEALC28	95	33	6,233	10.12
32	BEALC32	105	36	7,641	9.50
34	BEALC34	110	39	8,309	9.15
36	BEALC36	120	42	9,924	9.75
40	BEALC40	130	45	11,683	9.30
43	BEALC43	140	48	14,703	10.12
50	BEALC50	165	56	18,919	9.64
56	BEALC56	180	64	22,230	9.03

GRIPTEC

GRIPTEC headed bar is characterized with the swaging length (L_1), that obstruct the rebar deformation. Figure 20 shows GRIPTEC sleeve process. The dimensions of all bar sizes are listed in table 3 and 4.

The Griptec is a full performance (tension, compression, cyclic, fatigue) mechanical splice designed for the connection of concrete reinforcing bars.

Figure 20 GRIPTEC sleeve

It is guaranteed that each and every Griptec connection is proof-tested by pull test during the extrusion cycle. There is no reduction of the nominal cross section area of the bar.

Good fatigue performance. The 100% bar-break is also guaranteed. Figure 21 shows the bar-break performance of Griptec connection.

Figure 21 Bar-break performance of GRIPTEC sleeve connection

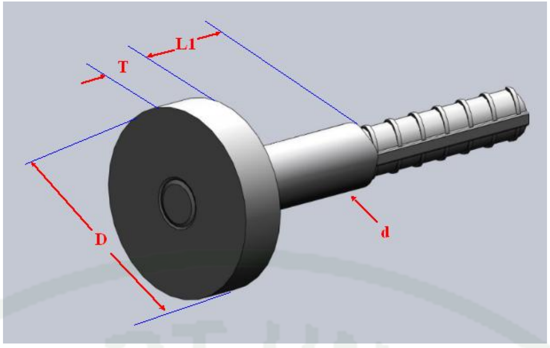

Figure 22 GRIPTEC headed bar

Table 3 GRIPTEC small headed bar dimension

Bar size	Model	Approximate external dimensions Small round heads				Net surface area (mm^2)	Surface ratio
		D	T	L1	d		
12	AGEASC12	34	12	68	19.0	624	5.52
14	AGEASC14	38	14	74	22.2	747	4.85
16	AGEASC16	42	16	97	25.3	883	4.39
20	AGEASC20	52	20	127	32.6	1,289	4.10
25	AGEASC25	65	22	116	37.8	2,196	4.47
26	AGEASC26	70	22	119	40.8	2,541	4.79
30	AGEASC30	80	28	138	47.0	3,292	4.66
32	AGEASC32	80	28	145	46.8	3,306	4.11
36	AGEASC36	90	32	143	53.8	4,088	4.02
40	AGEASC40	105	34	169	64.0	5,442	4.33
50	AGEASC50	125	47	205	74.5	7,913	4.03

Table 4 GRIPTEC large headed bar dimension

Bar size	Model	Approximate external dimensions Large round heads				Net surface area (mm^2)	Surface ratio
		D	T	L1	d		
12	AGALC12	45	12	68	19.0	1,307	11.56
14	AGEALC14	50	14	74	22.2	1,576	10.24
16	AGEALC16	55	16	97	25.3	1,873	9.32
20	AGEALC20	70	20	127	32.6	3,014	9.59
25	AGEALC25	90	22	116	37.8	5,240	10.67
26	AGEALC26	90	22	119	40.8	5,054	9.52
30	AGEALC30	105	28	138	47.0	6,924	9.80
32	AGEALC32	110	28	145	46.8	7,783	9.68
36	AGEALC36	125	32	143	53.8	9,999	9.82
40	AGEALC40	140	34	169	64.0	12,177	9.69
50	AGEALC50	170	47	205	74.5	18,339	9.34

Background on Strut-and-Tie Modeling

Strut-and-Tie Modeling (STM) is a detailing and ultimate strength calculation procedure for discontinuity regions within structures.

STM is ideal for deep members, joints, supporting brackets or corbels, dapped beam ends, anchorage zones for post-tensioning, and many other complex structural components.

STM is derived from plasticity theory. STM is a lower bound solution method. According to the theory of plasticity, any statically admissible stress field that is in equilibrium with the applied loads and in which stress levels are on or within the material yield surface constitutes a lower bound solution.

STM is a method involving the idealization of a complex structural member into a simple collection of struts, ties, and nodes representing, in a general manner, the flow of stress paths within the member. STM is ideal for deep members, joints, supporting brackets or corbels, dapped beam ends, anchorage zones for postensioning, and many other complex structural components.

STM involves the construction of a truss mechanism contained within the boundaries of the member being analyzed. The truss mechanism is composed of struts that model concrete compression fields, ties that model tensile steel reinforcement, and nodes that represent the localized zones in which the tensile steel is anchored into the concrete, and strut forces are transferred into the ties. The struts and ties carry only uniaxial stresses. This truss mechanism must be stable and properly balance the applied loads.

Failure of the truss mechanism is dictated by yielding of one or more ties or by excessive stresses within the struts or nodes or by an anchorage failure of the reinforcement at one of the nodes. When used properly to detail a structural member, only the first of the aforementioned failure modes should occur.

Figure 23 shows the three basic node types. A Compression-Compression-Compression (CCC) node is the intersection of three compression struts. A Compression-Compression-Tension (CCT) node is the intersection of two struts and a tension tie. A Compression-Tension-Tension (CTT) node represents the intersection of one compression strut with two tension ties. CCT and CTT nodes generally have lower effective strengths than CCC nodes due to the disruption effect created by the splitting associated with bond anchorage of the reinforcing bars.

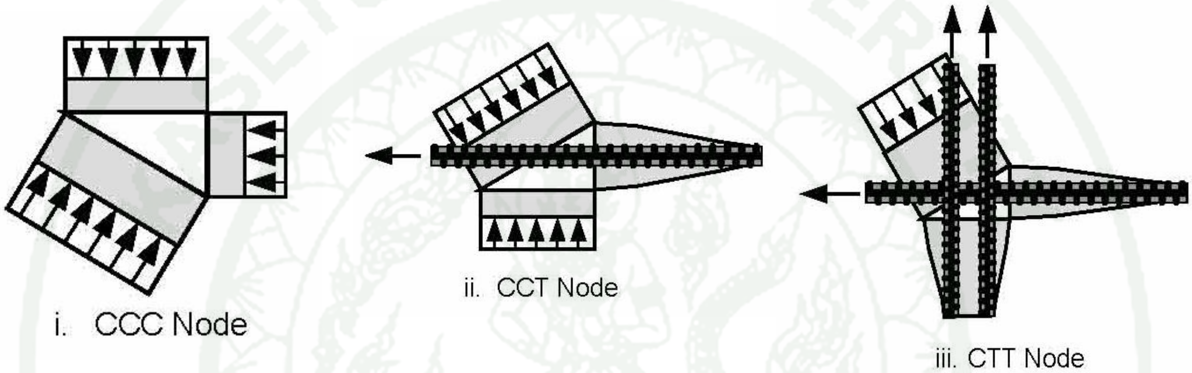

Figure 23 Basic node types

Source: Thompson et al. (2002)

Code Review

ACI STM Procedures

ACI 318-08 (American Concrete Institute, 2008) provides some guidance to determine the capacity of CCT nodes anchored by headed reinforcement i.e. the provisions of Appendix A can be used to analyze node and adjacent struts by using strut and tie model (STM) that can analyze node capacity as a function of compression stress on the faces of the node and struts. These provisions also require that sufficient anchorage length be provided to develop the tie bar in tension. In the case of headed bar anchorage of a tie, two components must be considered at failure: bearing of the head and bond. The ACI code does not present definitive criteria for the capacity of headed reinforcement. Figure 24 shows the typical critical node faces.

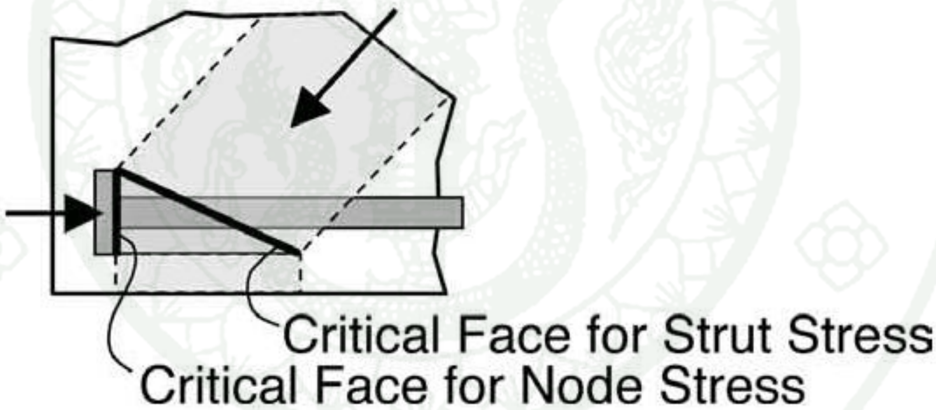

Figure 24 Critical node faces for STM stresses

Source: Thompson et al. (2002)

ACI Side Blow-out Model

Another existing provision of Appendix D of 318-08 (American Concrete Institute, 2008) also provides criteria for capacity of headed anchors. DeVries (1996) found that deeply embedded headed bars fail by side blowout and recommends a model similar to that provided in ACI 318-08 (American Concrete Institute, 2008), Section D.5.4, for side blowout of deeply embedded anchors. The side blowout provisions provide one model for the head-bearing component of anchorage.

ACI Bearing Capacity Model

Another model for head bearing can be found in ACI 318-08 (American Concrete Institute, 2008), Section 10.17, "Bearing Strength." The bond component can be modeled using the development length formula provided in ACI 318-08 (American Concrete Institute, 2008), Section12.2, "Development of Deformed Bars and Deformed Wire in Tension."

The ACI bearing capacity model (Section 10.17 of the ACI 318-08 (American Concrete Institute, 2008) and Section 5.7.5 of the AASHTO code (American Association of State Highway and Transportation Officials, 1998)) was used to calculate the contribution of the head to the tie bar anchorage. The bearing capacity equation depends on three main variables: the bearing area (or in this case, the net head area), Anh, the concrete compressive strength, fc', and the notional area projected beneath the surface of the loaded plate, A2.

Comparison to Design Recommendation following ACI Technical Paper

Based on bearing capacity model and side blow out model provisions in ACI 318, Thompson *et al* (2002) proposed design recommendations for headed bar anchorage performance which is provided by a combination of head bearing and bond.

The purpose of this design recommendation is to provide some calculation methods to determine the proper head size of headed reinforcement bars which is able to develop the rebar yield strength without breaking the concrete.

The experiment results are observed in comparison to the theoretical results proposed by this design recommendation.

Four strain gauges were placed along the bottom of the reinforcing bar to measure the stress profile along the tie bar. Bar stress at head can be calculated from strain gauge reading at 1db. Anchorage is carried primarily by bond until it reaches its peak capacity then it begins to decline as additional stress is applied to the bars. During the process of bond deterioration, bar anchorage is simultaneously transferred to the head, causing a rise in head bearing. Therefore anchorage capacity at failure is the combination of peak head bearing capacity and remaining bond at failure.

Model for Bearing Capacity

The proposed model for head bearing capacity is based on existing ACI code equations for bearing strength and side blowout capacity.
The equations used in the model are listed below.

$$f_{s,head} = n_{5\%} \cdot 2 \cdot f_c^{'} \cdot \left(\frac{c}{d_b}\right) \cdot \sqrt{\frac{A_{nh}}{A_b}} \cdot \psi \qquad (1)$$

Where,

$n_{5\%}$ is statistical adjustment parameter. A value of 0.7 is recommended

$f_c^{'}$ is concrete compression strength, from cylinder tests, MPa

c is minimum cover dimension, measured to bar center, mm

d_b is bar diameter, mm

A_b is bar area, mm^2

A_{nh} is net head area

ψ is radial disturbance factor, $0.6 + 0.4(c_2 / c) \leq 2.0$

c_2 is minimum cover dimension, measured in direction orthogonal to c, mm

Model for Bond Capacity

Under the proposed model, the bar stress contributed from bond is calculated using the ratio of available anchorage length *La* to development length *Ld.* assuming that the distribution of bar stress is linear over *Ld*.

This produces a baseline stress, $f_{s,bond} = \left(\frac{L_a}{L_d}\right) \cdot f_y$ (2)

The sum of these two components is the anchorage strength of headed reinforcement bar. If the anchorage strength is greater than the yield strength of rebar, the headed reinforcement bar is considered able to develop yield strength in rebar without breaking the concrete.

1. If a head is attached to the bar, then $f_{s,\ bond}$ must be reduced by the reduction factor

2. If $f_{s,head}$ is greater than the bar yield stress, f_y, the calculation is finished. The headed bar shall be installed with anchorage length of 6 times rebar diameter.

3. If $f_{s,head}$ is less than the bar yield stress, f_y, the remaining bar stress must be carried by bond. Use the following equation to solve for the required anchorage length, L_a.

$$f_{s,bond} = f_y - f_{s,head} = \chi \cdot \left(\frac{L_a}{L_d}\right) \cdot f_y \quad (3)$$

Where

L_a is anchorage length, measured from point at which tie bar first intersects strut boundary to end of tie bar, mm

L_d is development length using the equation in Chapter 12 of the ACI 318-08 (American Concrete Institute, 2008), mm

f_y is yield strength of reinforcement bar, MPa

χ is reduction factor, $\chi = 1 - 0.7\left(\frac{A_{nh} / A_b}{5}\right) \geq 0.3$ (4)

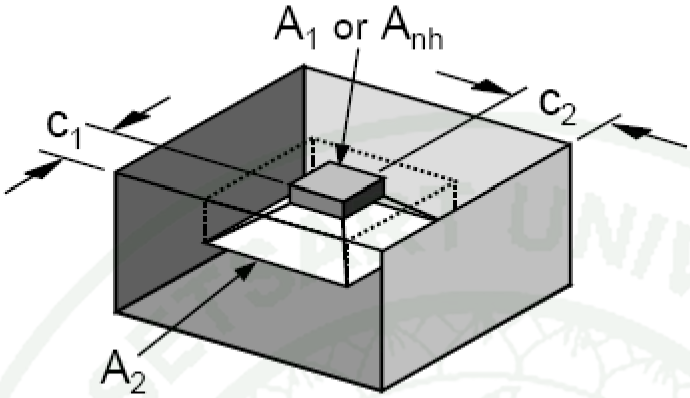

Figure 25 Important dimensions for bearing capacity model

Source: Thompson et al. (2002)

Figure 25 shows the important dimensions of bearing capacity model The dimension of each specimen for calculation head bearing capacity are listed in the appendix table 28.

The results of head bearing capacity from experimental of each specimen are listed in appendix table 29.

OBSTRUCTION EFFECT

It is stipulated in ACI 318-08 (American Concrete Institute, 2008) as following.

Clause 3.5.9 Headed deformed bars shall conform to ASTM A970 / A970M – 09 (American Society for Testing and Materials, 2009), and obstructions or interruptions of the bar deformations, if any, shall not extend more than *2db* from the bearing face of the head, see in Figure 26.

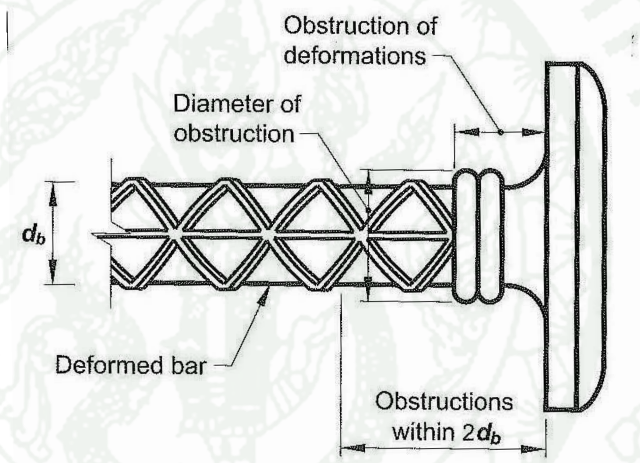

Figure 26 Headed deformed reinforcing bar with an obstruction that extends less than $2d_b$ from the bearing face of the head

Source: American Concrete Institute (2002)

The rebar deformation obstruction length of Griptec sleeve is 127 mm and 145 mm for diameter 20 mm and 32 mm respectively which is greater than 2db as stipulated in ACI 318-08 (American Concrete Institute, 2008).

MATERIALS AND METHODS

Specimen Fabrication and Testing Procedures

A total of 9 cases of CCT node specimens would be tested in the course of the project.

The basic test would be performed essentially on the simple beam test specimens and test frame as shown in Figure 27. However many small details of the test specimens and the testing procedure evolved over the course of the project.

Test Program

Eighteen (18) CCT node specimens will be casted as listed in table 5.

Specimen dimension 50 cm deep and 180 cm long with the width 6d that vary on the bars diameter (d)

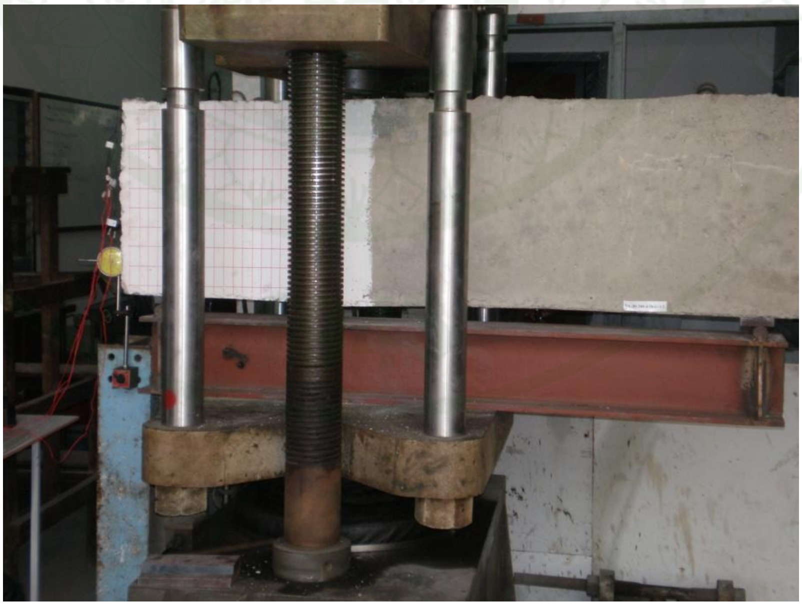

Figure 27 Placement specimen

Table 5 Dimension of specimen

Bar size (mm)	Width (cm)	Depth (cm)	Length (cm)	Number of specimen
20	12	50	180	16
32	20	50	180	2
Total numbers of specimen				18

Key Parameter

1. Bar size
   1.1. 20 mm
   1.2. 32 mm
2. Head type
   2.1. BARTEC with circular small head
   2.2. GRIPTEC with circular large head
   2.3. GRIPTEC with circular small head
   2.4. Standard hook 90˚
3. Concrete compressive strength
   3.1. Compressive strength 23.5 MPa
   3.2. Compressive strength 31.4 MPa

Nomenclature and List of Specimens

Each sample is clearly identified with the nomenclature as listed in table 6 - 8.

Table 6 Nomenclature of specimen

Confinement	Bar size	Compressive strength	Relative head area	Head type	Sample number
U	20 (32)	240(320)	4.10 (9.59)	B (G)	1 /1(2)
U= Unconfined	20 mm	240 ksc (23.5 MPa)	Relative head area = 4.10	B=Bartec	Sample number 1
	32 mm	320 ksc (31.4 MPa)	Relative head area = 9.59	G=Griptec	Sample number 2
			Relative head area = 0.00	H=Hooked	

Table 7 Example of specimen Nomenclature

U-20-240-4.00-B-1/1	Unconfined with 20 mm tie bar, 23.5 MPa concrete, Bartec headed with 4.0 relative head area, sample 1
U-32-240-9.00-B-1/1	Unconfined with 32 mm tie bar, 23.5 MPa concrete, Bartec headed with 9.0 relative head area, sample 1
U-20-240-0.00-H-1/1	Unconfined with 20 mm tie bar, 23.5 MPa concrete, standard hooked 90°, spacing sample 1
U-20-320-9.00-G-1/1	Unconfined with 20 mm tie bar, 31.4 MPa concrete, Griptec headed with 9.0 relative head area, spacing sample 1

Table 8 Nine cases of specimens

Item	Specimen ID	Condition	Strut angle	Width	Bar size	Head type	Relative head area
1	U-20-240-4.32-B-1/1,2	Unconfined	45˚	120	20	BARTEC with circular dh= 48 mm	4.32
2	U-20-240-9.59-B-1/1,2	Unconfined	45˚	120	20	GRIPTEC with circular dh= 70 mm	9.59
3	U-20-240-4.10-G-1/1,2	Unconfined	45˚	120	20	GRIPTEC with circular dh=52 mm	4.10
4	U-20-240-0.00-H-1/1,2	Unconfined	45˚	120	20	Hooked 90˚	0.00
5	U-20-320-4.32-B-1/1,2	Unconfined	45˚	120	20	BARTEC with circular dh= 48 mm	4.32
6	U-20-320-9.59-B-1/1,2	Unconfined	45˚	120	20	GRIPTEC with circular dh= 70 mm	9.59
7	U-20-320-4.10-G-1/1,2	Unconfined	45˚	120	20	GRIPTEC with circular dh=52 mm	4.10
8	U-20-320-0.00-H-1/1,2	Unconfined	45˚	120	20	Hooked 90˚	0.00
9	U-32-240-9.68-B-1/1,2	Unconfined	45˚	200	32	GRIPTEC with circular dh=110 mm	9.68

Specimen Details

The unconfined CCT node specimens will be tested. Unconfined specimens contain the tensile tie steel in the nodal zone region without stirrup.

Figure 28 and 29 show two types of headed bar i.e. BARTEC and GRIPTEC headed bar with the small and large circular shape used to study the effect of obstruction during bond development.

Figure 28 BARTEC Headed bars

Figure 29 GRIPTEC Headed bars

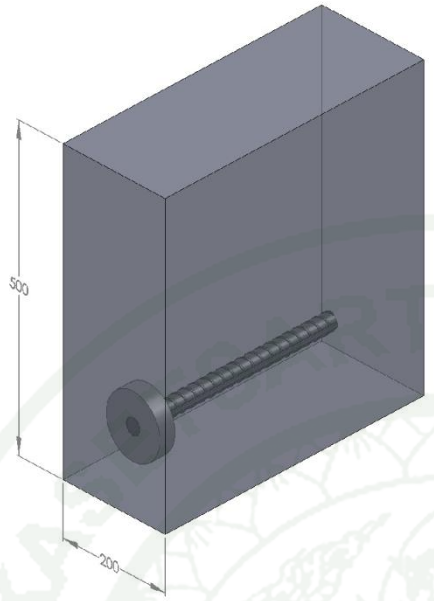

Figure 30 Headed bar dia 20 mm and 32 mm Specimen details

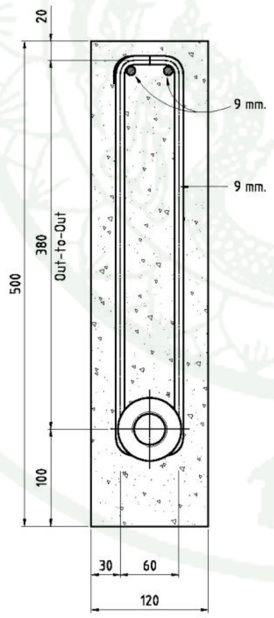

Figure 31 Specimen reinforcing details

Specimen with conventional 90˚ hooked bar will also be tested to compare the behavior with the headed bars specimens as shown in Figure 32.

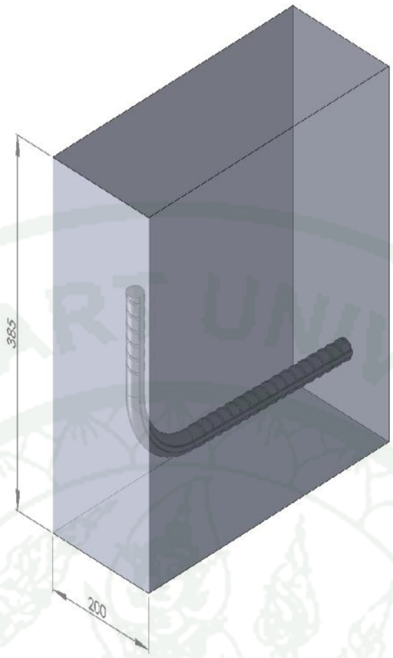

Figure 32 90° hooked bar dia 20 mm Specimen details

Figure 30 and 31 show two bar sizes i.e. dia 20 mm and 32 mm used as the longitudinal tied bars for each specimens.

The width of the specimens is changed depending on the size bar used in the primary tension tie. The width is generally 6db, where db is the diameter of the tension tie bar. 20 mm and 32 mm size bars will be tested with corresponding specimen widths of 120 mm and 200 mm respectively.

The tension tie is always centered at 10 cm from the bottom of the specimen. The yield strength (fy) of the ties is 450 MPa.

Two concretes with compressive strength i.e. 23.5 MPa and 31.4 MPa are used for this research.

Specimen Instrumentation

Three types of instrumentation will be used during the testing. Below is a list of the different instrumentation types and their purpose in the testing:

1. Strain gages will be used on the tie bar surface to provide information on the development of force in the tie bar in the nodal zone and in the stirrup reinforcement for confined condition.

2. Dial gauge will be used to measured horizontal slip of the head relative to the outside face of the concrete and to measure deflection of the specimen under the top load point.

The installation of this instrumentation is shown in Figure 33, 34 and 35. Figure 36 shows details of the typical CCT node test and instrument location along the node length. A hollow tube will be cast into every specimen to allow access to the head for slip measurements. The dial gauge will be connected to headed bars through a small diameter hollow tube to determine slip of head.

Figure 33 Strain gauges

Figure 34 Dial gauge

Figure 35 Data logger

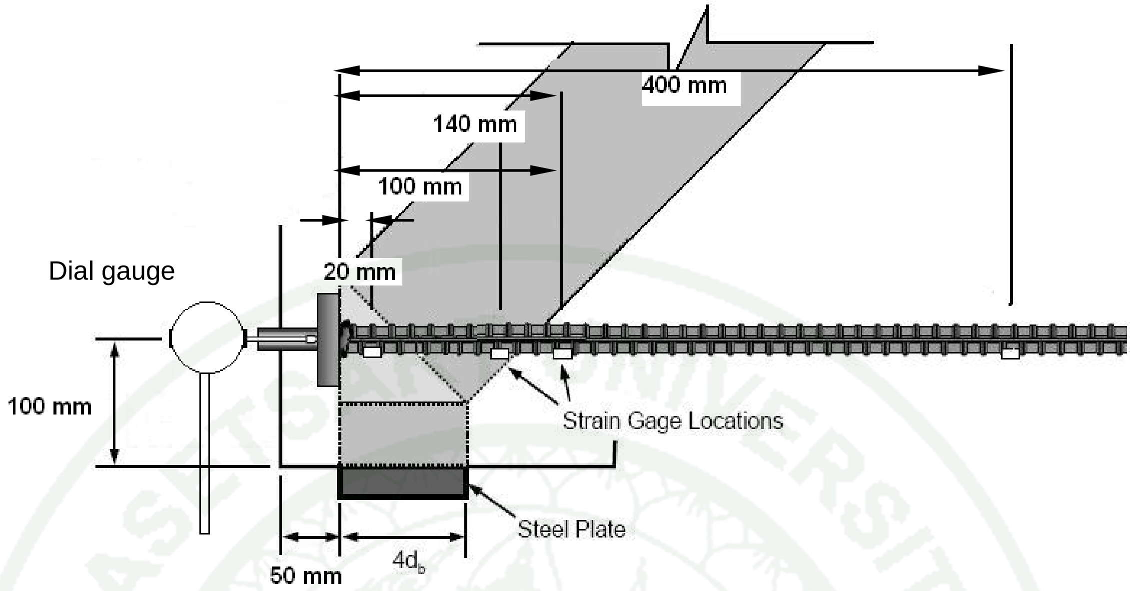

Figure 36 Placement of instrumentation in the nodal region of a typical specimen

Load Setup

The basic load setup for the CCT node specimens is pictured in Figures 37.

Essentially, the CCT node specimen is a deep beam that rests on two bearing supports.

Figure 37 A typical CCT node test

A hydraulic ram will exert load through a top bearing plate. The ram reacts against a steel cross-frame that is tied into the floor.

Testing Procedure

1. Pre-test preparation of the specimen

1.1. Preparation for testing involved

1.1.1. attach the top and bottom bearing plates. A 1 inch thick steel bearing plates will be used, with the full width of the specimen. The top and rear-bottom plates are each 6db long for all tests. The front bottom plate (the critical CCT node plate) is either 4db in length for all tests as shown in Figure 43. The bearing plates will be attached to the specimen with plaster. The plaster provides a uniform bearing between the plate and the concrete surface allowing for an even transfer of stress.

1.1.2. install the dial gauge for slip measurements of the head as shown in Figure 45.

1.1.3. draw the gridline in the nodal zone on the sides of the specimen in order to facilitate understanding the cracking patterns and provide a reference for picture taking.

1.2. Placing specimen

After the pre-test preparation, the specimen will be placed into position within the load frame (the top crosspiece was removable for this purpose) and the load ram and hemispherical head will be placed into position on the top of the specimen.

1.3. Install instrumentation

All instrumentation will be connected to the data acquisition equipment or data logger as shown in Figure 42 and 44 and a computerized check of the circuits is conducted.

2. Start testing

Once the instrumentation is properly installed, recheck the position of specimen and equipment to make sure it is located at the designed position and then start loading.

Load at CCT Node Support

The reading applied point load (P) and the calculated reaction load at front and rear support are characterized in Figure 38.

$$P\ max = \frac{112.5\ P}{150} \qquad P\ max = 0.75\ P$$

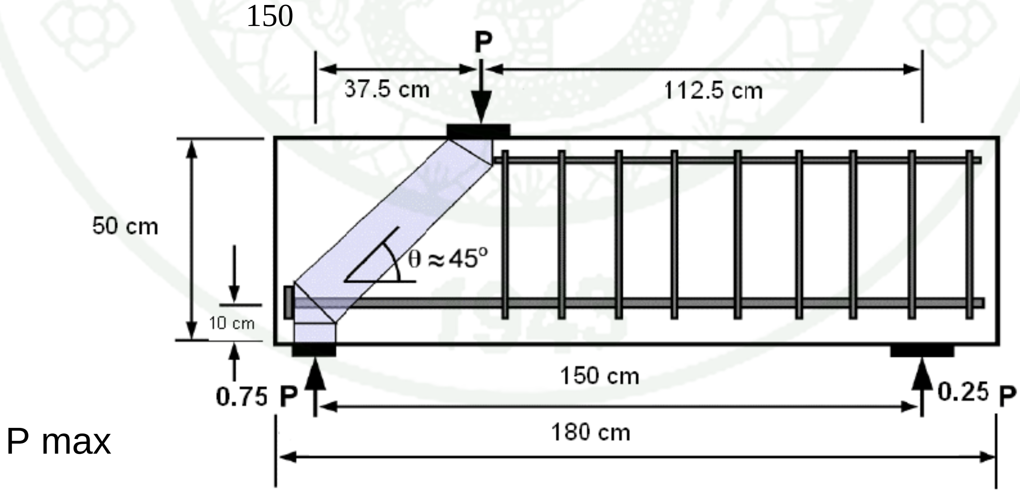

Figure 38 Typical CCT node specimen under applied load P

Figure 39 Strain gauges installation along bars

Figure 40 Strain gauges installation along bars

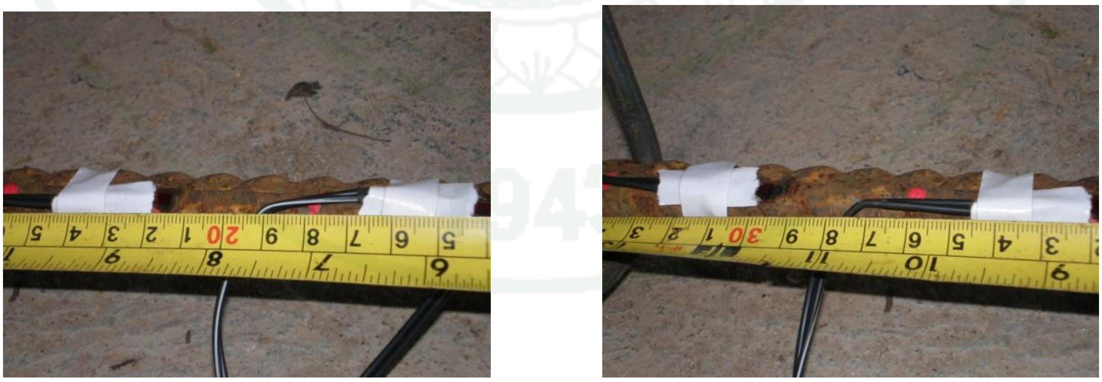

Figure 41 Strain gauges installation along bars

Figure 42 Loading specimen and monitoring

Figure 43 Steel plates at support

Figure 44 Strain monitoring devices

Figure 45 Data logger and dial gauges

EXPERIMENTAL RESULTS

Material Test Result

Concrete

Two cube specimens were cast for each cast. Mechanical properties of harden concrete (Compressive strength) of two casts were determined as per ASTM Standard C39/C39M-99 (American Society for Testing and Materials, 1999). Table 9 and 10 list the measured properties of two casts of concrete.

Table 9 Hardened concrete properties

Cast number	Sample number	Theoretical compressive strength	Cast date	Age (days)
1	1-1	24.5 MPa	22/11/2010	28
	1-2	24.5 MPa	22/11/2010	28
2	2-1	31.4 MPa	22/11/2010	28
	2-2	24.5 MPa	22/11/2010	28

Table 10 Concrete compressive strength

Cast number	Sample number	Ultimate load (kg)	Compressive strength cube	Compressive strength cylinder		Average cylinder compressive strength
1	1-1	60,149	267 ksc	237 ksc	23.2 MPa	23.15 MPa
	1-2	59,890	266 ksc	236 ksc	23.1 MPa	
2	2-1	78,816	350 ksc	310 ksc	30.4 MPa	30.6 MPa
	2-2	79,853	355 ksc	314 ksc	30.8 MPa	

Rebar Tensile Test

Thai rebar grade SD40 diameter 20 mm and 32 mm were tested as per ASTM A370-09 (American Society for Testing and Materials, 2009) to evaluate the mechanical properties as listed in table 11.

Table 11 Rebar mechanical properties

Rebar size	Specimen number	Steel grade	Area (mm^2)	Yield load (kN)	Ultimate load (KN)	Yield strength (MPa)	Tensile strength (MPa)
20	20-1	SD40	314.2	141	200	449.6	636.4
	20-2	SD40	314.1	141	200	449.8	637.8
	Average			141	200	449.7	637.1
32	32-1	SD40	804.3	359	510	446.8	634.6
	32-2	SD40	804.3	360	512	447.2	636.0
	Average			359	511	447.0	635.3

Table 12 Strain gauges location

Item	Specimen ID	Bar size	Head type	Relative head area	Strain gauge location (mm)			
					1	2	3	4
1	U-20-240-4.32-B-1/1	20	BARTEC with circular dh= 48 mm	4.32	20	140	260	420
2	U-20-240-4.32-B-1/2	20	BARTEC with circular dh= 48 mm	4.32	20	120	260	420
3	U-20-240-9.59-G-1/1	20	GRIPTEC with circular dh= 70 mm	9.59	20	100	140	300
4	U-20-240-9.59-G-1/2	20	GRIPTEC with circular dh= 70 mm	9.59	20	100	140	300
5	U-20-240-4.10-G-1/1	20	GRIPTEC with circular dh=52 mm	4.10	20	100	140	220
6	U-20-240-4.10-G-1/2	20	GRIPTEC with circular dh=52 mm	4.10	20	100	140	220
7	U-20-240-0.00-H-1/1	20	Hooked 90˚	0.00	20	140	225	355
8	U-20-240-0.00-H-1/2	20	Hooked 90˚	0.00	20	140	225	355
9	U-20-320-4.32-B-1/1	20	BARTEC with circular dh= 48 mm	4.32	20	140	260	420
10	U-20-320-4.32-B-1/2	20	BARTEC with circular dh= 48 mm	4.32	20	140	260	420
11	U-20-320-9.59-G-1/1	20	GRIPTEC with circular dh= 70 mm	9.59	20	100	140	300
12	U-20-320-9.59-G-1/2	20	GRIPTEC with circular dh= 70 mm	9.59	20	100	140	300
13	U-20-320-4.10-G-1/1	20	GRIPTEC with circular dh=52 mm	4.10	20	100	140	300
14	U-20-320-4.10-G-1/2	20	GRIPTEC with circular dh=52 mm	4.10	20	100	140	300

Table 12 (Continued)

Item	Specimen ID	Bar size	Head type	Relative head area	Strain gauge location (mm)			
					1	2	3	4
15	U-20-320-0.00-H-1/1	20	Hooked 90˚	0.00	20	140	225	355
16	U-20-320-0.00-H-1/2	20	Hooked 90˚	0.00	20	140	225	355
17	U-32-240-9.68-G-1/1	32	GRIPTEC with circular dh= 110 mm	9.68	20	100	140	300
18	U-32-240-9.68-G-1/2	32	GRIPTEC with circular dh= 110 mm	9.68	20	100	140	300

Cracking Behavior

Cracking of specimen was closely monitored and the applied load was also recorded at each cracking to monitor the cracking behavior. The results are listed in table 13.

Table 13 Cracking and ultimate load

Case No.	Description	P_{max} at support (kN)			
		1st crack	2nd crack	3rd crack	At failure
1	Bartec small head dia 20 mm, f'c = 23.5 MPa U-20-240-4.32-B-1/1-2	60.68	110.32	141.58	175.27
2	Griptec large head dia 20 mm f'c = 23.5 MPa U-20-240-9.59-G-1/1-2	30.76	72.50	85.36	154.80
3	Griptec small head dia 20 mm f'c = 23.5 MPa U-20-240-4.10-G-1/1-2	54.8	73.55	86.94	123.72
4	90° hooked dia 20 mm f'c = 23.5 MPa U-20-240-0.00-H-1/1-2	34.1	75.82	87.06	118.39
5	Bartec small head dia 20 mm, f'c = 31.4 MPa U-20-320-4.32-B-1/1-2	66.19	80.90	110.32	213.04

Table 13 (Continued)

Case No.	Description	P_{max} at support (kN)			
		1st crack	2nd crack	3rd crack	At failure
6	Griptec large head dia 20 mm f'c = 31.4 MPa U-20-320-9.59-G-1/1-2	74.81	86.94	121.36	204.82
7	Griptec small head dia 20 mm f'c = 31.4 MPa U-20-320-4.10-G-1/1-2	38.69	55.75	107.75	148.79
8	90° hooked dia 20 mm f'c = 31.4 MPa U-20-320-0.00-H-1/1-2	42.50	73.55	98.60	161.59
9	Griptec large head dia 32 mm f'c = 23.5 MPa U-32-240-9.68-G-1/2	55.16	73.55	91.90	161.59

The crack pattern for a CCT node specimen with a Griptec large headed 20 mm-diameter tie bar (relative head area = 9.59), strut angle of 45 degrees, and *fc′* of 23.5 MPa is shown in Figure 46, and is typical of the node tests. First cracking occurred at the point of maximum moment (directly beneath the load point). The measured front bearing reaction *P* was 32.4 kN Subsequent cracks formed at regular intervals toward the nodal zone (Crack 2 at *P* = 74.64 kN and Crack 3 at *P* = 86.48 kN) until the arch mechanism was fully developed and failure at maximum load P = 155.89 kN.

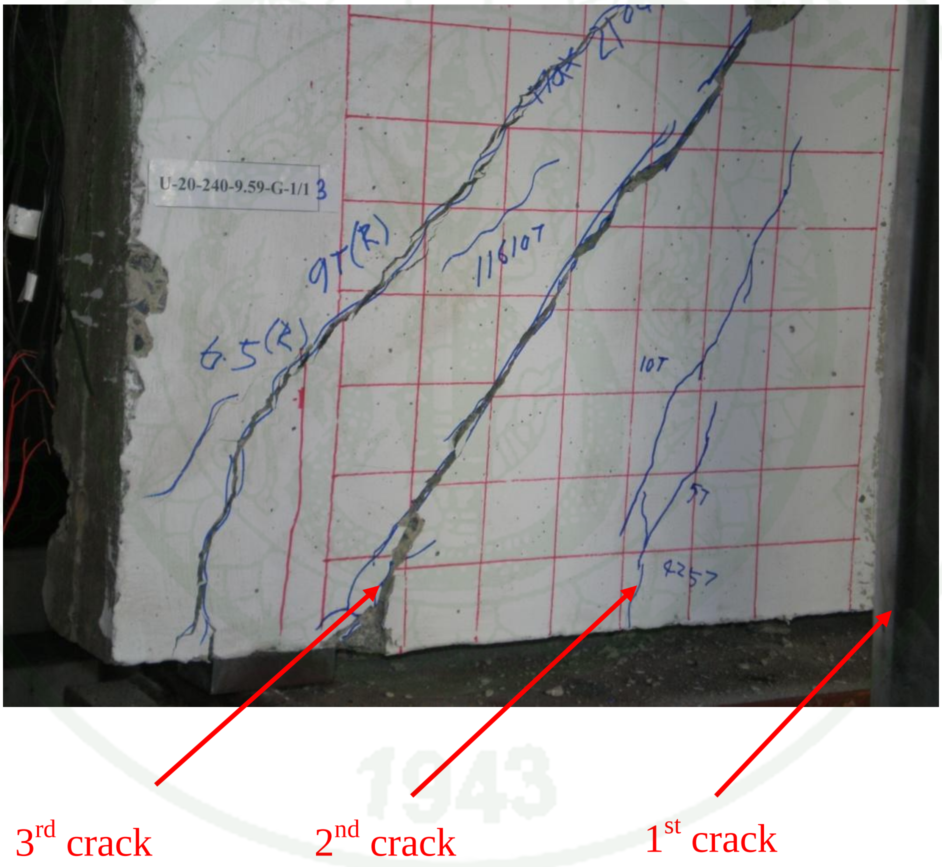

Figure 46 Cracking development of specimen Griptec large head dia 20 mm U-20-240-9.59-G-1/1

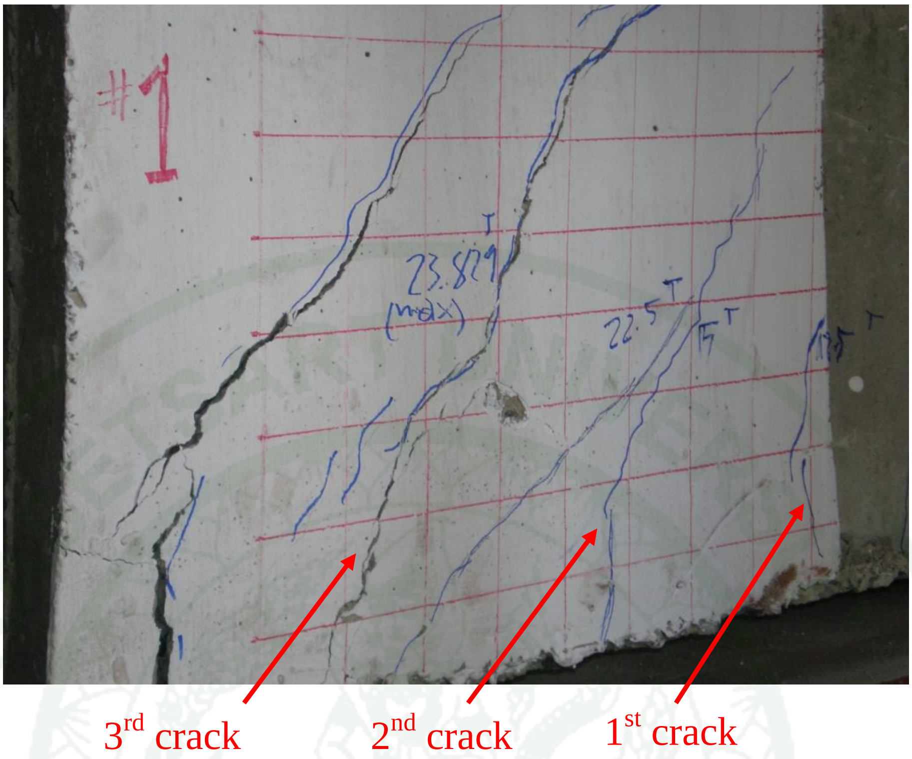

Figure 47 Cracking development of specimen Bartec small head dia 20 mm U-20-240-4.32-B-1/1

Similarly the crack pattern for a CCT node specimen with a Bartec small headed 20 mm-diameter tie bar (relative head area = 4.32), strut angle of 45 degrees, and *fc′* of 23.5 MPa is shown in Figure 47. First cracking occurred at the point of maximum moment (also directly beneath the load point) and the measured front bearing reaction *P* was 60.68 kN. The 2nd crack formed toward the nodal zone at the measured CCT nodal load, P = 110.32 kN and subsequently horizontal cracks formed between 1st and 2nd crack. When the measured load reached at P = 141.58 MPa the 3rd crack is immediately formed at the nodal face.

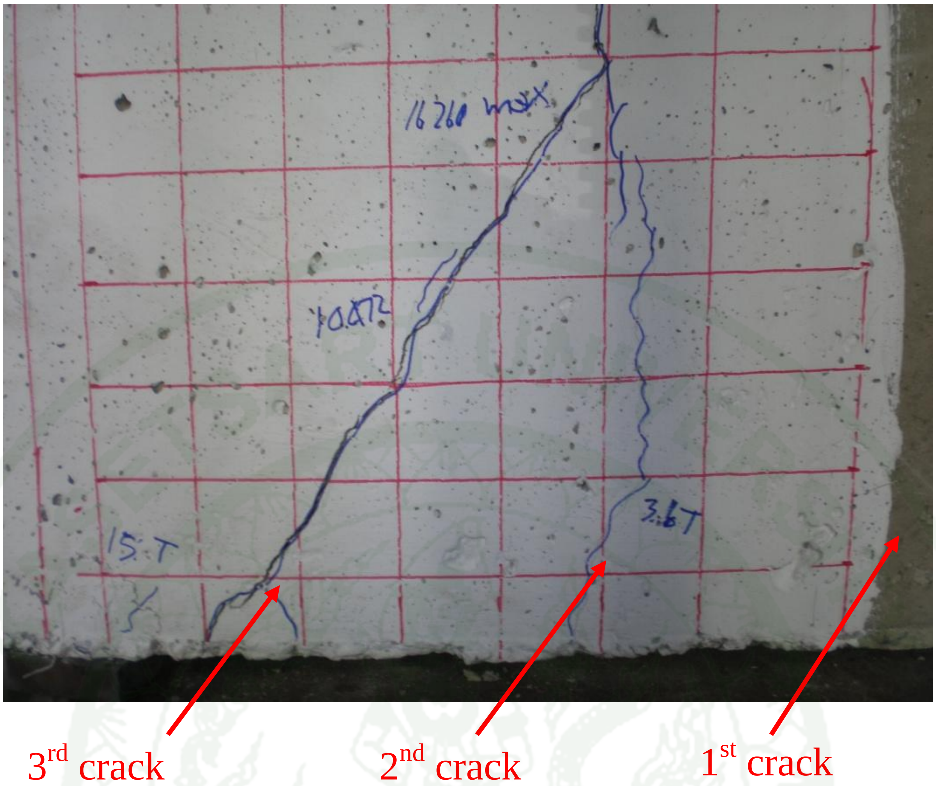

Figure 48 Cracking development of specimen 90° hooked dia 20 mm U-20-240-0.00-H-1/1

The crack pattern for a CCT node specimen with a 90° hooked 20 mm-diameter tie bar (relative head area = 0.00), strut angle of 45 degrees, and *fc′* of 23.5 MPa is shown in Figure 48. First cracking occurred at the point of maximum moment (also directly beneath the load point) and the measured front bearing reaction *P* was 34.10 kN. The 2nd crack formed toward the nodal zone at the measured CCT nodal load, P = 75.82 kN and subsequently horizontal cracks formed between 1st and 2nd crack. When the measured load reached at P = 87.06 MPa the 3rd crack is immediately formed at the nodal face.

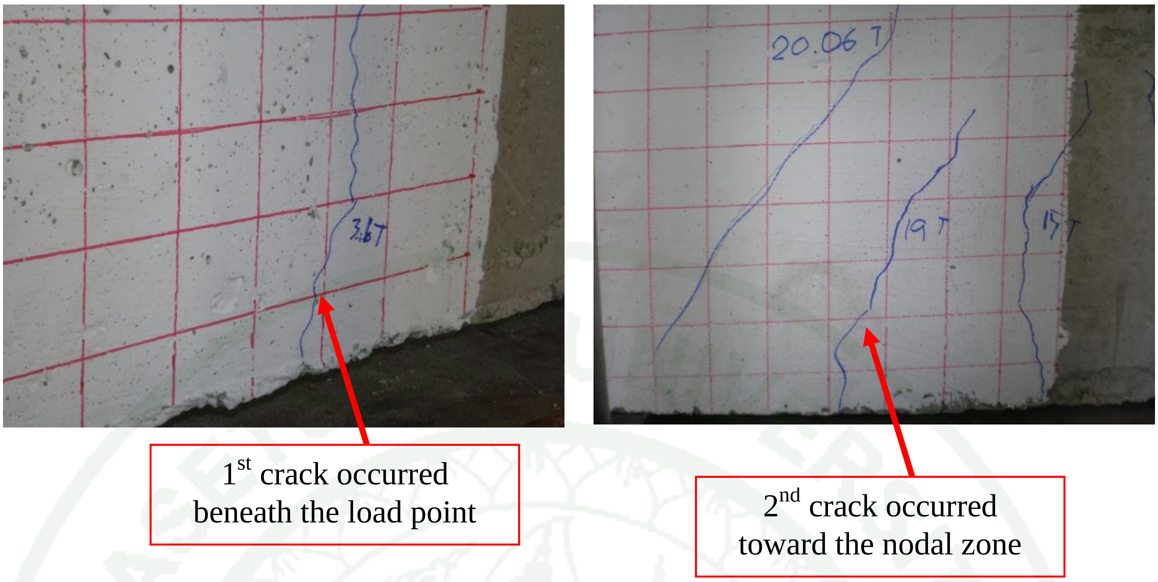

Figure 49 Cracking pattern development

Cracking development

Generally cracking patterns of all specimens are in the similar form as following as shown in Figure 49 and 50.

1. The first crack formed just under the applied point load.
2. The second crack formed closer toward the CCT nodal zone.
3. The first and second cracks then grew towards the top bearing plate at applied point load.
4. The third crack formed even closer to the CCT nodal zone and grew at an angle parallel to the diagonal strut.
5. The horizontal cracks grew from the second to the third cracks.
6. Brittle failure suddenly occurred and the front portion of specimen split away from the main body.

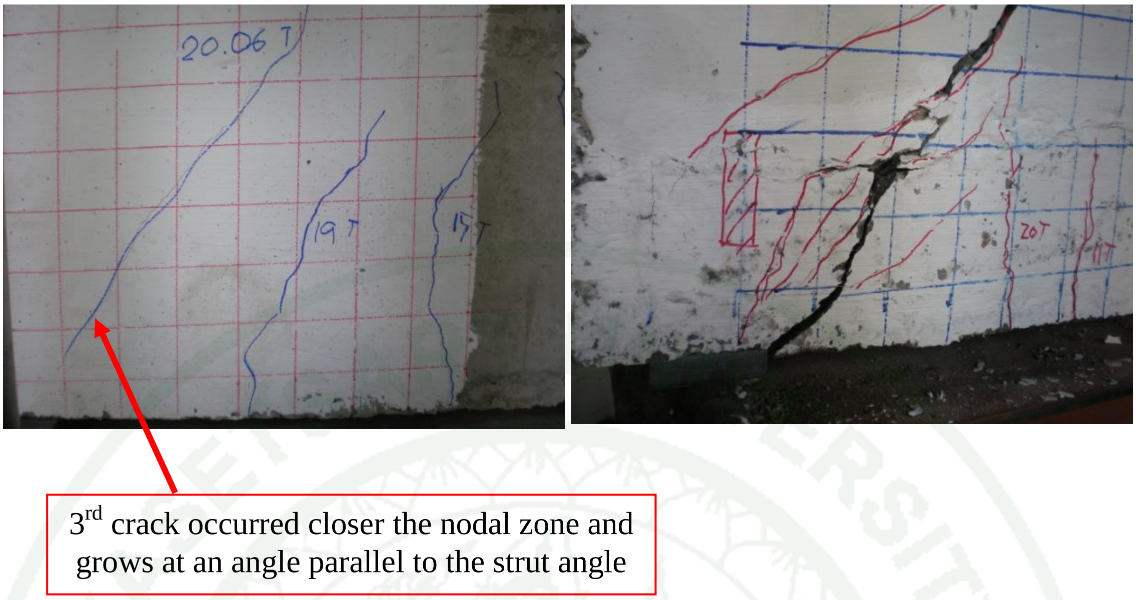

Figure 50 Cracking pattern development

Stress / Strain Development in the Bar

The tension strain of tie bars were measured from the four strain gauges attached along tie bars. The measured strain values for each specimen are listed in appendix table 18-27.

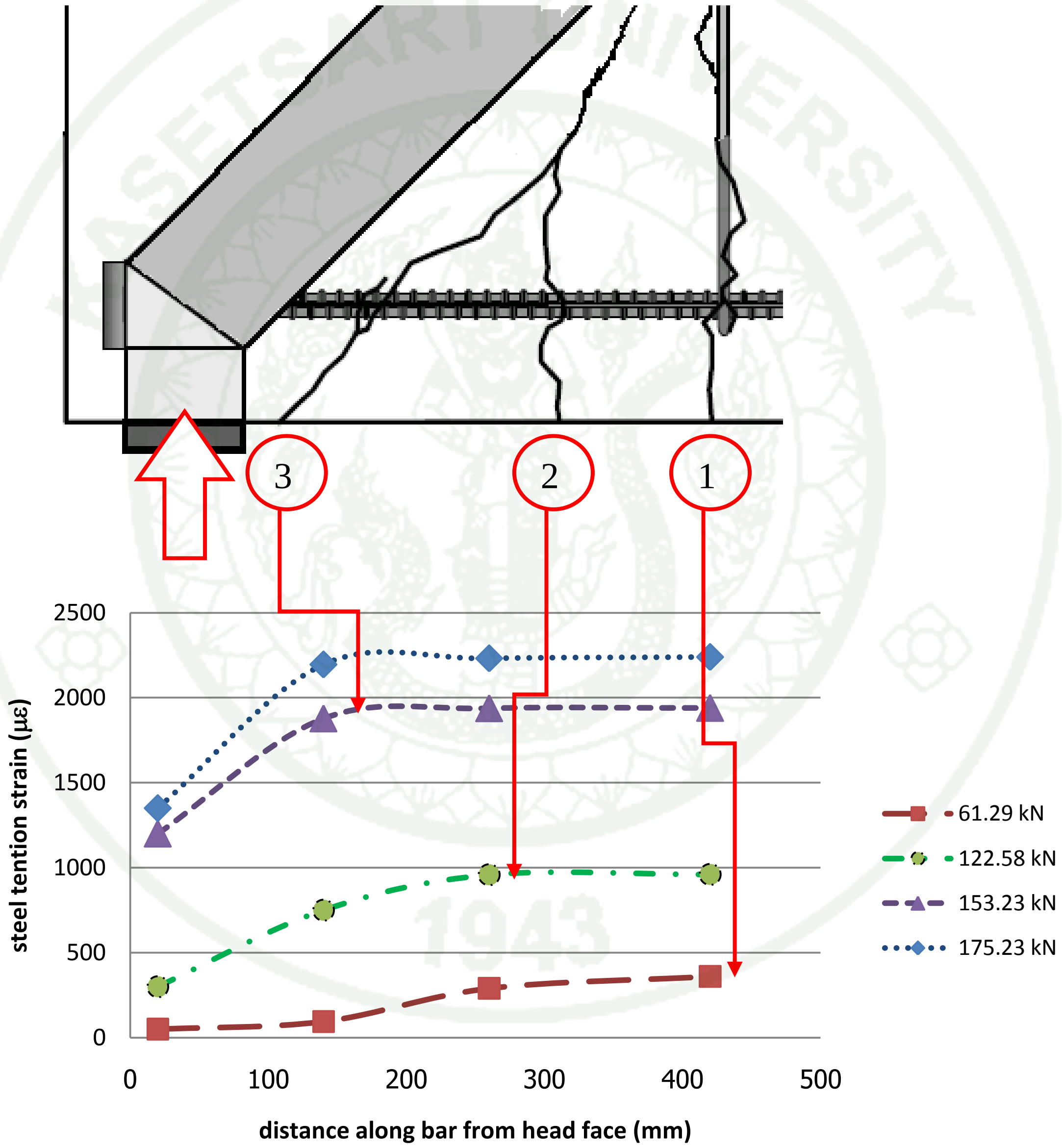

Figure 51 Measured tension strain along the bar for U-20-240-4.32-B-1/1

The strain distribution of specimen U-20-240-B-4.32-1/1 was plotted in Figure 51 and illustrated for a load of 61.29 kN that the largest strains in the bar correlate to the position of 1st crack. At the 2nd crack in the specimen that occurred around a load of 110.32 kN, the strain distribution at 122.58 kN shows that the zone of large tensile strains in the bar had extended to the location of 2nd crack. The third crack in the specimen appeared at a load of 141.58 kNs. The strain distribution at 153.23 kNs shows that the bar was strained beyond yield along nearly the entire gauged length. The final strain distribution at a load of 175.23 kNs shows that the bar had begun yielding. The full yielding of the bar was observed when the load reached 175.23 kNs.

Further to the reading tension strain of bar, the bar stresses were calculated from the measured strain shown in Figure 52. At a load of 61.29 kNs, the maximum stress in the bar was measured at 420 mm from the face of the head. At a load of 122.58 kNs, the maximum stress was reached at 260 mm. At a load of 153.23 kNs and higher, the maximum stress level in the bar was nearly uniform from a point of 140 mm away from the head. The final anchorage of the bar clearly occurred within the first 140 mm, the length roughly from the face of the head to the point where the bar passed out of the diagonal strut. The stresses at 20 mm in from the head provide an illustration of the bar force carried by the head while the stresses at 140 mm give an illustration of the total force in the bar.

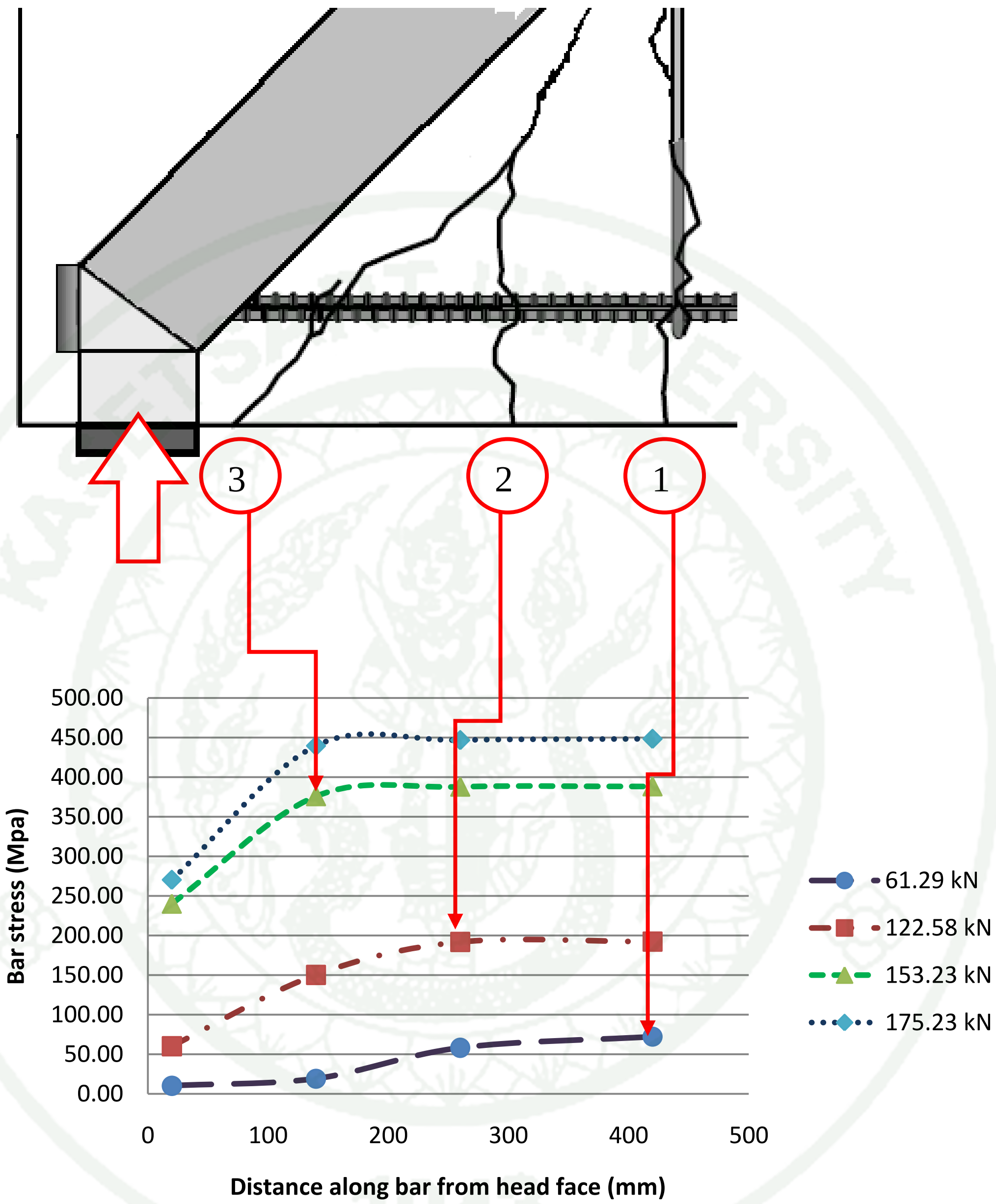

Figure 52 Bar stress development along the bar for U-20-240-4.32-B-1/1

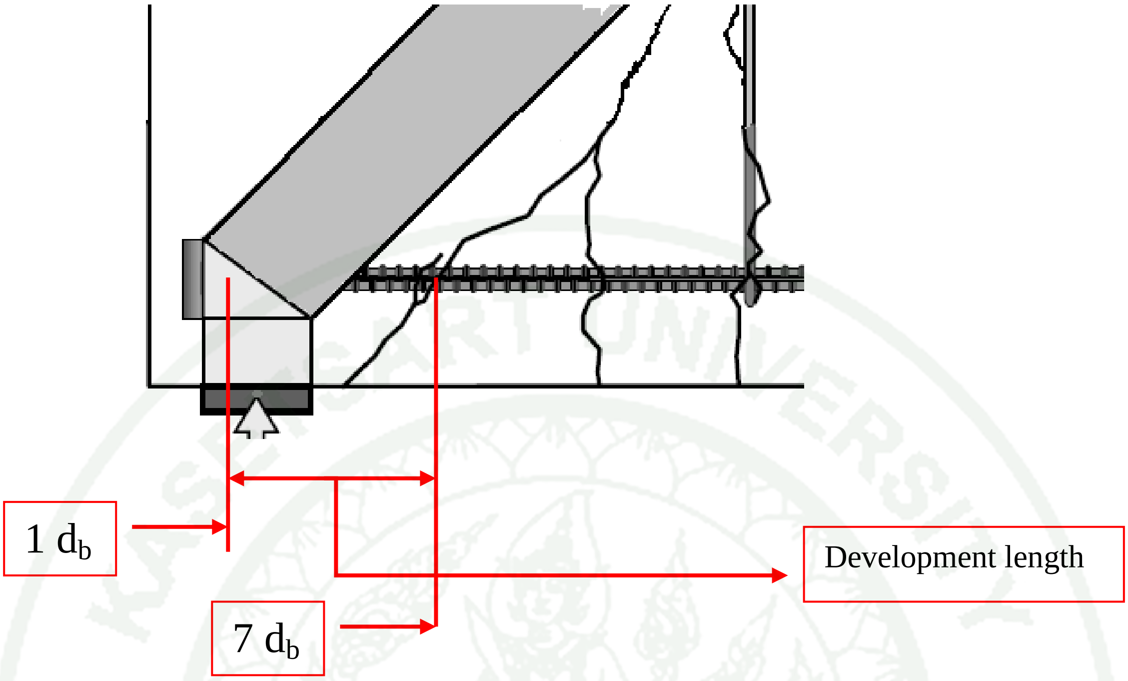

Figure 53 Typical Development length of CCT node

Figure 53 shows the typical development length of headed bar in CCT node that occurred between length 1db and 7db from the head face.

For other specimens, it was similarly illustrated characteristics of measured tension strain and rebar stress along the length from head surface as shown in Figure 54- 69.

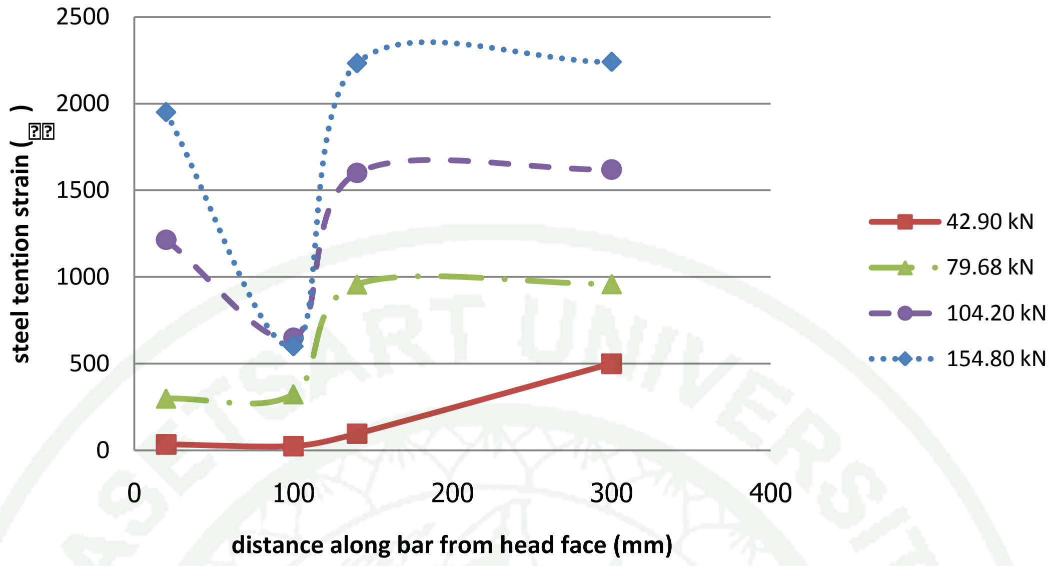

Figure 54 Measured tension strain along the bar for U-20-240-9.59-G-1/1

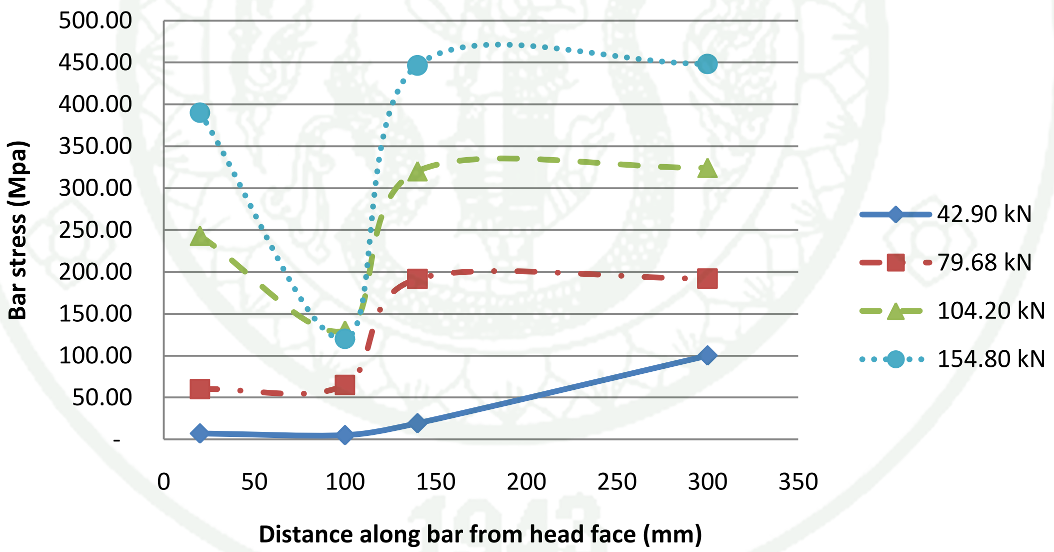

Figure 55 Bar stress development along the bar for U-20-240-9.59-G-1/1

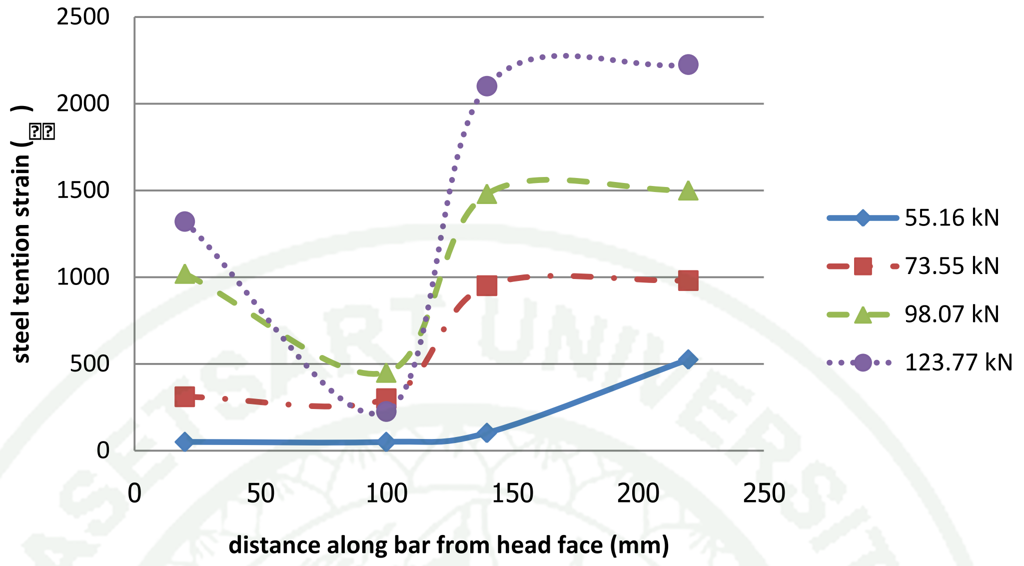

Figure 56 Measured tension strain along the bar for U-20-240-4.10-G-1/2

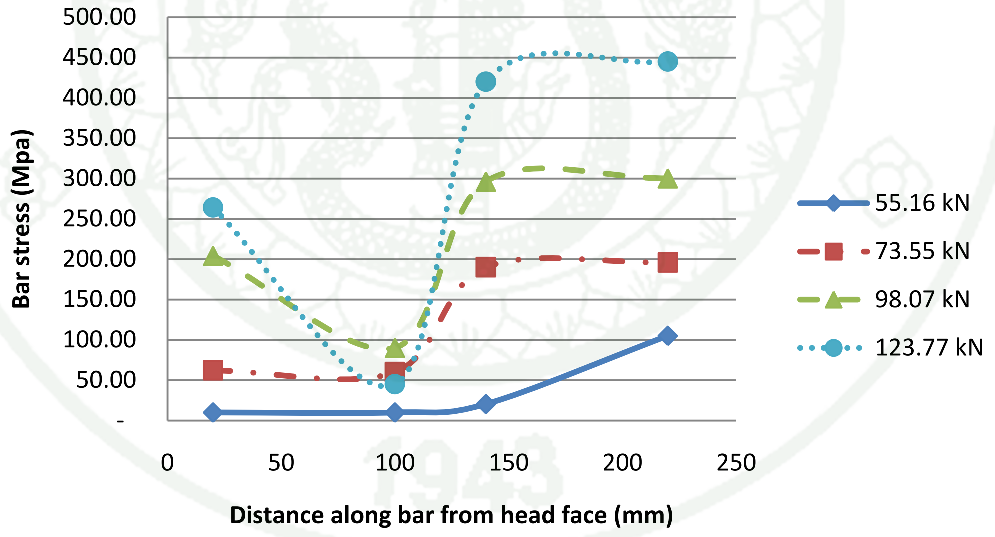

Figure 57 Bar stress development along the bar for U-20-240-4.10-G-1/1

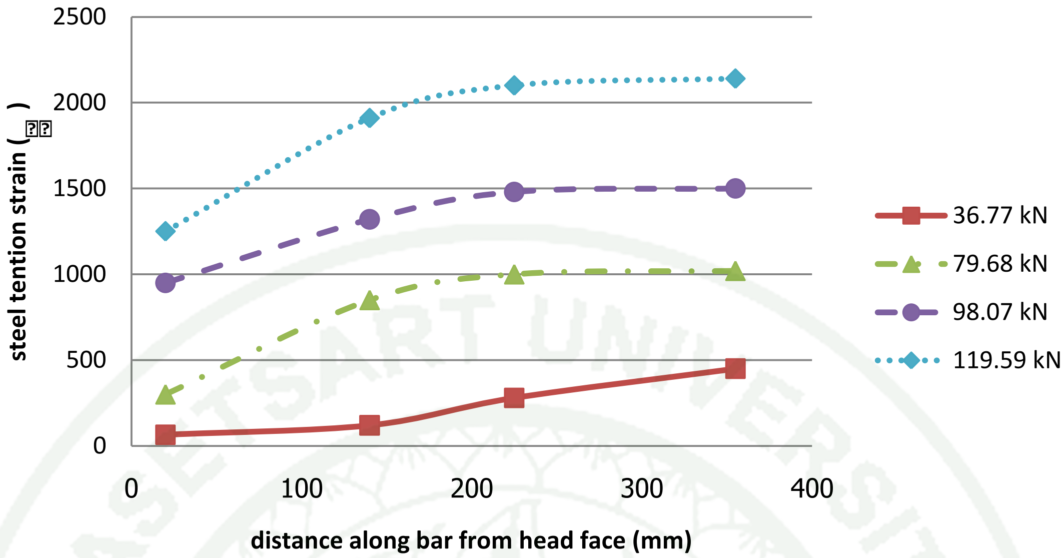

Figure 58 Measured tension strain along the bar for U-20-240-0.00-H-1/2

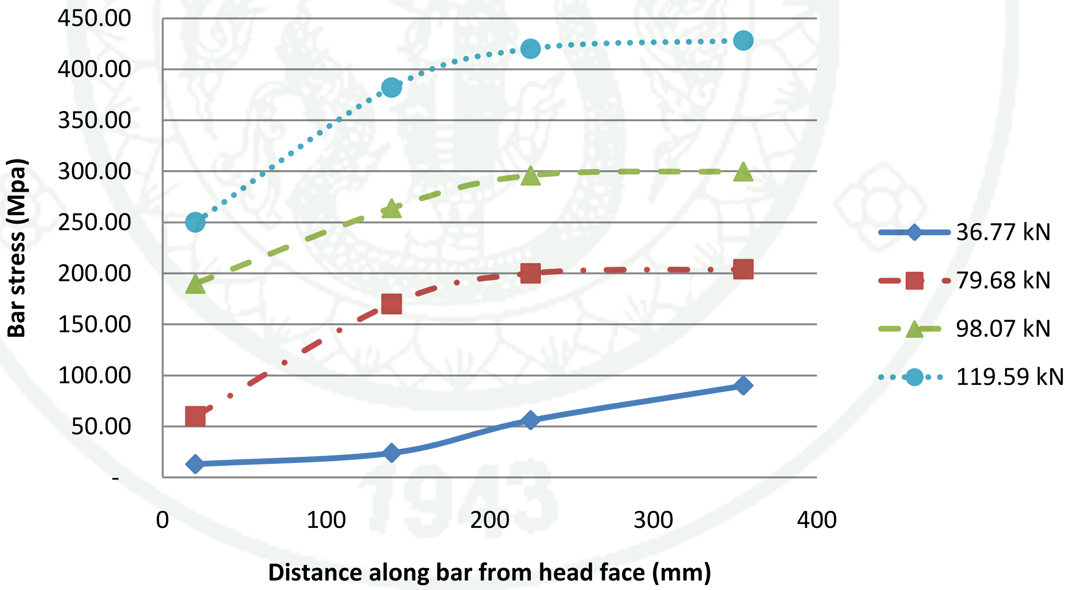

Figure 59 Bar stress development along the bar for U-20-240-0.00-H-1/1

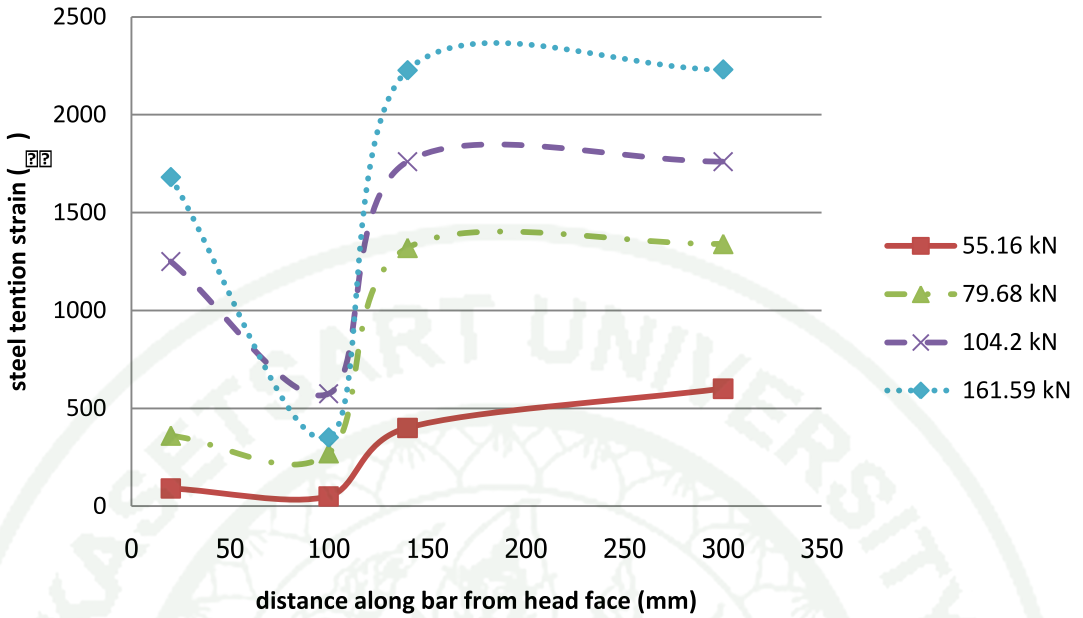

Figure 60 Measured tension strain along the bar for U-32-240-9.59-G-1/1

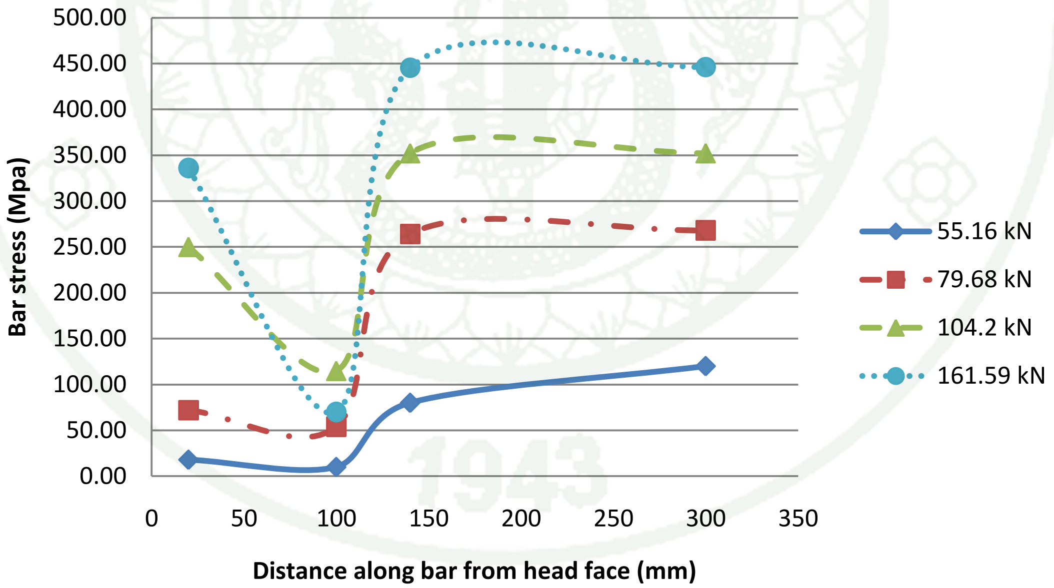

Figure 61 Bar stress development along the bar for U-32-240-9.68-G-1/1

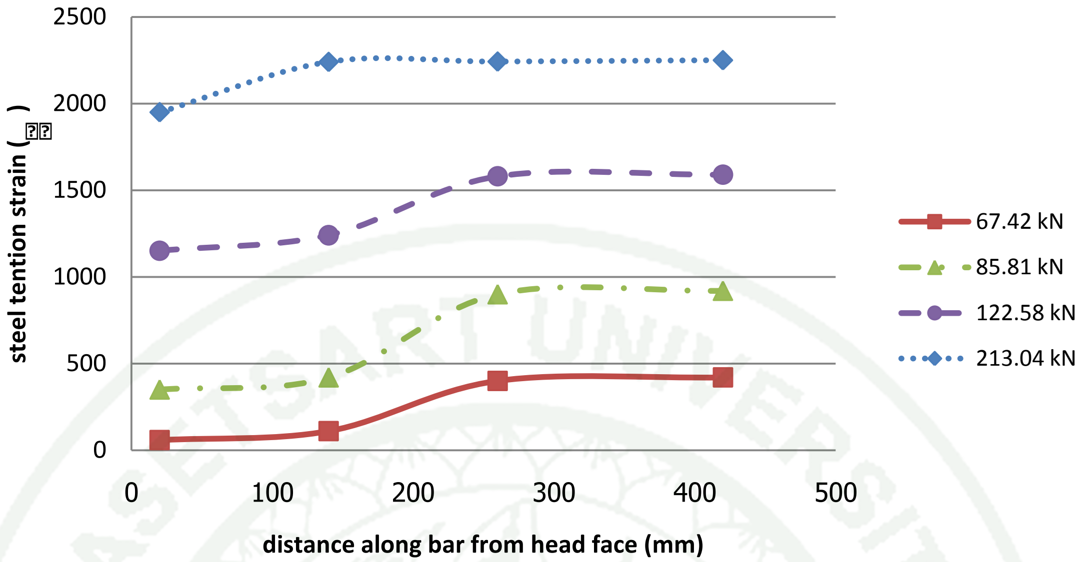

Figure 62 Measured tension strain along the bar for U-20-320-4.32-B-1/1

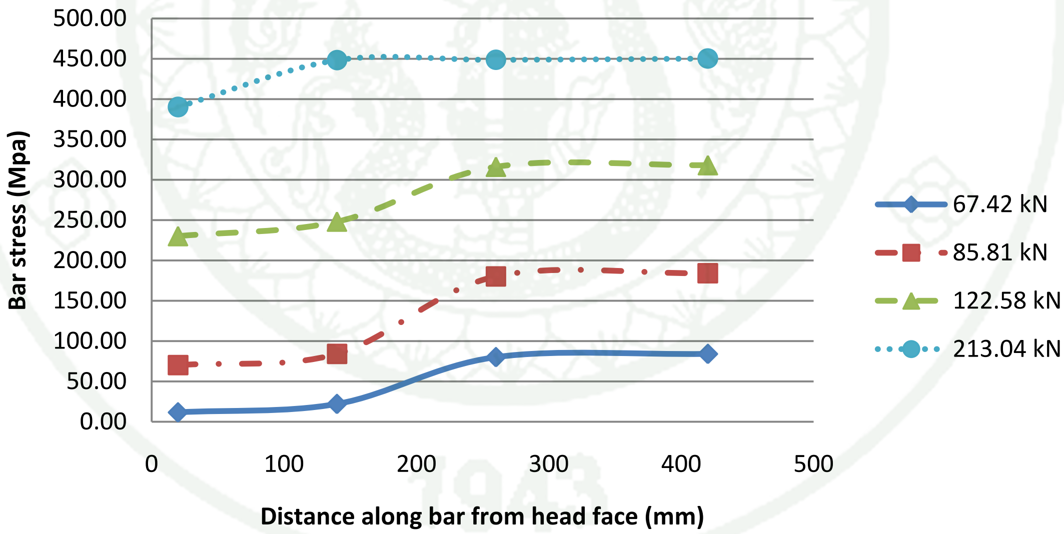

Figure 63 Bar stress development along the bar for U-20-320-4.32-B-1/1

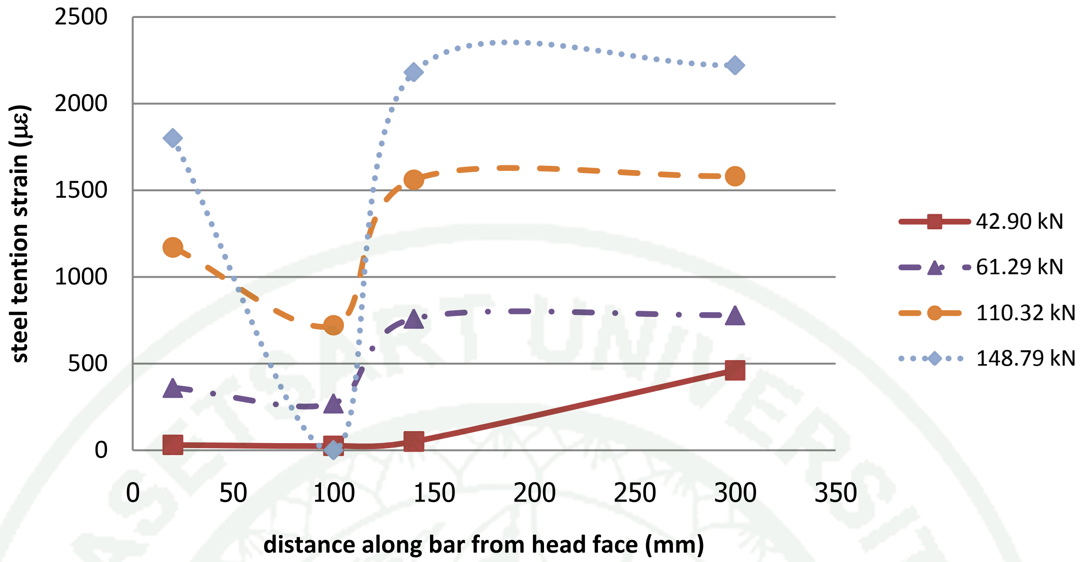

Figure 64 Measured tension strain along the bar for U-20-320-4.10-G-1/2

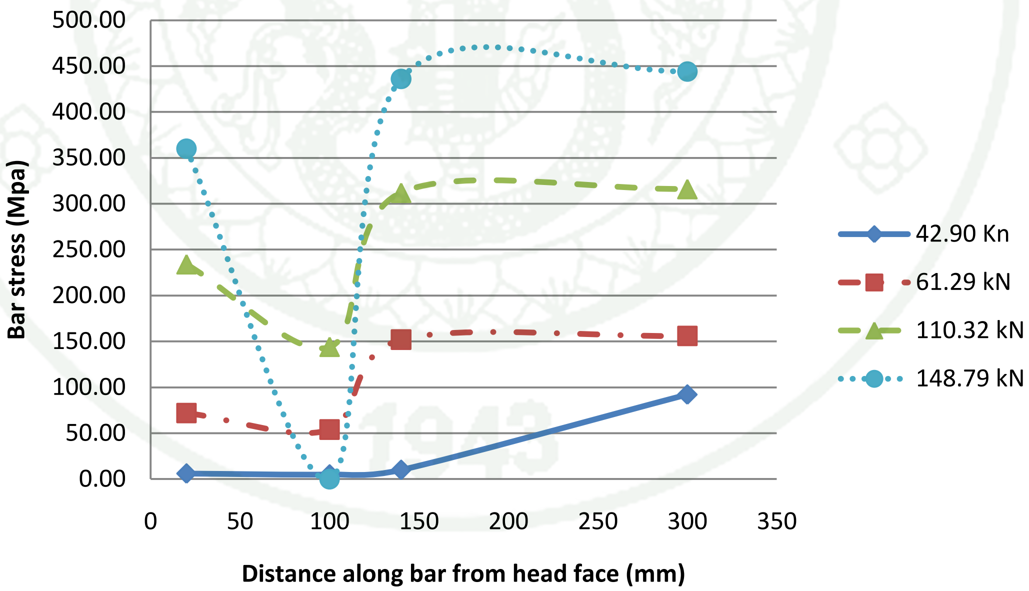

Figure 65 Bar stress development along the bar for U-20-320-4.10-G-1/1

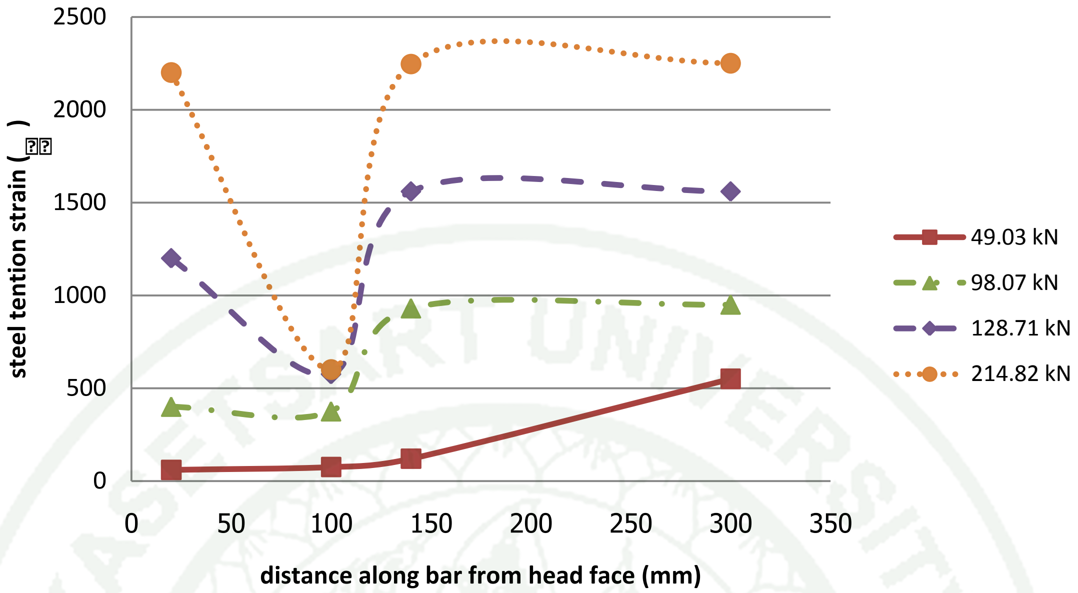

Figure 66 Measured tension strain along the bar for U-20-320-9.59-G-1/2

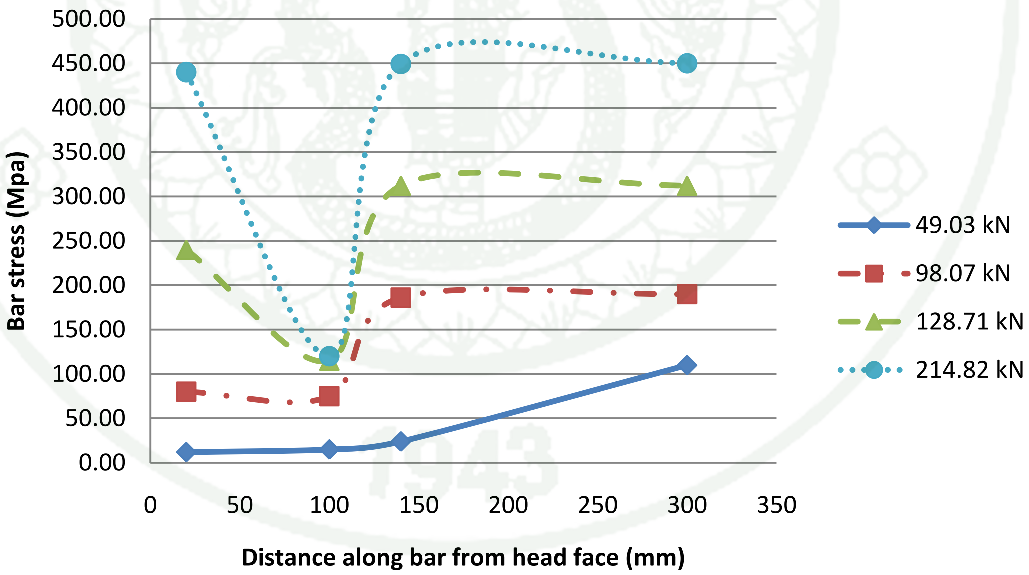

Figure 67 Bar stress development along the bar for U-20-320-9.59-G-1/1

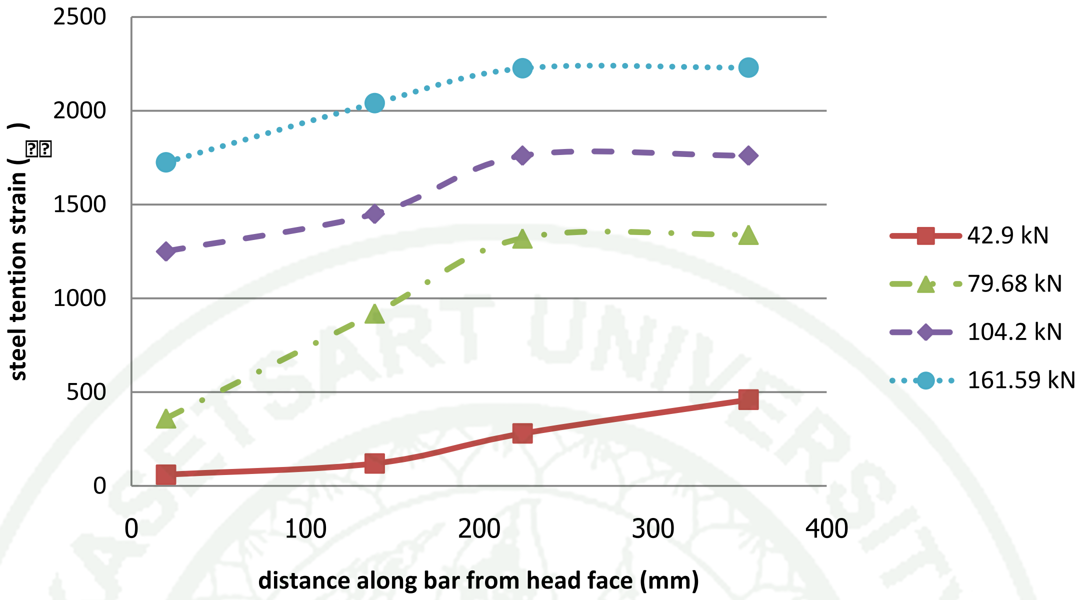

Figure 68 Measured tension strain along the bar for U-20-320-0.00-H-1/1

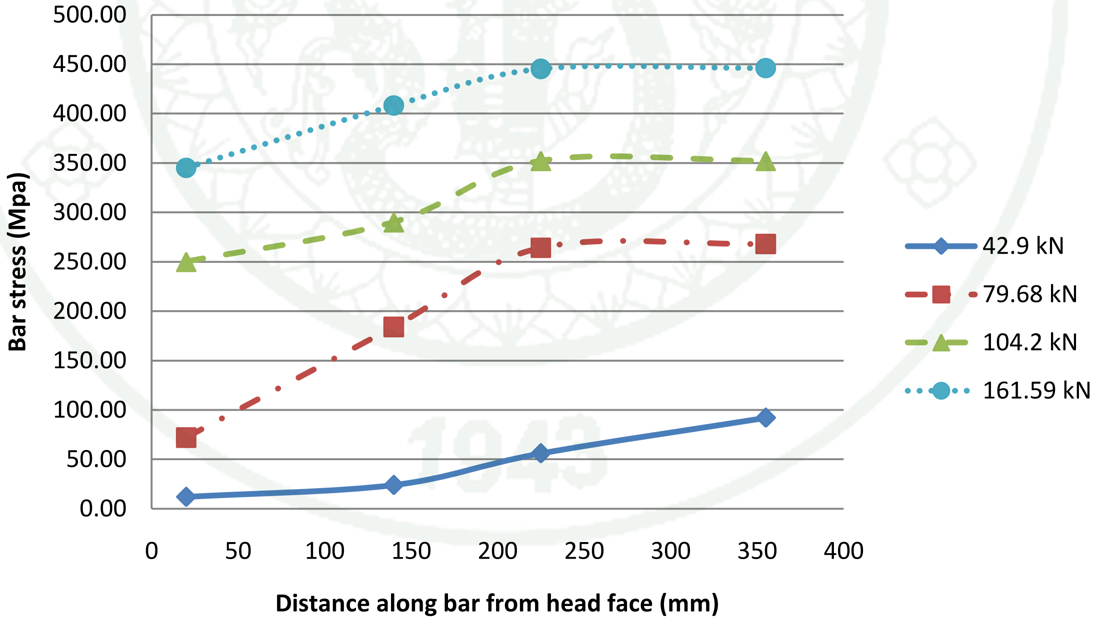

Figure 69 Bar stress development along the bar for U-20-320-0.00-H-1/1

Head Slip

Dial gauge was attached to the front end of beam as shown in Figure 71 and 72. The horizontal displacements of small and large Griptec heads were measured. The dial gauge reading is listed in appendix table 28 and 29.

Head slip : To compare the slip performance the head slips were measured from the variable head sized specimens. The results in Figure 70 is plotted against the bar stress at the head determined from a strain gauge placed at 1*db* from the head face. Data are presented for four specimens with 20 mm diameter tie bars. GRIPTEC small circular shape diameter 52 mm, and GRIPTEC large circular shape diameter 70 mm. Head slip typically did not initiate until cracking development, and then increased rapidly up to the point of failure. It obviously showed the delay of slip initiation and increment was delayed as head size increased.

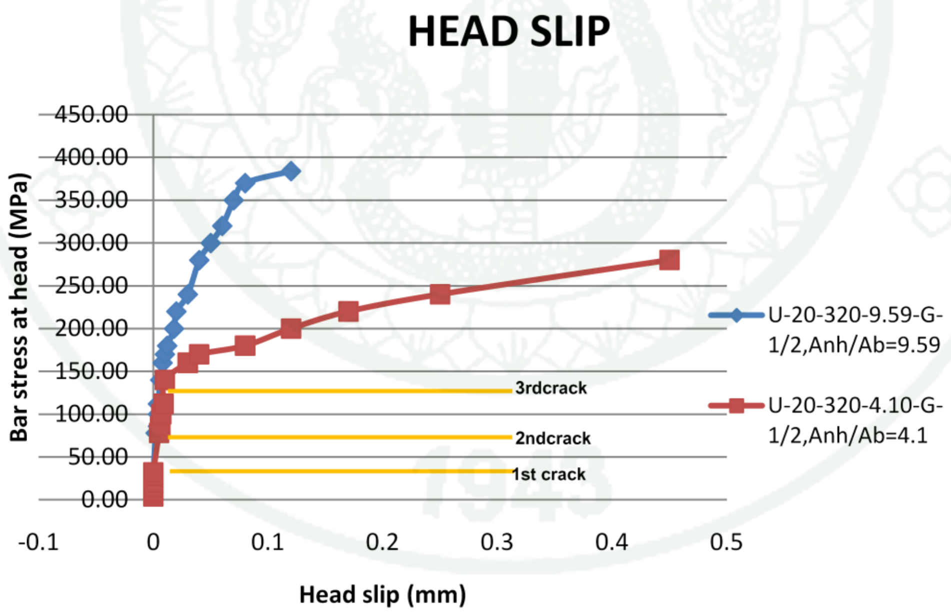

Figure 70 Correlation between Measured Head slip and bar stress at head

Figure 71 Head slip measurement for U-20-320-9.59-G-1/2

Figure 72 Head slip measurement for U-20-320-4.10-G-1/2

Failure Mode

The rupture failure of each specimen was observed after reaching maximum load. All specimens were characterized as strut compressive failure. That means the arch mechanism was fully performed on CCT node and rupture beyond the maximum load value.

The main characteristics of failure are as following.

1. Conical wedge shape of concrete behind the head as shown in Figure 73 – 76.
2. Cracking propagated along the diagonal compressive strut from the front support ahead to applied point load location on top beam as shown in Figure 77 and 78.
3. The left top portion above cracked diagonal plan cleaved apart as shown in Figure 79 and 80.
4. Spall failure of 90° hooked bar as shown in Figure 81.

Figure 73 Conical wedge shape behind head surface

Figure 74 Conical wedge shape behind head surface

Figure 75 Conical wedge shape behind head surface

Figure 76 Conical wedge shape behind head surface

Figure 77 Diagonal cracked plane

Figure 78 Diagonal cracked plane

Figure 79 Left top portion cleaved part

Figure 80 Left top portion cleaved part

Figure 81 Spall failure of 90° hooked bar

Contribution of Bond

To observe the correlation between bond stress and head bearing stress, the contributions to total bar stress provided by bond and head bearing in Specimen U-20-320-9.59-G-1/1 and U-20-320-4.10-G-1/1 were observed and plotted in Figure 82 and Figure 83. The stress from bond was measured over the bar length from 1db to 7db. Figure 83 shows that the contribution from bond peaked and then began to decrease before the contribution from head bearing reached its maximum capacity.

To determine the bond contribution to anchorage capacity, average bond stress was determined for the CCT node tests by using the difference between bar stress at 1*db* from the head and 7*db* from the head. The early rise in the bond component shows the bar force was initially transferred to the concrete primarily by bond. As the bar force increased, however, the bond component leveled off, and further increases in bar stress were transferred by head bearing. Eventually the bond contribution declined while the head bearing component rose rapidly. Peak bond stress did not occur simultaneously with peak head bearing. At failure, the anchorage capacity of the headed bar was provided by peak head bearing plus reduced bond.

Plots between total stress and bearing capacity and bond stress are presented in Figure 82 and Figure 83 to compare the effect of relative head area. Larger heads increased head bearing but resulted in larger decreases in the bond component. Increasing relative head area enlarges the gap between ultimate head bearing capacity and reduced bond.

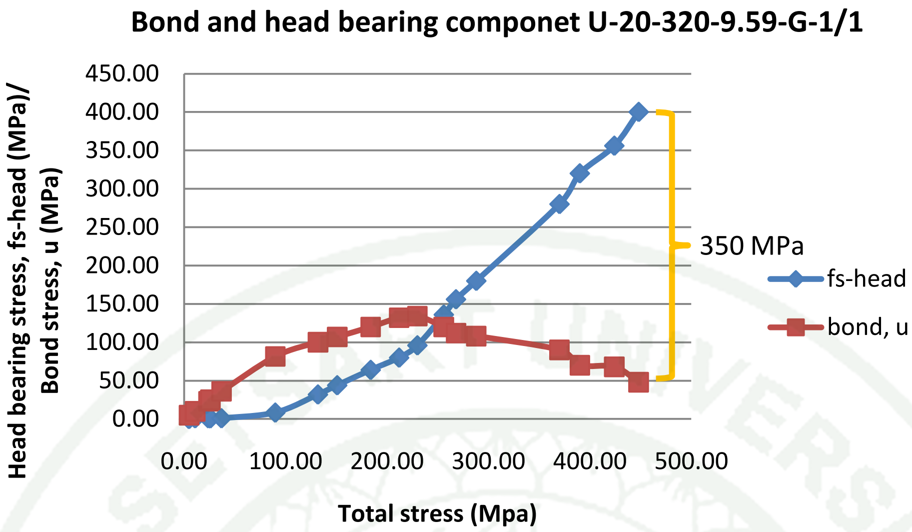

Figure 82 Bond and head bearing components for U-20-320-9.59-G-1/1

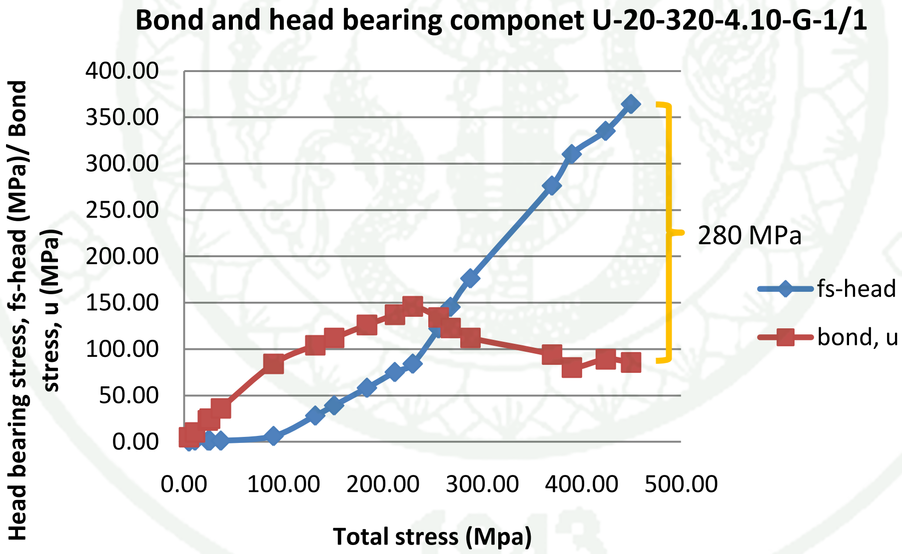

Figure 83 Bond and head bearing components for U-20-320-4.10-G-1/1

Obstruction Effect

As stipulated in ACI 318 (2008) clause 3.5.9 Headed deformed bars shall conform to ASTM A970 / A970M-09 (2009) and obstructions or interruptions of the bar deformations, if any, shall not extend more than *2db* from the bearing face of the head.

Reading from the steel tension strain in Figure 86, considering specimen U-20-320-4.10-G-1/2 the strain gauge reading attached on Griptec sleeve surface at the location 100 mm from the head face, at certain loads the strain reading significantly declined. This means the stress at this location declined as shown in Figure 89. However at location 1d (20 mm) and 7d (140 mm), it obviously showed that at the head bearing (1d) and the critical face of CCT node (7d) are perfectly performed as Bartec headed bar without obstruction U-20-320-4.32-B-1/1 as shown in Figure 85 and Figure 88.

It was similar with the Griptec large head specimen U-20-320-9.59-G-1/2 as shown in Figure 87 and 90.

Figure 83 Obstruction deformation of Griptec headed bar

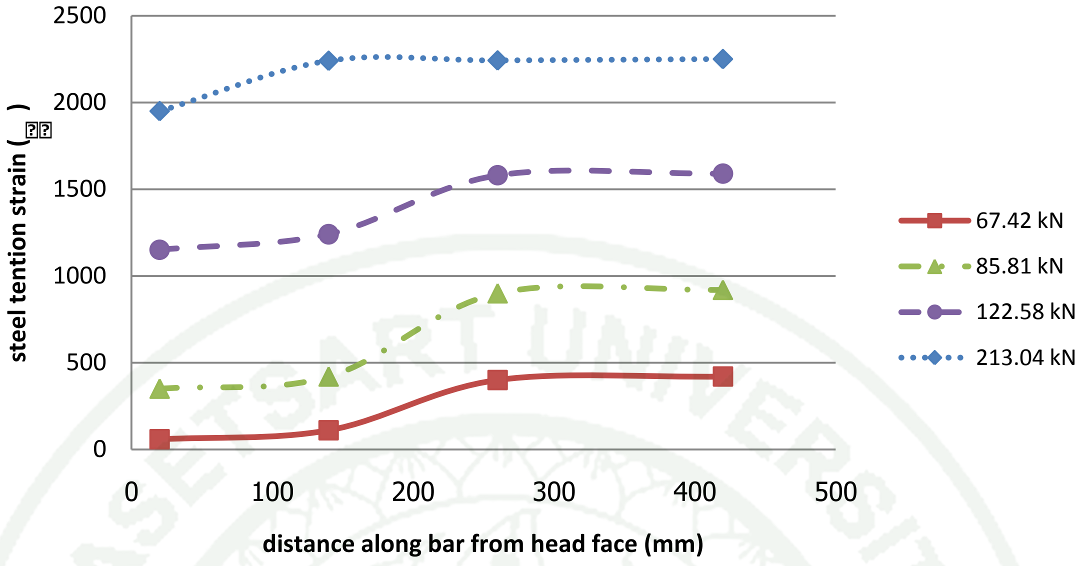

Figure 85 Tension strain along the bar for Bartec small head U-20-320-4.32-B-1/1

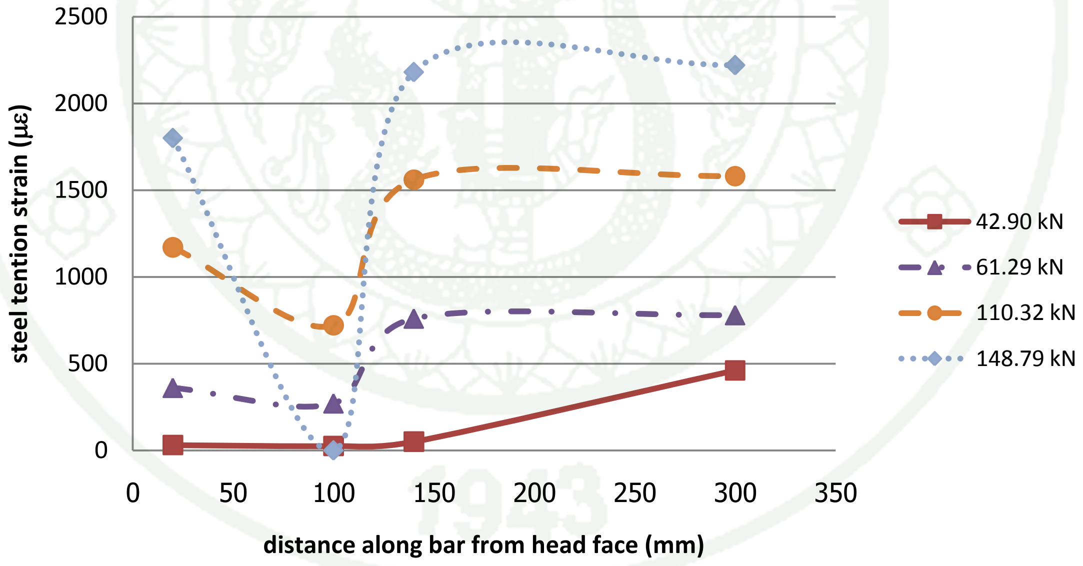

Figure 86 Tension strain along the bar for Griptec small head U-20-320-4.10-G-1/2

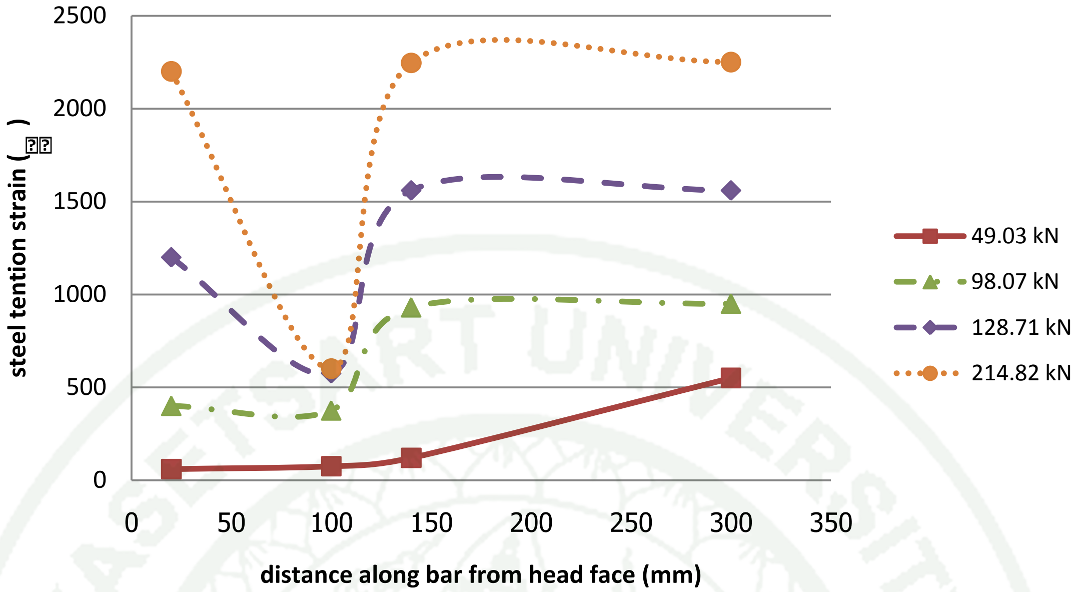

Figure 87 Tension strain along the bar for Griptec large head U-20-320-9.59-G-1/2

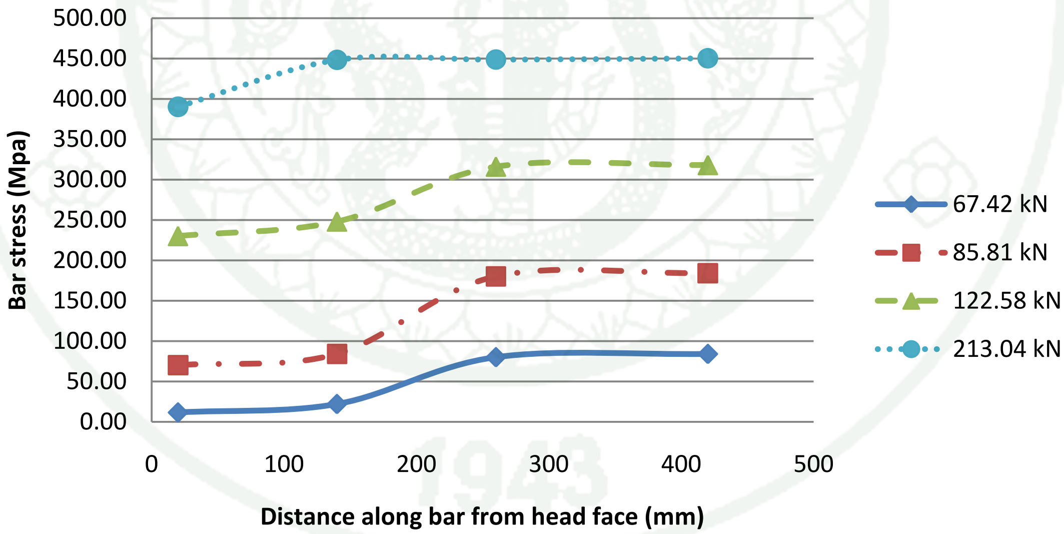

Figure 88 Bar stress along the bar for Bartec small head U-20-240-4.32-B-1/1

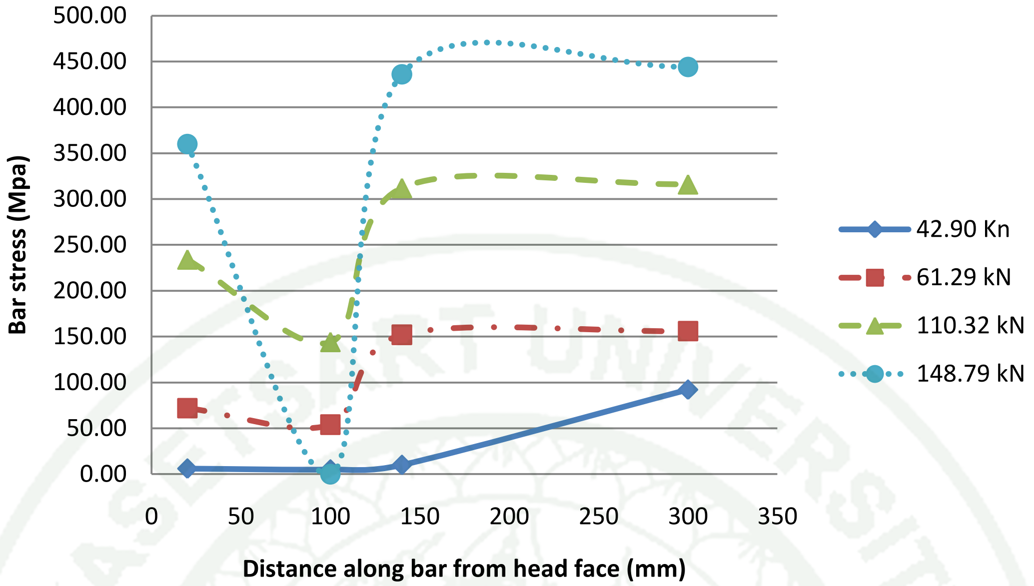

Figure 89 Bar stress along the bar for Griptec small head U-20-240-4.10-G-1/1

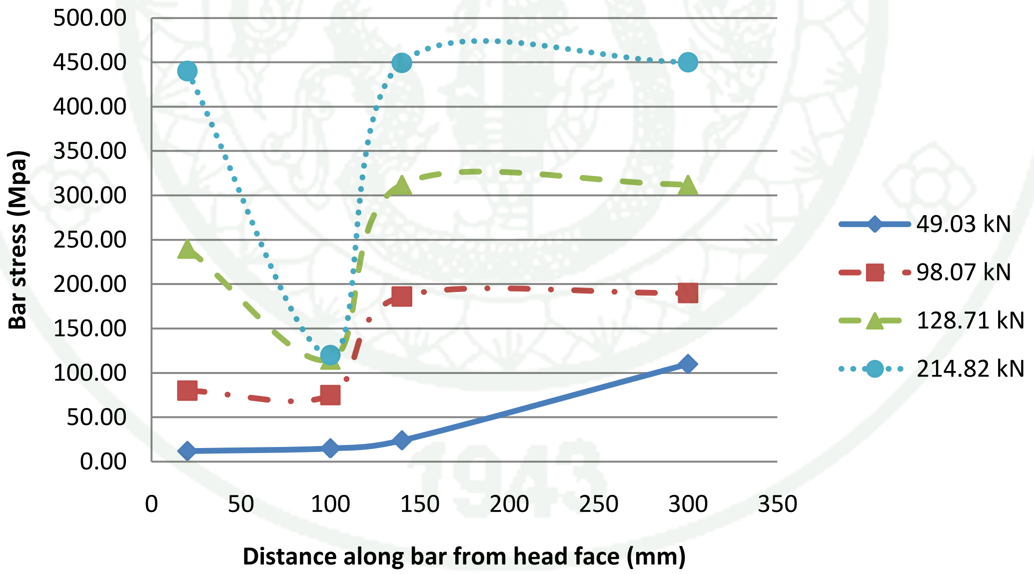

Figure 90 Bar stress along the bar for Griptec large head U-20-320-9.59-G-1/1

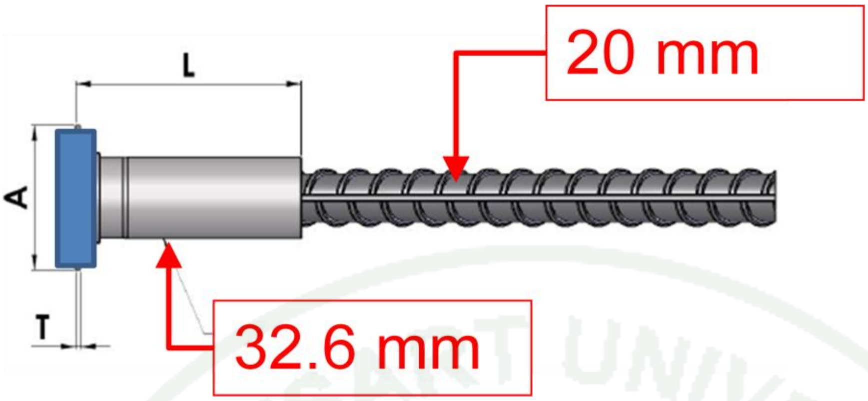

Figure 91 Griptec sleeve and rebar dimension

Figure 92 Bearing at Griptec sleeve end

Considering the dimension of swaged Griptec sleeve and rebar in Figure 91 at the end of sleeve the different outside diameter creates the end bearing that contributes to the total anchorage performance of Griptec headed bar as shown in Figure 92.

Correlation of Measured and Calculated Head Bar Stress Value

The theoretical values that were calculated from bearing capacity model of each head type are listed in appendix table 34-36.

To compare the measured value of head bar stress at failure listed in appendix table 33 and calculated value of head bearing capacity from proposed model, the correlation is plotted in Figure 93. It presents that the proposed model was reasonable performed.

Effect of Variable Head Type

The ultimate head bar stress for each variable head types are plotted in Figure 94 and Figure 95 to compare the head bearing capacity. It is obvious that increase of relative head area will increase head bearing capacity. For the similar relative head area Bartec head performed better than Griptec head.

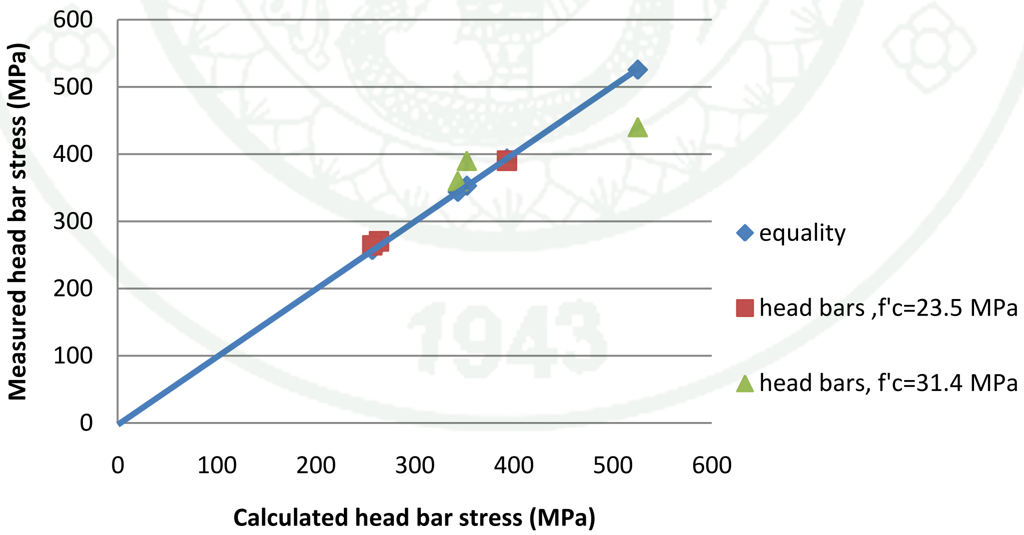

Figure 93 Correlation of measured and calculated value

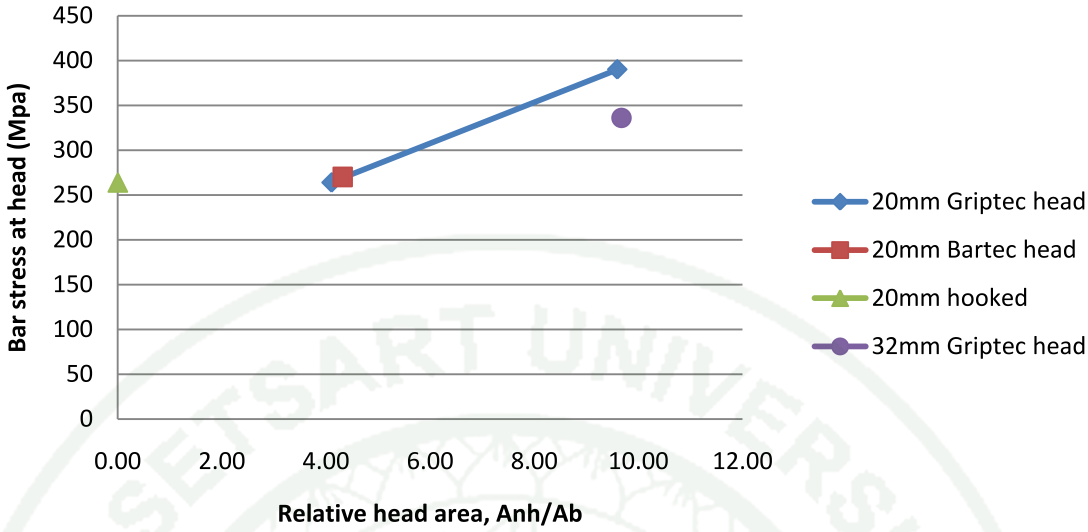

Figure 94 Correlation between relative head area, A_{nh}/a_b and head capacity for concrete compressive, f'_c = 23.5 MPa

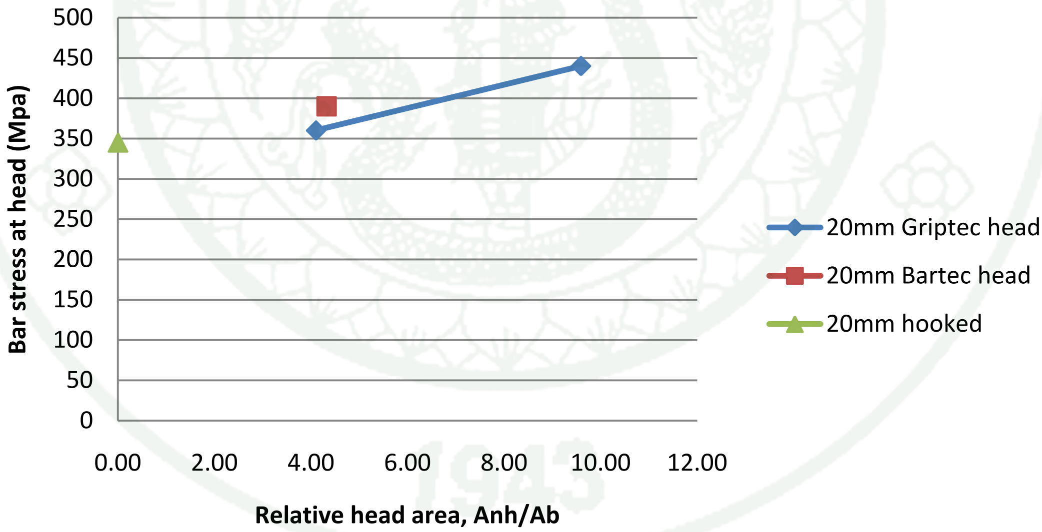

Figure 95 Correlation between relative head area, A_{nh}/a_b and head capacity for concrete compressive, f'_c = 31.4 MPa

Comparison to Hooked Bar

It is also obvious in Figure 93 and 94 that Bartec and Griptec headed bars had head bearing capacity greater than the hooked bars for both concrete compressive strength, f'_c 23.5 MPa and 31.4 MPa.

The Bartec small head had bearing capacity 13% greater than hooked bar, whereas the Griptec small head and Griptec large head had 4.3% and 27.5% greater respectively.

Effect of Bar Size

The bar stress at head of 32 mm bar was also plotted in Figure 94. The data point lay below the 20 mm bar for the similar relative head area. The decreased capacity of 32 mm bar may be due to the smaller relative bottom cover in that specimen.

CONCLUSION

1. Behavior of CCT Node

1.1. Cracking Behavior : Generally cracking patterns of all specimens are in the similar form as following.

1.1.1 The first crack formed just under the applied point load.

1.1.2 The second crack formed closer toward the CCT nodal zone.

1.1.3 The first and second cracks then grew towards the top bearing plate at applied point load.

1.1.4 The third crack formed even closer to the CCT nodal zone and grew at an angle parallel to the diagonal strut.

1.1.5 The horizontal cracks grew from the second to the third cracks.

1.1.6 Brittle failure suddenly occurred and the front portion of specimen split away from the main body.

1.2. Stress/Strain Development in the Bars

1.2.1 The bar stresses were calculated from the measured strain. Before the 1st crack formed at 20d_b away from head face, the maximum stress in the bar was recorded. At a higher load, the maximum stress was reached at the closer location from nodal face until the 2nd crack occurred. At a maximum load, the maximum stress level in the bar was nearly uniform from a point of 7d_b away from the head.

1.2.2 The final anchorage of the bar clearly occurred within the first 7d_b mm, the length roughly from the face of the head to the point where the bar passed out of the diagonal strut. The stresses at 1d_b mm in from the head provide an illustration of the bar force carried by the head while the stresses at 7d_b mm give an illustration of the total force in the bar.

1.3. Head Slip

1.3.1 Head slip typically did not initiate until cracking development, and then increased rapidly up to the point of failure.

1.3.2 It is obvious that with increased relative head area (A_{nh}/A_b) there is delay of slip initiation and increment.

1.4. Failure Mode : The main characteristics of failure are as following.

1.4.1 Cracking propagated along the diagonal compressive strut from the front support ahead to applied point load location on top beam.

1.4.2 The left top portion above cracked diagonal plan cleaved apart

1.4.3 Conical wedge shape of concrete behind the head

2. Obstruction Effect

2.1. The overall anchorage capacity of headed bar attached with Griptec sleeve was ultimately similar to the Bartec even though its sleeve surface obstructed the bar deformation larger than 2db as stipulated in ACI 318 clause 3.5.9.

3. Comparison to Standard Hooked Bar

3.1. All headed bar specimens reached the same anchorage capacity or higher than comparative hooked bars. This can confirm the use of headed bars in place of hooked bars.

3.2. The Bartec small head had bearing capacity 13% greater than hooked bar, whereas the Griptec small head and Griptec large head had 4.3% and 27.5% greater capacity respectively.

4. Comparison to the Theoretical Model

4.1 By bearing capacity model proposed by M. Keith Thompson, the measured value of head bar stress at failure was in line with the calculated value of head bearing capacity from proposed model.

LITERATURE CITED

American Association of State Highway and Transportation Officials. 1998. **AASHTO LRFD Bridge Design Specifications.** 2nd ed., Washington, DC.

American Concrete Institute. 2008. **ACI 318-08, Building Code Requirements for Structural Concrete and Commentary.** Farmington Hills, Michigan.

American Society for Testing and Materials. 2009. **ASTM A370-09 Standard Test Methods and Definitions for Mechanical Testing of Steel Products.** West Conshohocken, Pennsylvania.

American Society for Testing and Materials. 2009. **ASTM A970 / A970M - 09 Standard Specification for Headed Steel Bars for Concrete Reinforcement.** West Conshohocken, Pennsylvania.

American Society for Testing and Materials. 1999. **ASTM C39/C39M-99, Standard Test Method for Compressive Strength of Cylindrical Concrete Specimens**. West Conshohocken, Pennsylvania.

DeVries R.A. 1996. **Anchorage of Headed Reinforcement in Concrete,** The University of Texas at Austin, Austin, Texas.

Goto Yukimasa. 1971. Cracks Formed in Concrete Around Deformed Tension Bars, pp. 244-251. *In* **Proceedings Vol. 68, No. 4**, Journal of the American Concrete Institute. Detroit, Michigan.

Mains, R.M. 1951. Measurement of the Distribution of Tensile and Bond Stresses Along Reinforcing Bars, pp. 225-252. *In* **Proceedings Vol. 48, No. 3,** Journal of the American Concrete Institute. Detroit, Michigan.

Thompson, M. K., M. J. Young, J. O. Jirsa, J. E. Breen, and R. E. Klingner. 2002. **Anchorage Behavior of Headed Reinforcement : Literature review.** The University of Texas at Austin.

______, ______, ______, ______, ______. 2003. **Anchorage of Headed Reinforcement in CCT Nodes.** The University of Texas at Austin.

APPENDICES

Appendix A

Table

Appendix Table A1 Cracking and ultimate load for U-20-240-B-4.32-1/1

specimen #01(U-20-240-B-4.32-1/1)				Load at Cracking (kN)		
Time (min)	Applied load (kg)	Load at CCT node support (kgs)	Load at CCT node support (kN)	1st crack	2nd crack	3rd crack
0	0	0.00	0.00	60.68	110.32	141.58
4:48	2,500	1,875.00	18.39			
7:35	5,000	3,750.00	36.77			
9:56	7,500	5,625.00	55.16			
13:24	10,000	7,500.00	73.55			
16:46	12,500	9,375.00	91.94			
19:40	15,000	1,1250.00	110.32			
22:15	17,500	1,3125.00	128.71			
24:26	20,000	1,5000.00	147.10			
27:18	22,500	1,6875.00	165.49			
29:32	23,830	17,872.50	175.27			

Appendix Table A2 Cracking and ultimate load for U-20-240-9.59-G-1/1

specimen #3 (U-20-240-9.59-G-1/1)				Load at Cracking (kN)		
time (minute)	load (kg)	load at CCT node support (kg)	load at CCT node support (kN)	1st crack	2nd crack	3rd crack
0	0	0.00	0.00	32.4	74.64	86.48
4:47	2,500	1875.00	18.39			
7:38	5,000	3750.00	36.77			
10:45	7,500	5625.00	55.16			
13:47	10,000	7500.00	73.55			
17:36	12,500	9375.00	91.94			
19:37	15,000	11250.00	110.32			
21:36	17,500	13125.00	128.71			
24:03	20,000	15000.00	147.10			
25:45	21,195	15896.25	155.89			

Appendix Table A3 Cracking and ultimate load for U-20-240-9.59-G-1/2

specimen #04(U-20-240-G-9.59-1/2)				Load at Cracking (kN)		
Time (min)	Applied load (kg)	Load at CCT node support (kgs)	Load at CCT node support (kN)	1st crack	2nd crack	3rd crack
0	0	0.00	0.00	30.22	72.46	84.3
4:47	2,500	1,875.00	18.39			
7:38	5,000	3,750.00	36.77			
10:45	7,500	5,625.00	55.16			
13:47	10,000	7,500.00	73.55			
17:36	12,500	9,375.00	91.94			
19:37	15,000	11,250.00	110.32			
21:36	17,500	13,125.00	128.71			
24:03	20,000	15,000.00	147.10			
25:45	20,900	15675.00	153.71			

Appendix Table A4 Cracking and ultimate load for U-20-240- G-4.10-1/1

specimen #05(U-20-240-G-4.10-1/1)				Load at Cracking (kN)		
Time (min)	Applied load (kg)	Load at CCT node support (kgs)	Load at CCT node support (kN)	1st crack	2nd crack	3rd crack
0	0	0.00	0.00	56.8	75.56	93.95
4.13	2,500	1875.00	18.39			
8.32	5,000	3750.00	36.77			
11.58	7,500	5625.00	55.16			
15.00	10,000	7500.00	73.55			
17.80	12,500	9375.00	91.94			
20.00	15,000	11250.00	110.32			
23.00	17,500	13125.00	125.78			

Appendix Table A5 Cracking and ultimate load for U-20-240- G-4.10-1/2

specimen #06(U-20-240-G-4.10-1/2)				Load at Cracking (kN)		
Time (min)	Applied load (kg)	Load at CCT node support (kgs)	Load at CCT node support (kN)	1st crack	2nd crack	3rd crack
0	0	0.00	0.00	52.78	71.54	89.93
3.50	2,500	1,875.00	18.39			
7.20	5,000	3,750.00	36.77			
10:56	7,500	5,625.00	55.16			
13:59	10,000	7,500.00	73.55			
16:55	12,500	9,375.00	91.94			
20:45	15,000	11,250.00	110.32			
23:00	16,628	12,621.00	121.76			

Appendix Table A6 Cracking and ultimate load for U-20-240- G-4.10-1/2

specimen #07(U-20-240-H-0.00-1/1)				Load at Cracking (kN)		
Time (min)	Applied load (kg)	Load at CCT node support (kgs)	Load at CCT node support (kN)	1st crack	2nd crack	3rd crack
0	0	0.00	0.00	36.5	78.22	89.46
4:29	2,500	1,875.00	18.39			
7:47	5,000	3,750.00	36.77			
11:01	7,500	5,625.00	55.16			
14:14	10,000	7,500.00	73.55			
17:18	12,500	9,375.00	91.94			
19:32	15,000	11,250.00	110.32			
21:00	16,460	12,195.00	120.79			

Appendix Table A7 Cracking and ultimate load of U-20-240-H-0.00-1/2

specimen #08(U-20-240-H-0.00-1/2)				Load at Cracking (kN)		
Time (min)	Applied load (kg)	Load at CCT node support (kgs)	Load at CCT node support (kN)	1st crack	2nd crack	3rd crack
0.00	0	0.00	0.00	34.1	75.82	87.06
4.50	2,500	1875.00	18.39			
8.00	5,000	3750.00	36.77			
12.00	7,500	5625.00	55.16			
17.00	10,000	7500.00	73.55			
19:33	12,500	9375.00	91.94			
22.00	15,000	11,250	110.32			
24.00	16,100	12,075	118.39			

Appendix Table A8 Cracking and ultimate load of U-20-320-B-4.32-1/1

specimen #09(U-20-320-B-4.32-1/1)				Load at Cracking (kN)		
Time (min)	Applied load (kg)	Load at CCT node support (kgs)	Load at CCT node support (kN)	1st crack	2nd crack	3rd crack
0	0	0.00	0.00	68.4	83.11	112.53
4:43	2,500	1,875.00	18.39			
7:28	5,000	3,750.00	36.77			
10:45	7,500	5,625.00	55.16			
13:44	10,000	7,500.00	73.55			
17:56	12,500	9,375.00	91.94			
21:17	15,000	11,250.00	110.32			
24:16	17,500	13,125.00	128.71			
27:17	20,000	15,000.00	147.10			
30:28	22,500	16,875.00	165.49			
32:39	25,000	18,750.00	183.87			
36:24	27,500	20,625.00	202.26			
38:54	28,300	21,975.00	215.25			

Appendix Table A9 Cracking and ultimate load of U-20-320-B-4.32-1/2

specimen #10(U-20-320-B-4.32-1/2)				Load at Cracking (kN)		
Time (min)	Applied load (kg)	Load at CCT node support (kgs)	Load at CCT node support (kN)	1st crack	2nd crack	3rd crack
0	0	0.00	0.00	63.98	78.69	108.11
4:38	2,500	1,875.00	18.39			
7:48	5,000	3,750.00	36.77			
10:10	7,500	5,625.00	55.16			
13:01	10,000	7,500.00	73.55			
15:49	12,500	9,375.00	91.94			
18:55	15,000	11,250.00	110.32			
21:46	17,500	13,125.00	128.71			
26:25	20,000	15,000.00	147.10			
29:37	22,500	16,875.00	165.49			
33:10	25,000	18,750.00	183.87			
36:44	27,500	20,625.00	202.26			
39:34	28,500	21,723.75	210.83			

Appendix Table A10 Cracking and ultimate load of U-20-320-G-9.59-1/1

specimen #11(U-20-320-G-9.59-1/1)				Load at Cracking (kN)		
Time (min)	Applied load (kg)	Load at CCT node support (kgs)	Load at CCT node support (kN)	1st crack	2nd crack	3rd crack
0	0	0.00	0.00	77.2	94.33	123.75
4:43	2,500	1,875.00	18.39			
7:58	5,000	3,750.00	36.77			
10:55	7,500	5,625.00	55.16			
12:57	10,000	7,500.00	73.55			
16:26	12,500	9,375.00	91.94			
19:34	15,000	11,250.00	110.32			
22:35	17,500	13,125.00	128.71			
25:37	20,000	15,000.00	147.10			
30:38	22,500	16,875.00	165.49			
33:39	25,000	18,750.00	183.87			
36:40	27,500	20,625.00	202.26			
38:16	28,000	20,876.25	207.21			

Appendix Table A11 Cracking and ultimate load of U-20-320-G-9.59-1/2

specimen #12(U-20-320-G-9.59-1/2)				Load at Cracking (kN)		
Time (min)	Applied load (kg)	Load at CCT node support (kgs)	Load at CCT node support (kN)	1st crack	2nd crack	3rd crack
0	0	0.00	0.00	72.42	89.55	118.97
6:16	2,500	1875.00	18.39			
8:55	5,000	3750.00	36.77			
12:00	7,500	5625.00	55.16			
14:45	10,000	7500.00	73.55			
17:42	12,500	9375.00	91.94			
20:28	15,000	11250.00	110.32			
25:05	17,500	13125.00	128.71			
27:43	20,000	15000.00	147.10			
31:10	22,500	16875.00	165.49			
34:06	25,000	18750.00	183.87			
38:05	27,500	20625.00	202.26			
39:30	27,645	20883.75	202.43			

Appendix Table A12 Cracking and ultimate load of U-20-320-G-4.10-1/1

specimen #13(U-20-320-G-4.10-1/1)				Load at Cracking (kN)		
Time (min)	Applied load (kg)	Load at CCT node support (kgs)	Load at CCT node support (kN)	1st crack	2nd crack	3rd crack
0	0	0.00	0.00	40	57.06	109.06
3:28	2,500	1,875.00	18.39			
4:58	5,000	3,750.00	36.77			
6:42	7,500	5,625.00	55.16			
8:46	10,000	7,500.00	73.55			
10:36	12,500	9,375.00	91.94			
14:28	15,000	11,250.00	110.32			
16:47	17,500	13,125.00	128.71			
20:28	19,260	14,321.25	150.1			

Appendix Table A13 Cracking and ultimate load of U-20-320-G-4.10-1/2

specimen #14(U-20-320-G-4.10-1/2)				Load at Cracking (kN)		
Time (min)	Applied load (kg)	Load at CCT node support (kgs)	Load at CCT node support (kN)	1^{st} crack	2^{nd} crack	3^{rd} crack
0	0	0.00	0.00	37.38	54.44	106.44
3.45	2,500	1875.00	18.39			
4.48	5,000	3750.00	36.77			
6.28	7,500	5625.00	55.16			
9.02	10,000	7500.00	73.55			
10.25	12,500	9375.00	91.94			
14.36	15,000	11250.00	110.32			
17.03	17,500	13125.00	128.71			
23.24	20,000	15000.00	147.48			

Appendix Table A14 Cracking and ultimate load of U-20-320- H-0.00-1/1

specimen #15(U-20-320-H-0.00-1/1)				Load at Cracking (kN)		
Time (min)	Applied load (kg)	Load at CCT node support (kgs)	Load at CCT node support (kN)	1st crack	2nd crack	3rd crack
0.00	0	0.00	0.00	44	75.05	100.1
5:08	2,500	1875.00	18.39			
7:27	5,000	3750.00	36.77			
9:59	7,500	5625.00	55.16			
12:18	10,000	7500.00	73.55			
15:54	12,500	9375.00	91.94			
19:20	15,000	11250.00	110.32			
23:10	17,500	13125.00	128.71			
27:40	20,000	15000.00	147.10			
32:00	22,070	16477.50	163.09			

Appendix Table A15 Cracking and ultimate load of U-20-320- H-0.00-1/2

specimen #16 (U-20-320-H-0.00-1/2)				Load at Cracking (kN)		
Time (min)	Applied load (kg)	Load at CCT node support (kgs)	Load at CCT node support (kN)	1st crack	2nd crack	3rd crack
0.00	0	0.00	0.00	41	72.05	97.1
4.00	2,500	1875.00	18.39			
6.01	5,000	3750.00	36.77			
8.38	7,500	5625.00	55.16			
11.12	10,000	7500.00	73.55			
14.21	12,500	9375.00	91.94			
18.20	15,000	11250.00	110.32			
22.20	17,500	13125.00	128.71			
26.40	20,000	15000.00	147.10			
31.55	22,000	16650.00	160.09			

Appendix Table A16 Cracking and ultimate load of U-32-240-G-9.68-1/1

specimen #19(U-32-240-G-9.68-1/1)				Load at Cracking (kN)		
Time (min)	Applied load (kg)	Load at CCT node support (kgs)	Load at CCT node support (kN)	1st crack	2nd crack	3rd crack
0	0	0.00	0.00	57.2	75.59	93.98
3:08	2,500	1,875.00	18.39			
6:27	5,000	3,750.00	36.77			
9:09	7,500	5,625.00	55.16			
12:18	10,000	7,500.00	73.55			
15:04	12,500	9,375.00	91.94			
18:20	15,000	11,250.00	110.32			
20:10	17,500	13,125.00	128.71			
23:40	20,000	15,000.00	147.10			
26:00	22,500	16,875.00	165.49			
28:00	22,380	16,935.00	163.63			

Appendix Table A17 Cracking and ultimate load of U-32-240-G-9.68-1/2

specimen #20(U-32-240-G-9.68-1/2)				Load at Cracking (kN)		
Time (min)	Applied load (kg)	Load at CCT node support (kgs)	Load at CCT node support (kN)	1st crack	2nd crack	3rd crack
0.00	0	0.00	0.00	53.12	71.51	89.9
3.15	2,500	1,875.00	18.39			
6.7	5,000	3,750.00	36.77			
9.2	7,500	5,625.00	55.16			
12.5	10,000	7,500.00	73.55			
15.4	12,500	9,375.00	91.94			
18.6	15,000	11,250.00	110.32			
21.4	17,500	13,125.00	128.71			
24.8	20,000	15,000.00	147.10			
26.5	21,700	16,275.00	159.55			

Appendix Table A18 Tension Strain reading of Bartec small head U-20-240-4.32-B-1/1

Applied load (kg)	load at support (kg)	load at support (kN)	strain at distance from the head (mm)			
			20	140	260	420
0	-	0	0	0	0	0
833	625.00	6.13	10	12	20	25
1,667	1,250.00	12.26	15	18	25	30
2,500	1,874.99	18.39	20	25	30	55
3,333	2,499.99	24.52	22	28	40	65
4,167	3,124.99	30.65	26	30	50	100
5,000	3,749.99	36.77	32	38	75	160
5,833	4,374.98	42.90	35	48	96	225
6,667	4,999.98	49.03	38	62	140	285
7,500	5,624.98	55.16	40	74	220	385
8,333	6,249.98	61.29	50	95	290	360
9,167	6,874.97	67.42	58	100	360	420
10,000	7,499.97	73.55	65	116	400	450
10,833	8,124.97	79.68	70	126	460	520
11,667	8,749.97	85.81	80	140	540	560
12,500	9,374.96	91.94	86	220	620	680
13,333	9,999.96	98.07	120	380	660	730
14,167	10,624.96	104.20	160	480	750	820
15,000	11,249.96	110.32	200	560	790	860
15,833	11,874.95	116.45	230	620	820	900
16,667	12,499.95	122.58	300	750	958	960
17,500	13,124.95	128.71	460	820	1195	1200
18,333	13,749.95	134.84	680	1040	1390	1400

Appendix Table A18 (Continued)

Applied load (kg)	load at support (kg)	load at support (kN)	strain at distance from the head (mm)			
			20	140	260	420
19,167	14,374.94	140.97	850	1220	1580	1600
20,000	14,999.94	147.10	1050	1440	1845	1850
20,833	15,624.94	153.23	1200	1878	1938	1940
21,667	16,249.94	159.36	1335	2138	2134	2140
22,500	16,874.93	165.49	1345	2176	2175	2180
23,333	17,499.93	171.62	1348	2185	2196	2200
23,825	17,868.75	175.23	1350	2196	2232	2240

Appendix Table A19 Bar stress of Bartec small head U-20-240-4.32-B-1/1

Bar stress at each location							
20.00 mm		140.00 mm		260.00 mm		420.00 mm	
ksc	MPa	ksc	MPa	ksc	MPa	ksc	MPa
0.00	0.00	0.00	0.00	0.00	0.00	0.00	0.00
20.40	2.00	24.48	2.40	40.80	4.00	51.00	5.00
30.60	3.00	36.72	3.60	51.00	5.00	61.20	6.00
40.80	4.00	51.00	5.00	61.20	6.00	112.20	11.00
44.88	4.40	57.12	5.60	81.60	8.00	132.60	13.00
53.04	5.20	61.20	6.00	102.00	10.00	204.00	20.01
65.28	6.40	77.52	7.60	153.00	15.00	326.40	32.01
71.40	7.00	97.92	9.60	195.84	19.21	459.00	45.01
77.52	7.60	126.48	12.40	285.60	28.01	581.40	57.02
81.60	8.00	150.96	14.80	448.80	44.01	785.40	77.02
102.00	10.00	193.80	19.01	591.60	58.02	734.40	72.02
118.32	11.60	204.00	20.01	734.40	72.02	856.80	84.02
132.60	13.00	236.64	23.21	816.00	80.02	918.00	90.03
142.80	14.00	257.04	25.21	938.40	92.03	1,060.80	104.03
163.20	16.00	285.60	28.01	1,101.60	108.03	1,142.40	112.03
175.44	17.20	448.80	44.01	1,264.80	124.03	1,387.20	136.04
244.80	24.01	775.20	76.02	1,346.40	132.04	1,489.20	146.04
326.40	32.01	979.20	96.03	1,530.00	150.04	1,672.80	164.05
408.00	40.01	1,142.40	112.03	1,611.60	158.04	1,754.40	172.05
469.20	46.01	1,264.80	124.03	1,672.80	164.05	1,836.00	180.05

Appendix Table A19 (Continued)

Bar stress at each location							
20.00 mm		140.00 mm		260.00 mm		420.00 mm	
ksc	MPa	ksc	MPa	ksc	MPa	ksc	MPa
612.00	60.02	1,530.00	150.04	1,954.32	191.65	1,958.40	192.05
938.40	92.03	1,672.80	164.05	2,437.80	239.07	2,448.00	240.07
1,387.20	136.04	2,121.60	208.06	2,835.60	278.08	2,856.00	280.08
1,734.00	170.05	2,488.80	244.07	3,223.20	316.09	3,264.00	320.09
2,142.00	210.06	2,937.60	288.08	3,763.80	369.10	3,774.00	370.10
2,448.00	240.07	3,831.12	375.70	3,953.52	387.71	3,957.60	388.11
2,723.40	267.07	4,361.52	427.72	4,353.36	426.92	4,365.60	428.12
2,743.80	269.07	4,439.04	435.32	4,437.00	435.12	4,447.20	436.12
2,749.92	269.68	4,457.40	437.12	4,479.84	439.32	4,488.00	440.12
2,754.00	270.08	4,479.84	439.32	4,553.28	446.52	4,569.60	448.12

Appendix Table A20 Tension Strain reading of Griptec large head U-20-240-9.59-G-1/1

Applied load (kg)	load at support (kg)	load at support (kN)	strain at distance from the head (mm)			
			20	100	140	300
0	-	0.00	0	0	0	0
833	625.00	6.13	10	12	20	25
1,667	1,250.00	12.26	15	18	25	30
2,500	1,874.99	18.39	20	25	30	55
3,333	2,499.99	24.52	22	28	40	65
4,167	3,124.99	30.65	26	30	50	100
5,000	3,749.99	36.77	32	38	75	160
5,833	4,374.98	42.90	35	25	96	500
6,667	4,999.98	49.03	120	62	140	285
7,500	5,624.98	55.16	150	74	220	385
8,333	6,249.98	61.29	200	95	290	360
9,167	6,874.97	67.42	250	100	360	420
10,000	7,499.97	73.55	280	116	400	450
10,833	8,124.97	79.68	300	35	958	960
11,667	8,749.97	85.81	80	140	540	560
12,500	9,374.96	91.94	86	220	620	680
13,333	9,999.96	98.07	120	380	660	730
14,167	10,624.96	104.20	1215	180	1600	1620
15,000	11,249.96	110.32	200	560	790	860
15,833	11,874.95	116.45	230	620	820	900
16,667	12,499.95	122.58	300	750	958	960
17,500	13,124.95	128.71	460	820	1195	1200

Appendix Table A20 (Continued)

Applied load (kg)	load at support (kg)	load at support (kN)	strain at distance from the head (mm)			
			20	100	140	300
18,333	13,749.95	134.84	680	1040	1390	1400
19,167	14,374.94	140.97	850	1220	1580	1600
20,000	14,999.94	147.10	1050	1440	1845	1850
21,047	15,785.25	154.80	1950	300	2232	2240

Appendix Table A21 Bar stress of Griptec large head U-20-240-9.59-G-1/1

Bar stress at each location							
20.00 mm		140.00 mm		260.00 mm		420.00 mm	
ksc	MPa	ksc	MPa	ksc	MPa	ksc	MPa
0.00	0.00	0.00	0.00	0.00	0.00	0.00	0.00
20.40	2.00	24.48	2.40	40.80	4.00	51.00	5.00
30.60	3.00	36.72	3.60	51.00	5.00	61.20	6.00
40.80	4.00	51.00	5.00	61.20	6.00	112.20	11.00
44.88	4.40	57.12	5.60	81.60	8.00	132.60	13.00
53.04	5.20	61.20	6.00	102.00	10.00	204.00	20.01
65.28	6.40	77.52	7.60	153.00	15.00	326.40	32.01
71.40	7.00	51.00	5.00	195.84	19.21	1,020.00	100.03
244.80	24.01	126.48	12.40	285.60	28.01	581.40	57.02
306.00	30.01	150.96	14.80	448.80	44.01	785.40	77.02
408.00	40.01	193.80	19.01	591.60	58.02	734.40	72.02
510.00	50.01	204.00	20.01	734.40	72.02	856.80	84.02
571.20	56.02	236.64	23.21	816.00	80.02	918.00	90.03
612.00	60.02	71.40	7.00	1,954.32	191.65	1,958.40	192.05
163.20	16.00	285.60	28.01	1,101.60	108.03	1,142.40	112.03
175.44	17.20	448.80	44.01	1,264.80	124.03	1,387.20	136.04
244.80	24.01	775.20	76.02	1,346.40	132.04	1,489.20	146.04
2,478.60	243.07	367.20	36.01	3,264.00	320.09	3,304.80	324.09
408.00	40.01	1,142.40	112.03	1,611.60	158.04	1,754.40	172.05
469.20	46.01	1,264.80	124.03	1,672.80	164.05	1,836.00	180.05
612.00	60.02	1,530.00	150.04	1,954.32	191.65	1,958.40	192.05
938.40	92.03	1,672.80	164.05	2,437.80	239.07	2,448.00	240.07

Appendix Table A21 (Continued)

Bar stress at each location							
20.00 mm		140.00 mm		260.00 mm		420.00 mm	
ksc	MPa	ksc	MPa	ksc	MPa	ksc	MPa
1,387.20	136.04	2,121.60	208.06	2,835.60	278.08	2,856.00	280.08
1,734.00	170.05	2,488.80	244.07	3,223.20	316.09	3,264.00	320.09
2,142.00	210.06	2,937.60	288.08	3,763.80	369.10	3,774.00	370.10
3,978.00	390.11	612.00	60.02	4,553.28	446.52	4,569.60	448.12

Appendix Table A22 Tension Strain reading of Griptec small head U-20-240-4.10-G-1/2

Applied load (kg)	load at support (kg)	load at support (kN)	strain at distance from the head (mm)			
			20	100	140	220
0	0	0.00	0	0	0	0
833	625.00	6.13	15	5	20	25
1,667	1,250.00	12.26	20	5	30	30
2,500	1,874.99	18.39	10	10	40	55
3,333	2,499.99	24.52	10	15	50	65
4,167	3,124.99	30.65	20	20	65	95
5,000	3,749.99	36.77	20	10	75	40
5,833	4,374.98	42.90	30	25	80	225
6,667	4,999.98	49.03	40	10	90	10
7,500	5,624.98	55.16	50	50	102	525
8,333	6,249.98	61.29	100	50	240	625
9,167	6,874.97	67.42	180	40	635	820
10,000	7,499.97	73.55	310	40	950	980
10,833	8,124.97	79.68	560	70	1030	1120
11,667	8,749.97	85.81	725	80	1200	1250
12,500	9,374.96	91.94	820	85	1400	1480
13,333	9,999.96	98.07	1020	90	1480	1500
14,167	10,624.96	104.20	1280	120	1590	1640
15,000	11,249.96	110.32	1290	155	1700	1820
15,833	11,874.95	116.45	1300	170	1840	1940

Appendix Table A22 (Continued)

Applied load (kg)	load at support (kg)	load at support (kN)	strain at distance from the head (mm)			
			20	100	140	220
16,667	12,499.95	122.58	1310	190	2010	2180
16,828	12,621.00	123.77	1320	225	2100	2225

Appendix Table A23 Bar stress of Griptec small head U-20-240-4.10-G-1/2

Bar stress at each location							
20.00 mm		140.00 mm		260.00 mm		420.00 mm	
ksc	MPa	ksc	MPa	ksc	MPa	ksc	MPa
0.00	0.00	0.00	0.00	0.00	0.00	0.00	0.00
30.60	3.00	10.20	1.00	40.80	4.00	51.00	5.00
40.80	4.00	10.20	1.00	61.20	6.00	61.20	6.00
20.40	2.00	20.40	2.00	81.60	8.00	112.20	11.00
20.40	2.00	30.60	3.00	102.00	10.00	132.60	13.00
40.80	4.00	40.80	4.00	132.60	13.00	193.80	19.01
40.80	4.00	20.40	2.00	153.00	15.00	81.60	8.00
61.20	6.00	51.00	5.00	163.20	16.00	459.00	45.01
81.60	8.00	20.40	2.00	183.60	18.01	20.40	2.00
102.00	10.00	102.00	10.00	208.08	20.41	1,071.00	105.03
204.00	20.01	102.00	10.00	489.60	48.01	1,275.00	125.03
367.20	36.01	81.60	8.00	1,295.40	127.04	1,672.80	164.05
632.40	62.02	81.60	8.00	1,938.00	190.05	1,999.20	196.05
1,142.40	112.03	142.80	14.00	2,101.20	206.06	2,284.80	224.06
1,479.00	145.04	163.20	16.00	2,448.00	240.07	2,550.00	250.07
1,672.80	164.05	173.40	17.00	2,856.00	280.08	3,019.20	296.08
2,080.80	204.06	183.60	18.01	3,019.20	296.08	3,060.00	300.08
2,611.20	256.07	244.80	24.01	3,243.60	318.09	3,345.60	328.09
2,631.60	258.07	316.20	31.01	3,468.00	340.09	3,712.80	364.10
2,652.00	260.07	346.80	34.01	3,753.60	368.10	3,957.60	388.11
2,672.40	262.07	387.60	38.01	4,100.40	402.11	4,447.20	436.12
2,692.80	264.07	459.00	45.01	4,284.00	420.12	4,539.00	445.12

Appendix Table A24 Tension Strain reading of hooked bar U-20-240-0.00-H-1/2

Applied load (kg)	load at support (kg)	load at support (kN)	strain at distance from the head (mm)			
			20	140	225	355
0	0	0.00	0	0	0	0
833	625.00	6.13	15	15	25	40
1,667	1,250.00	12.26	20	25	35	30
2,500	1,874.99	18.39	10	30	50	55
3,333	2,499.99	24.52	10	40	55	75
4,167	3,124.99	30.65	45	50	80	110
5,000	3,749.99	36.77	65	120	280	450
5,833	4,374.98	42.90	76	125	340	500
6,667	4,999.98	49.03	90	240	420	600
7,500	5,624.98	55.16	120	350	580	680
8,333	6,249.98	61.29	180	520	750	800
9,167	6,874.97	67.42	240	650	860	840
10,000	7,499.97	73.55	260	725	920	900
10,833	8,124.97	79.68	300	850	1000	1020
11,667	8,749.97	85.81	540	1010	1180	1200
12,500	9,374.96	91.94	860	1280	1350	1380
13,333	9,999.96	98.07	950	1200	1480	1500
14,167	10,624.96	104.20	1020	1320	1480	1620
15,000	11,249.96	110.32	1060	1440	1560	1740
15,833	11,874.95	116.45	1140	1520	1840	1900
16,260	12,195.00	119.59	1250	1650	2100	2140

Appendix Table A25 Bar stress of hooked bar U-20-240-0.00-H-1/2

Bar stress at each location							
20.00 mm		140.00 mm		260.00 mm		420.00 mm	
ksc	MPa	ksc	MPa	ksc	MPa	ksc	MPa
0.00	0.00	0.00	0.00	0.00	0.00	0.00	0.00
30.60	3.00	30.60	3.00	51.00	5.00	81.60	8.00
40.80	4.00	51.00	5.00	71.40	7.00	61.20	6.00
20.40	2.00	61.20	6.00	102.00	10.00	112.20	11.00
20.40	2.00	81.60	8.00	112.20	11.00	153.00	15.00
91.80	9.00	102.00	10.00	163.20	16.00	224.40	22.01
132.60	13.00	244.80	24.01	571.20	56.02	918.00	90.03
155.04	15.20	255.00	25.01	693.60	68.02	1,020.00	100.03
183.60	18.01	489.60	48.01	856.80	84.02	1,224.00	120.03
244.80	24.01	714.00	70.02	1,183.20	116.03	1,387.20	136.04
367.20	36.01	1,060.80	104.03	1,530.00	150.04	1,632.00	160.04
489.60	48.01	1,326.00	130.04	1,754.40	172.05	1,713.60	168.05
530.40	52.01	1,479.00	145.04	1,876.80	184.05	1,836.00	180.05
612.00	60.02	1,734.00	170.05	2,040.00	200.06	2,080.80	204.06
1,101.60	108.03	2,060.40	202.06	2,407.20	236.07	2,448.00	240.07
1,754.40	172.05	2,611.20	256.07	2,754.00	270.08	2,815.20	276.08
1,938.00	190.05	2,448.00	240.07	3,019.20	296.08	3,060.00	300.08
2,080.80	204.06	2,692.80	264.07	3,019.20	296.08	3,304.80	324.09
2,162.40	212.06	2,937.60	288.08	3,182.40	312.09	3,549.60	348.10
2,325.60	228.06	3,100.80	304.08	3,753.60	368.10	3,876.00	380.11
2,550.00	250.07	3,366.00	330.09	4,284.00	420.12	4,365.60	428.12

Appendix Table A26 Tension strain reading of Griptec large headed bar U-32-240-9.59-G-1/1

Applied load (kg)	load at support (kg)	load at support (kN)	strain at distance from the head (mm)			
			20	100	140	300
0	0.00	0.00	0	0	0	0
833	625.00	6.13	5	10	15	20
1,667	1250.00	12.26	10	20	25	30
2,500	1874.99	18.39	15	25	32	55
3,333	2499.99	24.52	26	35	50	65
4,167	3124.99	30.65	46	40	80	110
5,000	3749.99	36.77	50	50	120	160
5,833	4374.98	42.90	60	40	280	460
6,667	4999.98	49.03	70	30	340	520
7,500	5624.98	55.16	90	20	400	600
8,333	6249.98	61.29	120	30	600	800
9,167	6874.97	67.42	200	35	840	920
10,000	7499.97	73.55	280	40	1110	1120
10,833	8124.97	79.68	360	50	1320	1340
11,667	8749.97	85.81	480	80	1450	1400
12,500	9374.96	91.94	760	120	1540	1600
13,333	9999.96	98.07	1100	160	1620	1680
14,167	10624.96	104.20	1250	200	1760	1760
15,000	11249.96	110.32	1290	220	1820	1850
15,833	11874.95	116.45	1340	250	1900	1920
16,667	12499.95	122.58	1390	270	1960	1980

Appendix Table A26 (Continued)

Applied load (kg)	load at support (kg)	load at support (kN)	strain at distance from the head (mm)			
			20	100	140	300
17,500	13124.95	128.71	1450	290	2000	2040
18,333	13749.95	134.84	1510	320	2040	2080
19,167	14374.94	140.97	1570	325	2080	2140
20,000	14999.94	147.10	1610	330	2100	2180
20,833	15624.94	153.23	1650	340	2200	2210
21,970	16477.50	161.59	1680	350	2226	2230

Appendix Table A27 Bar stress Griptec large headed bar U-32-240-9.68-G-1/1

Bar stress at each location							
20.00 mm		140.00 mm		260.00 mm		420.00 mm	
ksc	MPa	ksc	MPa	ksc	MPa	ksc	MPa
0.00	0.00	0.00	0.00	0.00	0.00	0.00	0.00
10.20	1.00	20.40	2.00	30.60	3.00	40.80	4.00
20.40	2.00	40.80	4.00	51.00	5.00	61.20	6.00
30.60	3.00	51.00	5.00	65.28	6.40	112.20	11.00
53.04	5.20	71.40	7.00	102.00	10.00	132.60	13.00
93.84	9.20	81.60	8.00	163.20	16.00	224.40	22.01
102.00	10.00	102.00	10.00	244.80	24.01	326.40	32.01
122.40	12.00	81.60	8.00	571.20	56.02	938.40	92.03
142.80	14.00	61.20	6.00	693.60	68.02	1,060.80	104.03
183.60	18.01	40.80	4.00	816.00	80.02	1,224.00	120.03
244.80	24.01	61.20	6.00	1,224.00	120.03	1,632.00	160.04
408.00	40.01	71.40	7.00	1,713.60	168.05	1,876.80	184.05
571.20	56.02	81.60	8.00	2,264.40	222.06	2,284.80	224.06
734.40	72.02	102.00	10.00	2,692.80	264.07	2,733.60	268.07
979.20	96.03	163.20	16.00	2,958.00	290.08	2,856.00	280.08
1,550.40	152.04	244.80	24.01	3,141.60	308.09	3,264.00	320.09
2,244.00	220.06	326.40	32.01	3,304.80	324.09	3,427.20	336.09
2,550.00	250.07	408.00	40.01	3,590.40	352.10	3,590.40	352.10
2,631.60	258.07	448.80	44.01	3,712.80	364.10	3,774.00	370.10
2,733.60	268.07	510.00	50.01	3,876.00	380.11	3,916.80	384.11
2,835.60	278.08	550.80	54.02	3,998.40	392.11	4,039.20	396.11

Appendix Table A27 (Continued)

Bar stress at each location							
20.00 mm		140.00 mm		260.00 mm		420.00 mm	
ksc	MPa	ksc	MPa	ksc	MPa	ksc	MPa
2,958.00	290.08	591.60	58.02	4,080.00	400.11	4,161.60	408.11
3,080.40	302.08	652.80	64.02	4,161.60	408.11	4,243.20	416.12
3,202.80	314.09	663.00	65.02	4,243.20	416.12	4,365.60	428.12
3,284.40	322.09	673.20	66.02	4,284.00	420.12	4,447.20	436.12
3,366.00	330.09	693.60	68.02	4,488.00	440.12	4,508.40	442.12
3,427.20	336.09	714.00	70.02	4,541.04	445.32	4,549.20	446.12

Appendix Table A28 Head slip of Griptec large head specimen U-20-320-G-9.59-1/1

Tension strain at 1db (με)	Bar stress at head (ksc)	Bar stress at head (MPa)	Head slip (mm)
20	40.8	4.00	0
40	81.6	8.00	0
45	91.8	9.00	0
50	102	10.00	0
90	183.6	18.01	0
75	153	15.00	0
100	204	20.01	0
140	285.6	28.01	0
160	326.4	32.01	0
390	795.6	78.02	0.002
430	877.2	86.02	0.004
500	1020	100.03	0.004
560	1142.4	112.03	0.004
700	1428	140.04	0.006
800	1632	160.04	0.008
850	1734	170.05	0.01
885	1805.4	180.00	0.012
980	1999.2	200.00	0.018

Appendix Table A28 (Continued)

Tension strain at 1db (με)	Bar stress at head (ksc)	Bar stress at head (MPa)	Head slip (mm)
1100	2244	220.06	0.02
1200	2448	240.07	0.03
1400	2856	280.08	0.04
1500	3060	300.08	0.05
1600	3264	320.09	0.06
1750	3570	350.10	0.07
1850	3774	370.10	0.08
1920	3916.8	384.11	0.12

Appendix Table A29 Head slip of Griptec small head specimen U-20-320-G-4.10-1/1

tension strain at 1_{db} (με)	Bar stress at head (ksc)	Bar stress at head (MPa)	Head slip (mm)
15	30.6	3.00	0
35	71.4	7.00	0
45	91.8	9.00	0
60	122.4	12.00	0
85	173.4	17.00	0
95	193.8	19.01	0
140	285.6	28.01	0
150	306	30.01	0
180	367.2	36.01	0.005
200	408	40.01	0.005
220	448.8	44.01	0.006
235	479.4	47.01	0.007
280	571.2	56.02	0.009
340	693.6	68.02	0.01
380	775.2	76.02	0.03
450	918	90.03	0.04
885	1805.4	180.00	0.08
980	1999.2	200.00	0.12
1160	2366.4	232.06	0.17
1350	2754	270.08	0.25
1400	2856	280.08	0.45

Appendix Table A30 Bond and head bearing component for U-20-320-9.59-G-1/1

Item	Time (min)	1d	7d	7d-1d	fs-head	Bond,u	Total stress
					Mpa	Mpa	
1	2	0	25	25	0.00	5.00	5.00
2	4	5	55	50	1.00	10.00	11.00
3	6	5	130	125	1.00	25.01	26.01
4	8	5	120	115	1.00	23.01	24.01
5	10	5	130	125	1.00	25.01	26.01
6	12	5	185	180	1.00	36.01	37.01
7	14	42	450	408	8.40	81.62	90.03
8	16	160	660	500	32.01	100.03	132.04
9	18	220	755	535	44.01	107.03	151.04
10	20	320	920	600	64.02	120.03	184.05
11	22	400	1060	660	80.02	132.04	212.06
12	24	480	1150	670	96.03	134.04	230.06
13	26	680	1280	600	136.04	120.03	256.07
14	28	780	1340	560	156.04	112.03	268.07
15	30	900	1440	540	180.05	108.03	288.08
16	32	1400	1850	450	280.08	90.03	370.10
17	34	1600	1950	350	320.09	70.02	390.11
18	36	1780	2120	340	356.10	68.02	424.12
19	38	2000	2240	240	400.11	48.01	448.12

Appendix Table A31 Bond and head bearing component for U-20-320-4.10-G-1/1

Item	Time (min)	1d	7d	7d-1d	fs-head	Bond,u	Total stress
					MPa	MPa	MPa
1	2	0	25	25	0.00	5.00	5.00
2	4	5	55	50	1.00	10.00	11.00
3	6	5	130	125	1.00	25.01	26.01
4	8	5	120	115	1.00	23.01	24.01
5	10	5	130	125	1.00	25.01	26.01
6	12	5	185	180	1.00	36.01	37.01
7	14	30	450	420	6.00	84.02	90.03
8	16	140	660	520	28.01	104.03	132.04
9	18	195	755	560	39.01	112.03	151.04
10	20	290	920	630	58.02	126.04	184.05
11	22	375	1060	685	75.02	137.04	212.06
12	24	420	1150	730	84.02	146.04	230.06
13	26	610	1280	670	122.03	134.04	256.07
14	28	726	1340	614	145.24	122.83	268.07
15	30	880	1440	560	176.05	112.03	288.08
16	32	1380	1850	470	276.08	94.03	370.10
17	34	1550	1950	400	310.09	80.02	390.11
18	36	1675	2120	445	335.09	89.02	424.12
19	38	1820	2248	428	364.10	85.62	449.73

Appendix Table A32 Important dimension of each specimen

Item	Bar size	Head type	A_{nh}/A_b	L_{plt}/d_b	c_2/d_b	c/d_b
1	20	BARTEC circular dh= 48 mm	4.32	4	5	3
2	20	BARTEC circular dh= 48 mm	4.32	4	5	3
3	20	GRIPTEC circular dh= 70 mm	9.59	4	5	3
4	20	GRIPTEC circular dh= 70 mm	9.59	4	5	3
5	20	GRIPTEC circular dh=52 mm	4.1	4	5	3
6	20	GRIPTEC circular dh=52 mm	4.1	4	5	3
7	20	Hooked 90˚	0	4	5	3
8	20	Hooked 90˚	0	4	5	3
9	20	BARTEC circular dh= 48 mm	4.32	4	5	3
10	20	BARTEC circular dh= 48 mm	4.32	4	5	3
11	20	GRIPTEC circular dh= 70 mm	9.59	4	5	3
12	20	GRIPTEC circular dh= 70 mm	9.59	4	5	3
13	20	GRIPTEC circular dh=52 mm	4.1	4	5	3
14	20	GRIPTEC circular dh=52 mm	4.1	4	5	3
15	20	Hooked 90˚	0	4	5	3
16	20	Hooked 90˚	0	4	5	3
17	32	GRIPTEC circular dh=110 mm	9.68	4	3.1	1.9
18	32	GRIPTEC circular dh=110 mm	9.68	4	3.1	1.9

Appendix Table A33 Results from experiment

Item	Bar size	Head type	f'c , kcs	f_s at $1d_b$, MPa	f_s at $7d_b$, MPa	max load at support (kN)	Failure mode
1	20	BARTEC circular dh= 48 mm	240	290	436	175.27	Splitting
2	20	BARTEC circular dh= 48 mm	240	----	----	----	----
3	20	GRIPTEC circular dh= 70 mm	240	390	446	155.89	Splitting
4	20	GRIPTEC circular dh= 70 mm	240	387	442	153.71	Splitting
5	20	GRIPTEC circular dh=52 mm	240	170	416	125.78	Splitting
6	20	GRIPTEC circular dh=52 mm	240	264	420	121.76	Splitting
7	20	Hooked 90˚	240	225	378	120.79	Splitting
8	20	Hooked 90˚	240	250	382	118.39	Splitting
9	20	BARTEC circular dh= 48 mm	320	388	442	215.25	Splitting
10	20	BARTEC circular dh= 48 mm	320	390	448	210.83	Splitting
11	20	GRIPTEC circular dh= 70 mm	320	438	447	207.21	Splitting
12	20	GRIPTEC circular dh= 70 mm	320	440	449	202.43	Splitting
13	20	GRIPTEC circular dh=52 mm	320	356	430	150.1	Splitting
14	20	GRIPTEC circular dh=52 mm	320	360	436	147.48	Splitting
15	20	Hooked 90˚	320	345	408	163.09	Splitting
16	20	Hooked 90˚	320	256	404	160.09	Splitting
17	32	GRIPTEC circular dh=110 mm	240	340	446	163.63	Splitting
18	32	GRIPTEC circular dh=110 mm	240	332	440	159.55	Splitting

Appendix Table A34 Calculated value for dia 20 mm with f'_c = 23.5 MPa

			BARTEC	GRIPTEC	
			small	small	large
Rebar diameter	d_b	mm	20	20	20
Rebar cross-section area	A_b	mm^2	314	314	314
Rebar nominal yield	f_y	MPa	450	450	450
Head net bearing area	A_{nh}	mm^2	1357	1289	3014
			4.32	4.10	9.59
Concrete compressive strength	f'_c	MPa	23.5	23.5	23.5
Concrete strength used in calculation	f'_c	MPa	23.15	23.15	23.15
Rebar spacing	c_2	mm	100	100	100
Concrete cover	c	mm	60	60	60
Statistical correction factor	$n_{5\%}$		0.7	0.7	0.7
Development length	L_d	mm	300	300	300
Radial disturbance factor	Ψ		1.27	1.27	1.27
Bar stress provided by the head	$fs_{,head}$	MPa	264	257	393
Reduction factor	x		0.39	0.43	0.30
Minimum computed anchorage length	L_a	mm	314	302	126
Minimum required anchorage length	L_a	mm	314	302	160
head bearing capacity from experiment			270	264	390

Appendix Table A35 Calculated value for dia 20 mm with f'_c = 34.5 MPa

			BARTEC	GRIPTEC	
			small	small	large
Rebar diameter	d_b	mm	20	20	20
Rebar cross-section area	A_b	mm^2	314	314	314
Rebar nominal yield	f_y	MPa	450	450	450
Head net bearing area	A_{nh}	mm^2	1357	1289	3014
			4.32	4.10	9.59
Concrete compressive strength	f'_c	MPa	30.6	30.6	30.6
Concrete strength used in calculation	f'_c	MPa	30.6	30.6	30.6
Rebar spacing	c_2	mm	100	100	100
Concrete cover	c	mm	60	60	60
Statistical correction factor	$n_{5\%}$		0.7	0.7	0.7
Development length	L_d	mm	300	300	300
Radial disturbance factor	Ψ		1.27	1.27	1.27
Bar stress provided by the head	$fs,_{head}$	MPa	353	344	525
Reduction factor	x		0.39	0.43	0.30
Minimum computed anchorage length	L_a	mm	164	167	-168
Minimum required anchorage length	L_a	mm	164	167	160
head bearing capacity from experiment			390	360	440

Appendix Table A36 Calculated value for dia 32 mm with f'$_c$ = 23.5 MPa

			BARTEC	GRIPTEC	
			small	small	large
Rebar diameter	db	mm	32	32	32
Rebar cross-section area	A_b	mm^2	804	804	804
Rebar nominal yield	f_y	MPa	450	450	450
Head net bearing area	A_{nh}	mm^2	3400	3306	7783
			4.23	4.11	9.68
Concrete compressive strength	f'_c	MPa	23.15	23.15	23.15
Concrete strength used in calculation	f'_c	MPa	23.15	23.15	23.15
Rebar spacing	c_2	mm	100	100	100
Concrete cover	c	mm	100	100	100
Statistical correction factor	$n_{5\%}$		0.7	0.7	0.7
Development length	L_d	mm	300	300	300
Radial disturbance factor	Ψ		1.00	1.00	1.00
Bar stress provided by the head	$fs,_{head}$	MPa	215	212	325
Reduction factor	x		0.41	0.42	0.30
Minimum computed anchorage length	L_a	mm	384	374	278
Minimum required anchorage length	L_a	mm	384	374	278
head bearing capacity from experiment			----	----	336

Appendix B

Figure

Appendix Figure B1 Dia 20 mm and 32 mm control bars SD40

Appendix Figure B2 Tensile testing of control bars

Appendix Figure B3 DEXTRA's headed bars

Appendix Figure B4 GRIPTEC's headed bars

Appendix Figure B5 GRIPTEC Large and small headed bars dia 20 mm and 32 mm

Appendix Figure B6 GRIPTEC Large and small headed bars dia 20 mm and 32 mm

Appendix Figure B7 GRIPTEC Large and small headed bars dia 32 mm

Appendix Figure B8 GRIPTEC Large and small headed bars dia 20 mm

Appendix Figure B9 BARTEC small headed bars dia 20 mm and 32 mm

Appendix Figure B10 BARTEC and GRIPTEC large and small headed bars dia 20

Appendix Figure B11 Strain gauges

Appendix Figure B12 Strain gauges

Appendix Figure B13 Strain gauge installation

Appendix Figure B14 Strain gauge installation

Appendix Figure B15 Strain gauge installation

Appendix Figure B16 Strain gauge installation along bars

Appendix Figure B17 Rebar fixing

Appendix Figure B18 Rebar fixing

Appendix Figure B19 Rebar fixing and formwork

Appendix Figure B20 Rebar fixing

Appendix Figure 21 Rebar fixing and formwork

Appendix Figure B22 Rebar fixing and formwork

Appendix Figure B23 Concrete placing

Appendix Figure B24 Concrete placing


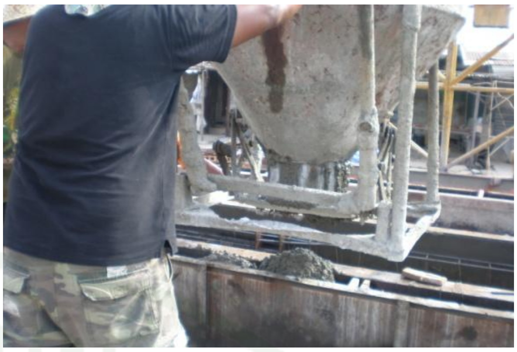

Appendix Figure B25 Concrete placing


Appendix Figure B26 Concrete placing


Appendix Figure B27 Concrete placing

Appendix Figure B28 Concrete placing and identification

Appendix Figure B29 Loading specimen and identification

Appendix Figure B30 Loading specimen and instrument setting

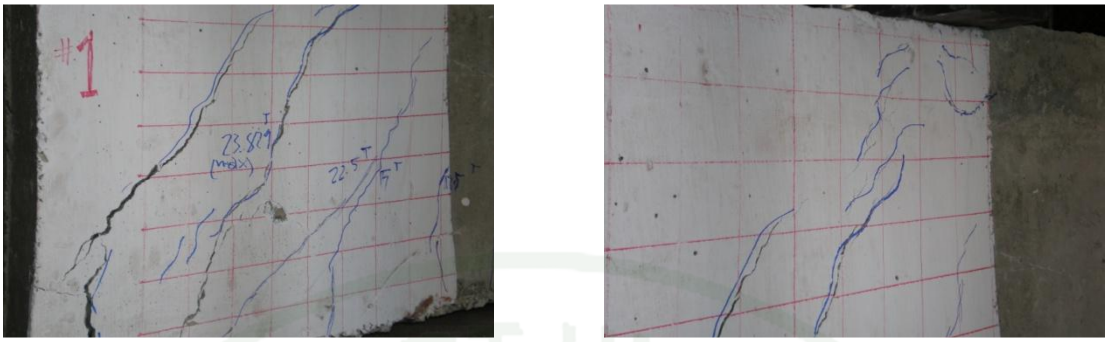

Appendix Figure B31 Cracking behavior for U-20-240-4.32-B-1/1

Appendix Figure B32 Cracking behavior for U-20-240-9.59-G-1/1

Appendix Figure B33 Cracking behavior for U-20-240-9.59-G-1/2

Appendix Figure B34 Cracking behavior for U-20-240-4.10-G-1/1

Appendix Figure B35 Cracking behavior for U-20-240-4.10-G-1/2

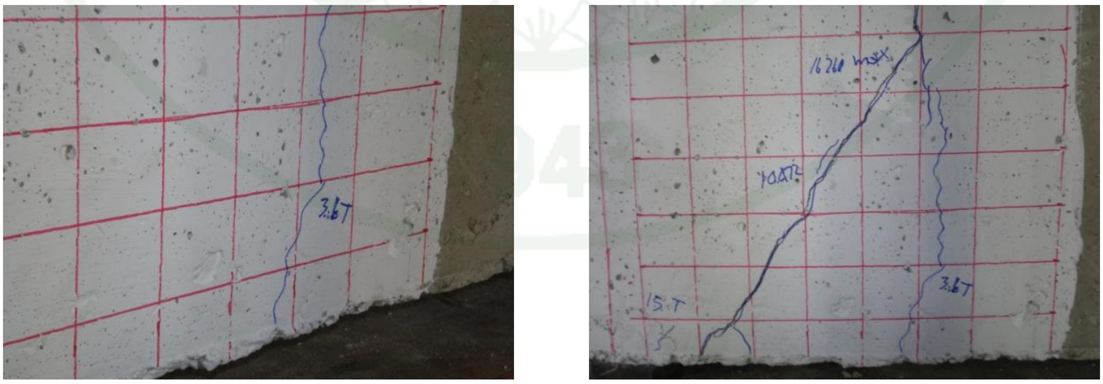

Appendix Figure B36 Cracking behavior for U-20-240-0.00-H-1/1

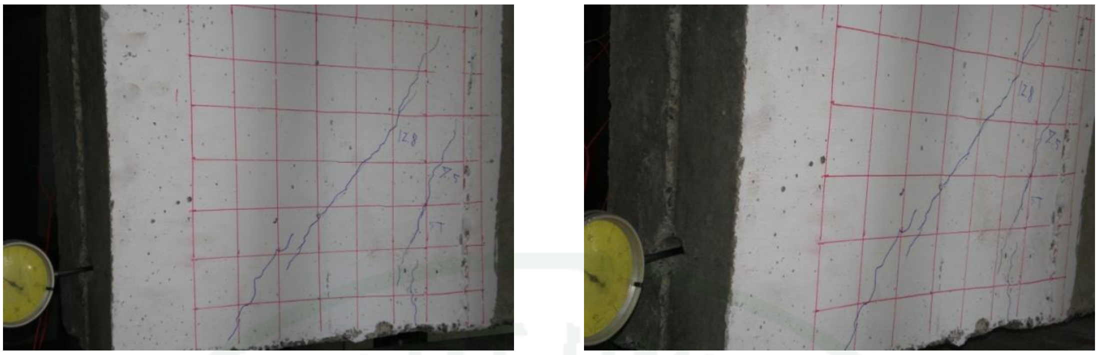

Appendix Figure 37 Cracking behavior for U-20-240-0.00-H-1/2

Appendix Figure B38 Cracking behavior for U-20-320-4.32-B-1/1

Appendix Figure B39 Cracking behavior for U-20-320-4.32-B-1/2

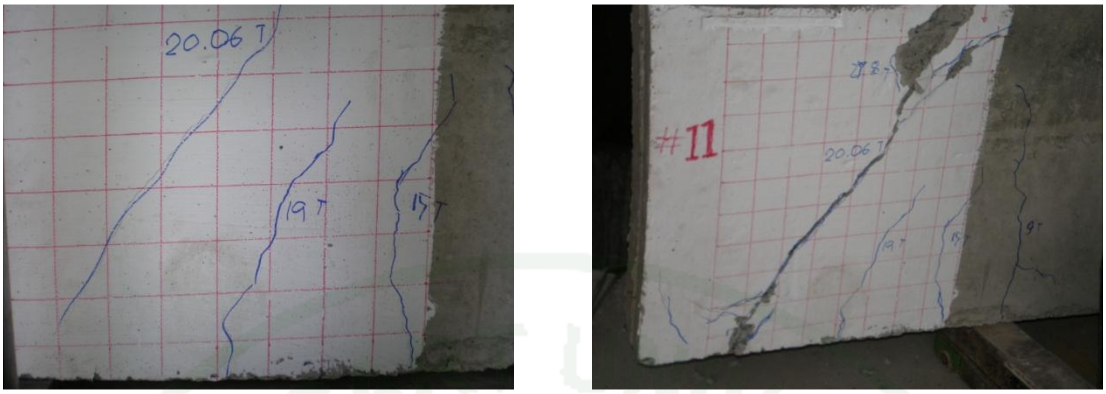

Appendix Figure B40 Cracking behavior for U-20-320-9.59-G-1/1

Appendix Figure B41 Cracking behavior for U-20-320-9.59-G-1/2

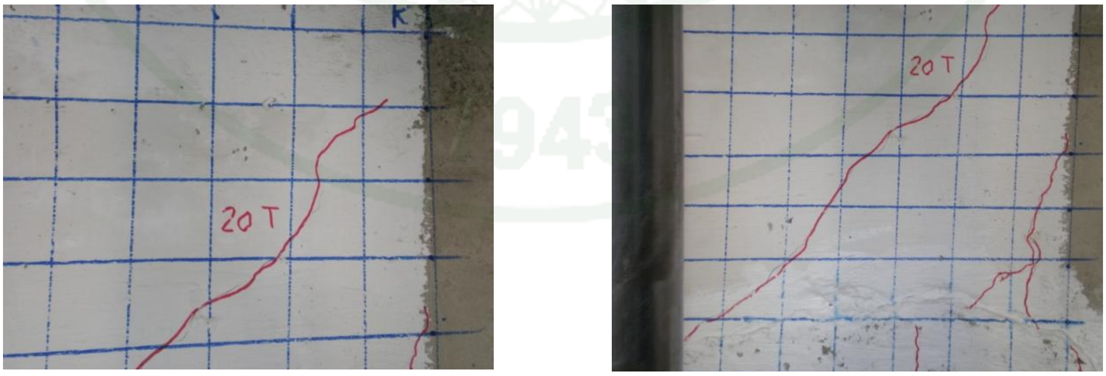

Appendix Figure B42 Cracking behavior for U-20-320-4.10-G-1/1

Appendix Figure B43 Cracking behavior for U-20-320-4.10-G-1/2

Appendix Figure B44 Cracking behavior for U-20-320-0.00-H-1/1

Appendix Figure 45 Cracking behavior for U-20-320-0.00-H-1/2

CURRICULUM VITAE

NAME : Mr. Wichian Kaewkhampa

BIRTH DATE : October 5, 1965

BIRTH PLACE : Phayao, Thailand

EDUCATION :

YEAR	INSTITUTE	DEGREE/DIPLOMA
1987	Chiangmai Univ.	B.Eng (Civil Engineering)
2011	Kasetsart Univ.	M.Eng (Civil Engineering)

POSITION /TITLE : Project Manager

WORK PLACE : Dextra Manufacturing Co., Ltd.